

Copyright  
by  
Sungmo Kang  
2009

The Dissertation Committee for Sungmo Kang  
certifies that this is the approved version of the following dissertation:

**Reducible and Toroidal  
Dehn Filling with Distance 3**

Committee:

---

Cameron Gordon, Supervisor

---

John Luecke

---

Alan Reid

---

Seungsang Oh

---

Hossein Namazi

**Reducible and Toroidal  
Dehn Filling with Distance 3**

by

**Sungmo Kang, B.S.**

**DISSERTATION**

Presented to the Faculty of the Graduate School of  
The University of Texas at Austin  
in Partial Fulfillment  
of the Requirements  
for the Degree of

**DOCTOR OF PHILOSOPHY**

THE UNIVERSITY OF TEXAS AT AUSTIN

August 2009

Dedicated to my wife Jiyoung and my son Austin, and my parents.

## Acknowledgments

First and foremost, I wish to thank my PhD advisor, Cameron Gordon, for his great encouragement and constant enthusiasm as well as the many hours spent discussing mathematics and life. I also wish to thank Sungbok Hong for first stimulating my interest in topology. I also wish to thank my PhD committee, John Luecke, Alan Reid, Seungsang Oh and Hossein Namazi.

This dissertation is a milestone on my path of learning that began at an early age. Growing up, my parents enthusiastically supported me in a variety of educational activities. I wish to acknowledge my parents for their amazing unconditional support. I am incredibly grateful for their willingness to let me make my decisions unrestricted by their concerns and for their full support once I have made them.

I also wish to acknowledge the countless number of family, friends, colleagues and teachers who have contributed so much to my life, including the support to follow my heart in pursuit of my ideals. The completion of this dissertation is but a small result of the care and attention that has been given to me by so many.

Finally, I wish to thank my wife Jiyoung for her great support and my son Austin for giving me a lot of happiness. I am deeply proud of my wife and my son.

# **Reducible and Toroidal Dehn Filling with Distance 3**

Publication No. \_\_\_\_\_

Sungmo Kang, Ph.D.

The University of Texas at Austin, 2009

Supervisor: Cameron Gordon

This dissertation is an investigation into the classification of all hyperbolic manifolds which admit a reducible Dehn filling and a toroidal Dehn filling with distance 3. The first example was given by Boyer and Zhang. They used the Whitehead link. Eudave-Muñoz and Wu gave an infinite family of such hyperbolic manifolds using tangle arguments. I show in this dissertation that these are the only hyperbolic manifolds admitting a reducible Dehn filling and a toroidal Dehn filling with distance 3. The main tool to prove this is to use the intersection graphs on surfaces introduced and developed by Gordon and Luecke.

# Table of Contents

<b>Acknowledgments</b>	<b>v</b>
<b>Abstract</b>	<b>vi</b>
<b>List of Tables</b>	<b>ix</b>
<b>List of Figures</b>	<b>x</b>
<b>Chapter 1. Introduction</b>	<b>1</b>
1.1 Basics of 3-manifolds . . . . .	1
1.1.1 3-manifolds . . . . .	1
1.1.2 Surfaces in 3-manifolds . . . . .	1
1.2 Dehn Surgeries . . . . .	4
1.3 Some Classifications on Exceptional Pairs . . . . .	5
1.4 Main Result . . . . .	7
<b>Chapter 2. Intersection Graphs on Surfaces</b>	<b>11</b>
2.1 Introduction . . . . .	11
2.2 Binary Faces and the Subgraph $\Lambda$ of $G_1^+$ . . . . .	13
2.2.1 Terminology and Lemmas . . . . .	14
2.2.2 Existence of a White Bigon . . . . .	19
2.3 A $B(\alpha, \beta)$ Bigon and a Black Trigon . . . . .	24
2.3.1 Isomorphic Disk Faces and Dual Graph of $G^+$ . . . . .	24
2.3.2 Ordinary Cycles and Boundary Cycles . . . . .	31
2.3.3 Proof of Theorem 2.3.1 . . . . .	37
2.4 A $B(\alpha, \beta)$ Bigon and a White Trigon . . . . .	40
2.4.1 A $W(\alpha, \delta)$ Trigon with Two $\delta$ -edges and One $\alpha$ -edge . .	40
2.4.2 A $W(\alpha, \delta)$ Trigon with Two $\alpha$ -edges and One $\delta$ -edge . .	50
2.4.3 A $W(\beta, \gamma)$ Trigon, a $W(\beta, \delta)$ Trigon and a $W(\alpha, \gamma)$ Trigon	54

<b>Chapter 3. The Toroidal Dehn Filling</b>	<b>59</b>
3.1 Topological Description of the Toroidal Dehn Filling $M(r_2)$ . . .	59
3.2 A Link Surgery Description of the Toroidal Dehn Filling $M(r_2)$	65
<b>Chapter 4. Dehn Fillings on a Link and Tangle Fillings on a Tangle</b>	<b>72</b>
4.1 Tangle Description of $M$ with Tangle Slopes . . . . .	72
4.2 Some Restrictions on Tangle Slopes $\theta, \varphi$ and $\omega$ . . . . .	75
4.3 The Proof of $\theta = 2$ . . . . .	82
4.3.1 The Case that $\varphi = -3$ . . . . .	82
4.3.2 The Case that $\varphi = 3$ . . . . .	85
4.3.3 The Case that $\omega = -1/3$ . . . . .	86
4.3.4 The Proof of Proposition 4.3.1 . . . . .	89
4.4 The Proof of Theorem 4.1.1 . . . . .	90
<b>Bibliography</b>	<b>91</b>
<b>Vita</b>	<b>96</b>

# List of Tables

1.1	Upper bounds for distances. . . . .	6
-----	-------------------------------------	---

## List of Figures

1.1	The tangles and the $1/0$ - and $1/3$ -rational tangle fillings used in Theorem 1.4.1. . . . .	9
2.1	Orientations on an edge. . . . .	13
2.2	6 edge classes on $\widehat{F}_2$ . . . . .	16
2.3	Two equivalent figures of $H_W$ or $H_B$ . . . . .	19
2.4	The intersection of $H_B$ and the corners of a $B(\alpha, \beta)$ face. . . .	20
2.5	A $B(\alpha, \beta)$ bigon, a $B(\gamma, \delta)$ trigon and the intersection on $H_B$ . . . .	26
2.6	Two orientations $\omega$ and $\omega'$ to the edges of $\Lambda^*$ . . . . .	28
2.7	Four distinct types of interior vertices. . . . .	32
2.8	Boundary cycles with respect to $\omega$ . . . . .	33
2.9	Boundary cycles with respect to $\omega'$ . . . . .	34
2.10	Three occurrences of label $x$ on $v_1$ and $v_2$ . . . . .	35
2.11	The intersection of the white corners of a bad $W(\beta, \gamma)$ face and $H_W$ , and the local configuration at an interior vertex of type (i). . . . .	38
2.12	The intersection of the white corners of a $W(\alpha, \gamma)$ face and $H_W$ , and the local configuration at an interior vertex of type (ii). . . . .	39
2.13	The intersection of the white corners of a $W(\alpha, \delta)$ trigon and the intersection of the black corners of a $B(\alpha, \beta)$ bigon and $H_B$ . . . . .	41
2.14	Local configurations of a boundary vertex (i), (ii), and an interior vertex with a $\delta$ -edge incident (iii), (iv). . . . .	41
2.15	The intersection of $H_W$ and the white corners of a $W(\alpha, \delta)$ trigon and a bad $W(\beta, \delta)$ face, and the intersection of the black corners of a $B(\alpha, \beta)$ bigon and $H_B$ . . . . .	44
2.16	A non-exceptional vertex having a $W(\delta, \delta)$ corner (i), a vertex having a $W(\delta, \beta)$ corner of a $W(\beta, \delta)$ face (ii), and an interior vertex (iii). . . . .	45
2.17	The intersection of the white corners of a $W(\alpha, \delta)$ trigon and $H_W$ , and the intersection of $H_B$ and the black corners of a $B(\alpha, \beta)$ bigon and a bad $B(\beta, \delta)$ face. . . . .	47

2.18	Local configurations of an interior vertex (i), (ii), and a non-exceptional vertex having a $B(\beta, \beta)$ corner (iii).	48
2.19	The intersection of $H_W$ and the white corners of a $W(\alpha, \delta)$ trigon and a bad $W(\alpha, \gamma)$ face, and the intersection of the black corners of a $B(\alpha, \beta)$ bigon and $H_B$ .	51
2.20	A non-exceptional vertex having a $W(\alpha, \alpha)$ corner (i), and local configurations of an interior vertex (ii), (iii).	52
2.21	The intersection of the white corners of a $W(\alpha, \delta)$ trigon and $H_W$ , and the intersection of $H_B$ and the black corners of a $B(\alpha, \beta)$ bigon and a bad $B(\beta, \delta)$ face.	53
2.22	Local configurations at an interior vertex (i), (ii), and a non-exceptional vertex having a $B(\beta, \beta)$ corner of a bad $B(\beta, \delta)$ face (iii).	54
2.23	The intersection of the white corners of a $W(\beta, \delta)$ trigon and $H_W$ , and the intersection of the black corners of a $B(\alpha, \beta)$ bigon and $H_B$ .	55
2.24	Local configurations at a boundary vertex.	56
3.1	A black bigon with negative edges and with a $(\epsilon_N, \epsilon'_S)$ corner and a $(\epsilon_S, \epsilon'_N)$ corner.	60
3.2	A vertex of valency 3 in $\overline{G}$ .	62
3.3	A trigon with two negative edges and one positive edge.	64
3.4	The external interval of $f$ .	65
3.5	The external intervals of $f_1$ and $f_2$ .	66
3.6	The link $L_0 = K_1 \cup K'_1 \cup K_2 \cup K'_2$ .	67
3.7	The link $L = K_1 \cup K'_1 \cup K_2 \cup K'_2 \cup K_0$ .	68
3.8	The $r_1$ -framing.	70
4.1	The strong invertibility of $L$ and the quotient of $(S^3, L)$ .	73
4.2	The pentangle $P(\theta', \varphi', 1/2, \omega', *) =$ the tangle $Q(-1/\theta', -1/\varphi', -1/\omega', *)$ .	74
4.3	$W(*) = Q(*, \varphi, \omega, 1/0)$ and the rational tangle fillings.	76
4.4	$W'(*) = Q(\theta, \varphi, *, 1/0)$ and the rational tangle fillings.	77
4.5	$W(*) = Q(*, \varphi, \omega, -1/3)$ and the rational tangle fillings.	78
4.6	$W'(*) = Q(\theta, \varphi, *, -1/3)$ and the rational tangle fillings.	80
4.7	$W(*) = Q(\theta, *, \omega, -1/3)$ and the rational tangle fillings.	81
4.8	$Q(\theta, \varphi, \omega, 1/0)$ .	89

# Chapter 1

## Introduction

### 1.1 Basics of 3-manifolds

#### 1.1.1 3-manifolds

A *3-manifold* is a topological space in which every point has a neighborhood homeomorphic to standard 3-dimensional space  $\mathbb{R}^3$ . We will be concerned with 3-manifolds that are *compact*, that is, for any cover of the manifold by open sets there is a finite subcover. Examples of compact 3-manifolds include the 3-sphere, lens spaces, knot complements, and Seifert fibered spaces. A 3-manifold is *closed* if it is compact and has empty boundary.

A 3-manifold  $M$  is *orientable* if it is possible to give every open set a consistent orientation. Taking a triangulation of  $M$ , this is equivalent to the statement that the vertices of every tetrahedron can be ordered so that the induced orientations on the 2 simplices of each tetrahedron disagree when attached together to form  $M$ . All 3-manifolds that we discuss will be compact and orientable.

#### 1.1.2 Surfaces in 3-manifolds

This subsection is based on the lecture notes of Cameron Gordon at the 2006 Park City Mathematics Institute Graduate Summer School.

Surfaces, or 2-manifolds, have played an important role in our understanding of the topology of 3-manifolds. Examples of surfaces are disks, annuli, spheres or tori. One of the most important types of surfaces are *incompressible* surfaces, which were introduced by Haken in the 1960s.

An *incompressible* surface  $F$  in a 3-manifold  $M$  is a properly embedded surface such that for every embedded disk  $D$  in  $M$  with  $D \cap F = \partial D$ ,  $\partial D$  bounds a disk in  $F$ . A surface  $F$  is essential if it is incompressible and not parallel into  $\partial M$ .

A compact orientable surface  $F$  with nonnegative Euler characteristic is either a sphere, a disk, a torus, or an annulus. These surfaces are called *small*. If a 3-manifold  $M$  contains such an essential surface, then it is said to be *reducible*,  *$\partial$ -reducible*, *toroidal*, or *annular*, respectively. Otherwise,  $M$  is called *irreducible*,  *$\partial$ -irreducible*, *atoroidal*, or *anannular*, respectively.

The importance of small surfaces in the theory of 3-manifolds is well known. For example, every compact orientable 3-manifold can be decomposed into canonical pieces by cutting it up along such surfaces. For spheres, Kneser's Theorem says the following:

**Theorem 1.1.1** (Kneser [24]). *Every oriented 3-manifold can be decomposed along a finite disjoint union of 2-spheres to give a collection of irreducible 3-manifolds  $M_1, M_2, \dots, M_n$ . The  $M_i$ 's are unique up to orientation-preserving homeomorphism and insertion or deletion of copies of  $S^3$ .*

A *Seifert fiber space* is a 3-manifold  $M$  that is a disjoint union of circles

(*fibers*), such that each fiber has a *fibred solid torus* neighborhood, i.e.  $D^2 \times I$  with  $D^2 \times \{0\}$  and  $D^2 \times \{1\}$  identified by a rotation  $\rho$  through  $\frac{2\pi p}{q}$  ( $q \geq 1$ ,  $(p, q) = 1$ ). The *fibers* are the images of the arc  $(0, 0) \times I$  (the central fiber) and the union of the arcs  $x \times I, \rho(x) \times I, \dots, \rho^{q-1}(x) \times I, x \neq (0, 0)$ . We will say that the fibers other than the central fiber are  $(p, q)$ -*curves* in the solid torus. If  $q \geq 2$  the central fiber is an *exceptional fiber of multiplicity*  $q$ . The quotient space of  $M$  obtained by identifying each fiber to a point is a surface, the *base* surface of  $M$ . A *small* Seifert fibered space is a Seifert fibered space with base space the 2-sphere and at most three singular fibers.

For annuli and tori we have the following theorem due to Jaco-Shalen and independently Johannson:

**Theorem 1.1.2** (Jaco-Shalen [21], Johannson [22]). *In an irreducible,  $\partial$ -irreducible 3-manifold  $M$ , there is a collection  $\mathcal{F}$  of disjoint essential annuli and tori such that each component of  $M$  cut along  $\mathcal{F}$  is either a Seifert fibered space, and  $I$ -bundle over a surface, or simple. A minimal such collection is unique up to isotopy.*

We say that  $M$  is a *simple manifold* if it contains no small essential surfaces. Then a simple manifold is expected to have a nice geometric structure.  $M$  is *hyperbolic* if  $M$  with boundary tori removed admits a finite volume hyperbolic structure with totally geodesic boundary. Then the following theorem, which is essentially the Geometrization conjecture, says that this is equivalent to being simple.

**Theorem 1.1.3** (Thurston [38], if  $\partial M \neq \emptyset$ ; Perelman [35], [36], [37], if  $\partial M = \emptyset$ ). *M is simple if and only if either*

1. *M is hyperbolic; or*
2. *M is a small Seifert fibered space; or*
3.  *$M \cong B^3$ .*

## 1.2 Dehn Surgeries

The operation of removing a solid torus from a 3-manifold and then reattaching it in some fashion, known as a *Dehn Surgery*, has become one of the fundamental methods used to represent 3-manifolds. It was introduced by Dehn [3] as a method for constructing "Poincaré spaces", that is non-simply-connected 3-manifolds which possess the same homology as the 3-sphere. The Lickorish-Wallace Theorem shows how important Dehn surgery is to study 3-manifolds.

**Theorem 1.2.1** (Lickorish [31], Wallace [40]). *Any closed, connected orientable 3-manifold can be obtained from the 3-sphere by Dehn surgery on a link in the 3-sphere.*

Let us define Dehn filling on 3-manifolds. Let  $M$  be a compact connected orientable 3-manifold with a torus boundary component  $\partial_0 M$  and  $r$  a *slope*, the isotopy class of an essential unoriented simple closed curve, on  $\partial_0 M$ . The manifold obtained by *r-Dehn filling* is defined to be  $M(r) = M \cup V$ , where

$V$  is a solid torus glued to  $M$  along  $\partial_0 M$  so that  $r$  bounds a disk in  $V$ . For a pair of slopes  $r_1$  and  $r_2$  on  $\partial_0 M$ , the distance  $\Delta(r_1, r_2)$  denotes the minimal geometric intersection number.

We are interested in obtaining restrictions on when a Dehn filling on a hyperbolic manifold fails to be hyperbolic. Such a filling is said to be *exceptional*. The Hyperbolic Dehn Surgery Theorem shows that the set of exceptional Dehn fillings are finite.

**Theorem 1.2.2** (Thurston [39]). *If  $M$  is hyperbolic then  $r$ -Dehn filling  $M(r)$  is hyperbolic for all but finitely many slopes  $r$  on  $\partial_0 M$ .*

The following theorem shows that it is unreasonable to try to describe all exceptional Dehn fillings.

**Theorem 1.2.3** (Myers [33]). *Any 3-manifold  $N$  is of the form  $M(r)$  for some simple 3-manifold  $M$  and some slope  $r$ .*

However, it turns out that it is rare for a hyperbolic 3-manifold to have more than one exceptional filling. So if we define an *exceptional pair*  $(M; r_1, r_2)$  to be a hyperbolic 3-manifold  $M$  with non-hyperbolic fillings  $M(r_1)$  and  $M(r_2)$ ,  $r_1 \neq r_2$ , then maybe we can classify all exceptional pairs.

### 1.3 Some Classifications on Exceptional Pairs

The first stage to classify exceptional pairs  $(M; r_1, r_2)$  is to find the upper bounds for  $\Delta(r_1, r_2)$  (the upper bounds are now proved to be at most 8 by Lackenby and Meyerhoff [25]).

We say that a 3-manifold is of *type*  $S, D, A$  or  $T$  if it contains an essential sphere, disk, annulus or torus. We also say that it is of *type*  $S^H$  or  $T^H$  if it contains a Heegaard sphere or torus.

Thurston's Geometrization conjecture implies that  $M$  is not hyperbolic if and only if  $M$  is one of six types  $S, D, A, T, S^H$  or  $T^H$  or  $M$  is a Seifert fibered space over the sphere with three exceptional fibers.

Here we shall focus on the first six types. In other words, consider a hyperbolic 3-manifold  $M$  which admits two exceptional Dehn fillings  $M(r_1)$  and  $M(r_2)$  with  $M(r_1), M(r_2) \in \{S, D, A, T, S^H, T^H\}$ .

Then upper bounds for  $\Delta(r_1, r_2)$  have been established in almost all cases, and are summarized in Table 1.1 (The entries marked - obviously do not occur.).

Table 1.1: Upper bounds for distances.

	$S$	$D$	$A$	$T$	$S^H$	$T^H$
$S$	1	0	2	3	?	1
$D$		1	2	2	-	-
$A$			5	5	-	-
$T$				8	2	?
$S^H$					0	1
$T^H$						1

For references for the entries in Table 1.1, see [9].

Some classifications of hyperbolic manifolds realizing the upper bounds in Table 1.1 are made by several people as follows.  $(S, A)$  and  $(D, T)$ : Lee

[27] and [26] respectively;  $(A, A)$  and  $(A, T)$ : Gordon and Wu [18] and [17] respectively;  $(T, T)$ : Gordon;  $(T, S^H)$ : Gordon and Luecke [12].

There are more classifications for some distances less than the maximal distance.  $(T, T)$  at distances 6 and 7: Gordon [6];  $(A, A)$  at distance 4,  $(A, T)$  at distance 5, and  $(T, T)$  at distances 4 and 5: Gordon and Wu [18], [17], and [19] respectively.

The method used in the classification theorems is based on the combinatorial and topological theory of intersection graphs which is originated in the work of Litherland [32] and was later developed into a powerful tool in a series of papers by Gordon and Luecke (see, e.g., [2], [12], [13]). An excellent introduction to this subject may be found in [7].

This dissertation establishes the classification of the case of  $(S, T)$  at distance 3.

## 1.4 Main Result

Consider a hyperbolic manifold  $M$  and slopes  $r_1$  and  $r_2$  such that the  $r_1$ -Dehn filling  $M(r_1)$  is reducible and the  $r_2$ -Dehn filling  $M(r_2)$  is toroidal. Then the least upper bound for  $\Delta(r_1, r_2)$  is known to be 3 by Oh [34] and independently Wu [42].

The first example of such a manifold with  $\Delta(r_1, r_2) = 3$  was given by Boyer and Zhang [1] in 1996. They constructed the manifold  $M = W(6)$ , where  $W(6)$  is the manifold obtained by Dehn filling with slope 6 under the

standard meridian-longitude coordinates on one boundary component of the exterior of the Whitehead link  $W$  in  $S^3$ . Then  $M(1)$  is reducible and  $M(4)$  is toroidal and  $\Delta(1, 4) = 3$ . In 1999, Eudave-Muñoz and Wu [4] explicitly described an infinite family of manifolds  $M$  realizing  $\Delta(r_1, r_2) = 3$  by means of tangle arguments. More specifically,  $M$  is the double branched cover of one of the tangles illustrated in Figure 1.1 where  $p$  is an integer no less than 3. However,  $p$  can be extended to any integer no less than 2. When  $p = 2$ , then the double branched cover of the tangle corresponds to  $W(6)$ .

The main result of this dissertation is to show that the manifolds  $M$  described above are the only examples of simple manifolds admitting a reducible Dehn filling and a toroidal Dehn filling with distance 3.

**Theorem 1.4.1.** *Let  $M$  be a simple 3-manifold with a torus boundary component  $\partial_0 M$  such that  $M(r_1)$  is reducible,  $M(r_2)$  is toroidal and  $\Delta(r_1, r_2) = 3$ . Then  $M$  is the double branched cover of one of the tangles with  $p \geq 2$  as described in Figure 1.1 (i).  $M(r_1)$ , corresponding to the  $1/3$ -rational tangle filling, is a connected sum of two lens spaces  $L(3, 1)$  and  $L(2, 1)$ , and  $M(r_2)$ , corresponding to the  $1/0$ -rational tangle filling, is toroidal and is not Seifert fibered. See Figure 1.1 (ii), (iii).*

In order to prove Theorem 1.4.1, we need the following.

**Theorem 1.4.2.** *Let  $M$  be a simple 3-manifold as in Theorem 1.4.1. Then  $M(r_2)$  is the union of  $M_1$  and  $M_2$ , where  $M_i$ ,  $i = 1, 2$ , is a Seifert fibered space*



1/3- and 1/0-rational tangles filled respectively. Notice that the toroidal Dehn filling  $M(4)$  is the union of  $M_1$  and  $M_2$ , where  $M_i$ ,  $i = 1, 2$ , is a Seifert fibered space over a disk with two exceptional fibers, along an incompressible torus and the fibers of  $M_1$  and  $M_2$  intersect exactly once on the incompressible torus i.e.  $M(4)$  is not Seifert fibered. We have thus shown that if  $M(r_2)$  contains a Klein bottle, then Theorem 1.4.1 and Theorem 1.4.2 hold.

Therefore, throughout this paper we may assume that  $M(r_2)$  does not contain a Klein bottle. Also, we may assume that  $M(r_2)$  is irreducible by [14] and  $M(r_1)$  is not homeomorphic to  $S^2 \times S^1$  by [29]. Then Theorem 1.4.1 and Theorem 1.4.2 follow immediately from Theorem 4.1.1 and Theorem 3.1.4 respectively.

As an immediate consequence of Theorem 1.4.2, we have the following.

**Corollary 1.4.3.** *Let  $M$  be a simple manifold with a torus boundary component. If  $M(r_1)$  is reducible and  $M(r_2)$  is a toroidal Seifert fibered manifold, then  $\Delta(r_1, r_2) \leq 2$ .*

It is unknown whether or not the upper bound 2 in Corollary 1.4.3 is the best possible.

The above results have been published in [23]

## Chapter 2

### Intersection Graphs on Surfaces

#### 2.1 Introduction

From now on we assume that  $M$  is a simple 3-manifold with a torus boundary component  $\partial_0 M$  and that  $r_1$  and  $r_2$  are slopes on  $\partial_0 M$  such that  $M(r_1)$  is reducible and  $M(r_2)$  contains an essential torus and  $\Delta(r_1, r_2) = 3$ .

Over all reducing spheres in  $M(r_1)$  which intersect the attached solid torus  $V_1$  in a family of meridian disks, we choose a 2-sphere  $\widehat{F}_1$  so that  $F_1 = \widehat{F}_1 \cap M$  has the minimal number, say  $n_1$ , of boundary components. Similarly let  $\widehat{F}_2$  be an essential torus in  $M(r_2)$  which intersects the attached solid torus  $V_2$  in a family of meridian disks, the number of which, say  $n_2$ , is minimal over all such surfaces and let  $F_2 = \widehat{F}_2 \cap M$ . Let  $u_1, u_2, \dots, u_{n_1}$  be the disks of  $\widehat{F}_1 \cap V_1$ , labeled as they appear along  $V_1$ . Similarly let  $v_1, v_2, \dots, v_{n_2}$  be the disks of  $\widehat{F}_2 \cap V_2$ . Then  $F_1$  is an essential planar surface, and  $F_2$  is an essential punctured torus in  $M$ . We may assume that  $F_1$  and  $F_2$  intersect transversely and the number of components of  $F_1 \cap F_2$  is minimal over all such surfaces. Then no circle component of  $F_1 \cap F_2$  bounds a disk in either  $F_1$  or  $F_2$  and no arc component is boundary-parallel in either  $F_1$  or  $F_2$ . In this section, the subscripts  $i$  and  $j$  will denote 1 or 2 with the convention that if they both

appear, then  $\{i, j\} = \{1, 2\}$ . The components of  $\partial F_i$  are numbered  $1, 2, \dots, n_i$  according to the labels of the corresponding disks of  $\widehat{F}_i \cap V_i$ . We obtain a graph  $G_i$  in  $\widehat{F}_i$  by taking as the (fat) vertices of  $G_i$  the disks in  $\widehat{F}_i \cap V_i$  and as the edges of  $G_i$  the arc components of  $F_1 \cap F_2$  in  $F_i$ . Each endpoint of an edge of  $G_i$  has a label, that is, the label of the corresponding component of  $\partial F_j$ ,  $i \neq j$ . Since each component of  $\partial F_i$  intersects each component of  $\partial F_j$  in  $\Delta$  points, the labels  $1, 2, \dots, n_j$  appear in order around each vertex of  $G_i$  repeatedly  $\Delta$  times.

For a graph  $G$ , the *reduced graph*  $\overline{G}$  of  $G$  is defined to be the graph obtained from  $G$  by amalgamating each family of mutually parallel edges into a single edge. For an edge  $\alpha$  of  $\overline{G}$ , the *weight* of  $\alpha$ , denoted by  $w(\alpha)$ , is the number of edges of  $G$  in  $\alpha$ .

Orient all components of  $\partial F_i$  so that they are mutually homologous on  $\partial_0 M$ ,  $i = 1, 2$ . Let  $e$  be an edge in  $G_i$ . Since  $e$  is a properly embedded arc in  $F_i$ , it has a disk neighborhood  $D$  in  $F_i$  with  $\partial D = a \cup b \cup c \cup d$ , where  $a$  and  $c$  are arcs in  $\partial F_i$  with induced orientation from  $\partial F_i$ . On  $D$ , if  $\partial D$  can be oriented so that  $a$  and  $c$  have the same orientation as that induced from  $\partial F_i$ , then  $e$  is called *positive*, otherwise *negative*. See Figure 2.1. Then we have the parity rule:

*An edge is positive on one graph if and only if it is negative on the other graph.*

Orient the core of  $V_i$ . Then we can give a sign to each vertex of  $G_i$

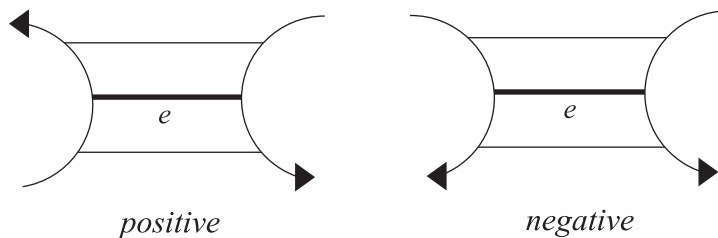


Figure 2.1: Orientations on an edge.

according to the sign of its intersection with the core of  $V_i$ . Two vertices (possibly equal) of  $G_i$  are called *parallel* if they have the same sign, otherwise *antiparallel*. A positive edge connects parallel vertices while a negative one connects antiparallel vertices. Let  $G_i^+$  denote the subgraph of  $G_i$  consisting of all the vertices and all the positive edges of  $G_i$ .

Let  $G$  be  $G_1$  or  $G_2$  and let  $x$  be a label of  $G$ . An  $x$ -edge is an edge of  $G$  with the label  $x$  at one endpoint. An  $x$ -cycle is a cycle of positive  $x$ -edges which can be oriented so that the tail of each edge has the label  $x$ . A cycle in  $G$  is a *Scharlemann cycle* if it bounds a disk face, and the edges in the cycle are all positive and have the same label pair. If the label pair is  $\{x, y\}$ , then we refer to such a Scharlemann cycle as an  $(x, y)$ -Scharlemann cycle.

## 2.2 Binary Faces and the Subgraph $\Lambda$ of $G_1^+$

In this section, we analyze the graphs  $G_1$  and  $G_2$  defined in section 2.1 and find the subgraph  $\Lambda$  of  $G_1$  which is easier to analyze.

### 2.2.1 Terminology and Lemmas

In this subsection, we will define binary faces in  $G_1^+$  and see some properties of binary faces. Since the arguments here are exactly the same as in [16] and in [28], we use the terminologies and several lemmas without proof described in [16] and in [28].

**Lemma 2.2.1.** *If  $G_i$  has a Scharlemann cycle, then  $\widehat{F}_j$  is separating.*

*Proof.* This follows from [42, Lemma 1.2]. □

**Lemma 2.2.2.**  *$G_2$  has exactly two vertices and the two vertices of  $G_2$  are antiparallel.*

*Proof.* By Theorem 1.3 in [30],  $G_2$  has exactly two vertices  $v_1$  and  $v_2$ . Assume that  $v_1$  and  $v_2$  are parallel. Then all the edges of  $G_2$  are positive. Since  $M$  is simple,  $n_1 \geq 3$ . Thus by Lemma 1.5 in [42] we can take a label  $x$  which is not a label of a Scharlemann cycle in  $G_2$ . Consider the subgraph  $\Gamma$  of  $G_2$  consisting of all vertices and all  $x$ -edges of  $G_2$ . Let  $V, E$  and  $F$  be the numbers of vertices, edges and disk faces of  $\Gamma$ , respectively. Since  $V < E$ , we have  $0 = \chi(\widehat{F}_2) \leq V - E + F < F$ , so  $\Gamma$  contains a disk face, which is an  $x$ -face in  $G_2$ . This contradicts [30, Theorem 4.4]. □

We assume without loss of generality that the ordering of the labels around  $v_1$  is anticlockwise while the ordering around  $v_2$  is clockwise. Since the two vertices of  $G_2$  are antiparallel, an Euler characteristic argument on

$G_1^+$  shows that there is a disk face in  $G_1^+$ , which is a  $(1, 2)$ -Scharlemann cycle. Then  $\widehat{F}_2$  is separating in  $M(r_2)$  by Lemma 2.2.1. We will call one side of  $\widehat{F}_2$  in  $M(r_2)$  the  $W$ (hite) side, denoted by  $\widehat{M}_W$  and the other the  $B$ (lack) side, denoted by  $\widehat{M}_B$ . Then  $F_2$  has a  $W$  side and a  $B$  side in  $M$ , which are denoted by  $M_W, M_B$  respectively. The faces of  $G_1$  are called  $W$  and  $B$  according to which side of  $F_2$  a neighborhood of their boundary lies.

$G_2$  has at most 6 *edge classes*, the isotopy classes in  $\widehat{F}_2$  relative to the fat vertices of  $G_2$  by [6, Lemma 5.2]. We label these edge classes  $\alpha, \beta, \gamma, \delta, \epsilon, \epsilon'$  as in Figure 2.2. An edge in  $G_1$  or  $G_2$  is called an  $\eta$ -*edge* if, being regarded as an edge in  $G_2$ , it lies in class  $\eta, \eta \in \{\alpha, \beta, \gamma, \delta, \epsilon, \epsilon'\}$ . The  $\epsilon$ -edges and  $\epsilon'$ -edges are positive in  $G_2$  while the others are negative by Lemma 2.2.2. Since  $v_1$  and  $v_2$  have the same valency,  $w(\epsilon) = w(\epsilon')$ . In Figure 2.2, an  $\epsilon$ -edge has two endpoints on  $\partial v_1$ . If the endpoint lies between the edge class  $\beta$  and the edge class  $\gamma$ , we say that the endpoint lies in class  $\epsilon_N$ , otherwise  $\epsilon_S$ . If the endpoint of an  $\epsilon'$ -edge lies between the edge class  $\alpha$  and the edge class  $\delta$  on  $\partial v_2$ , we say that the endpoint lies in class  $\epsilon'_N$ , otherwise  $\epsilon'_S$ .

Let  $\lambda, \mu$  be two elements of  $\{\alpha, \beta, \gamma, \delta\}$ . Then a  $(\lambda, \mu)$  *face* of  $G_1$  is one whose edges lie in classes  $\lambda, \mu$  on  $G_2$ . Lemma 3.1 of [12] shows that any such face must have edges in both classes  $\lambda$  and  $\mu$ . We call any such face a *binary face* of  $G_1$ .

A  $(\lambda, \mu)$  face  $f$  is  $\lambda$ -*good* if no two consecutive edges in the boundary of  $f$  belong to class  $\lambda$ . A  $(\lambda, \mu)$  face is *good* if it is either  $\lambda$ -good or  $\mu$ -good. A *bad* face is a binary face that is not good. To indicate the coloring of an  $(\lambda, \mu)$

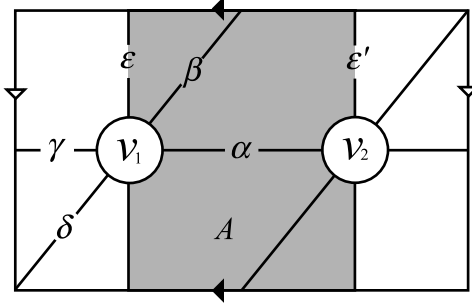


Figure 2.2: 6 edge classes on  $\widehat{F}_2$ .

face we will often call it an  $X(\lambda, \mu)$  face where  $X$  is to take the value  $B$  or  $W$ .

If  $c$  is an  $X$  corner of  $G_1$  for which the edge incident to label 1 is in class  $\lambda$  and the edge incident to label 2 is in class  $\mu$ , we call  $c$  an  $X(\lambda, \mu)$  corner, where  $X \in \{B, W\}$ . Then notice that a bad  $X(\lambda, \mu)$  face of  $G_1$  must contain  $X(\lambda, \lambda)$ ,  $X(\lambda, \mu)$ ,  $X(\mu, \lambda)$  and  $X(\mu, \mu)$  corners. For negative edges, there are four different types of corners i.e.  $X(\epsilon_N, \epsilon'_N)$ ,  $X(\epsilon_N, \epsilon'_S)$ ,  $X(\epsilon_S, \epsilon'_N)$  and  $X(\epsilon_S, \epsilon'_S)$  corners.

Then we have the theorem which gives topological information from combinatorial information.

**Theorem 2.2.3.** *Assume that  $G_1$  contains a good  $X(\lambda, \mu)$  face of length  $n$ . Then the  $X$  side of  $\widehat{F}_2$  in  $M(r_2)$  is a Seifert fibered space over the disk with exactly two exceptional fibers, one of which has order  $n$ . Moreover the Seifert*

fiber of this fibration is the curve on  $\widehat{F}_2$  formed by  $\lambda \cup \mu$ .

*Proof.* This is exactly Theorem 4.1 in [16]. □

*Remark:* In the proof of Theorem 4.1 of [16], we can isotope the annulus which separates the  $X$  side into two solid tori, so that the intersection of the core of  $V_2$  and the  $X$  side lies on the annulus.

The following lemmas are shown in Section 3 of [16].

**Lemma 2.2.4.** *Let  $c_1, c_2, \dots, c_n$  be a collection of  $X$  corners of  $G_1$ ,  $X \in \{B, W\}$ . The anticlockwise ordering of the endpoints of the edges of these corners on vertex  $v_1$  of  $G_2$  is the same as the clockwise ordering of the edge endpoints on vertex  $v_2$  of  $G_2$ .*

**Lemma 2.2.5.**  *$G_1$  cannot contain a vertex  $v$  with two edges in the same edge class incident to  $v$  at the same label.*

**Lemma 2.2.6.** *Given  $X \in \{B, W\}$ ,  $G_1$  does not contain  $X(\lambda, \lambda)$  corners for three distinct edge classes  $\lambda$ .*

**Lemma 2.2.7.** *If  $G_1$  contains a good  $X(\lambda, \mu)$  face, then any binary  $X$ -face of  $G_1$  on an edge class pair distinct but not disjoint from  $\{\lambda, \mu\}$  is bad.*

To make it easier to analyze graphs, we need to find a subgraph which has good properties. However, [28, Proposition 4.3] guarantees the existence of such a subgraph. That is,  $G_1^+$  contains a connected subgraph  $\Lambda$  satisfying the following properties;

- (1) for all vertices  $u_x$  of  $\Lambda$  but at most one (an exceptional vertex), there are an edge with edge class  $\alpha$  or  $\beta$ , and an edge with edge class  $\gamma$  or  $\delta$  in  $\Lambda$  which are incident to  $u_x$  with label  $i$  for each  $i = 1, 2$ ;
- (2) for the exceptional vertex  $u_{x_0}$ , if it exists, there are at least two edges in  $\Lambda$  incident to  $u_{x_0}$ ;
- (3) there is a disk  $D_\Lambda \subset \widehat{F}_1$  such that  $\text{Int}D_\Lambda \cap G_1^+ = \Lambda$ ; and
- (4)  $\Lambda$  has no cut vertex.

A vertex of  $\Lambda$  is a *boundary vertex* if there is an arc connecting it to  $\partial D_\Lambda$  whose interior is disjoint from  $\Lambda$ , and an *interior vertex* otherwise. Similarly for a *boundary edge* and an *interior edge* of  $\Lambda$ .

**Lemma 2.2.8.**  *$\Lambda$  contains a bigon.*

*Proof.* This follows from the proof of [28, Lemma 4.8]. □

**Lemma 2.2.9.**  *$\Lambda$  contains a face bounded only by  $\alpha$ - or  $\beta$ -edges, or only by  $\gamma$ - or  $\delta$ -edges. In other words,  $\Lambda$  contains a  $X(\lambda, \mu)$  face where  $\{\lambda, \mu\} = \{\alpha, \beta\}$  or  $\{\gamma, \delta\}$  and  $X \in \{B, W\}$ .*

*Proof.* This follows from [28, Lemma 4.6]. □

## 2.2.2 Existence of a White Bigon

By Lemma 2.2.9, from now on, throughout this paper we may assume without loss of generality that  $\Lambda$  contains a  $B(\alpha, \beta)$  face. Then we show that there is a white bigon in  $\Lambda$ .

Let  $\widehat{H}_B$  (resp.  $\widehat{H}_W$ ) be the intersection of  $V_2$  and  $\widehat{M}_B$  (resp.  $\widehat{M}_W$ ). Let  $H_B$  (resp.  $H_W$ ) be the intersection of  $V_2$  and  $M_B$  (resp.  $M_W$ ). Then  $V_2 = \widehat{H}_B \cup \widehat{H}_W$  and  $\partial V_2 = H_B \cup H_W$ . For the purpose of sections 2.3 and 2.4 there are two equivalent figures of  $H_B$  or  $H_W$  as in Figure 2.3 where corners of faces in  $G_1$  appear. Figure 2.3 (ii) is obtained by cutting  $H_B$  or  $H_W$  along the arc  $a$  in Figure 2.3 (i) such that one endpoint of  $a$  lies between the edge class  $\alpha$  and the edge class  $\epsilon_S$  at  $\partial v_1$  and the other lies between the edge class  $\alpha$  and the edge class  $\beta$  at  $\partial v_2$ .

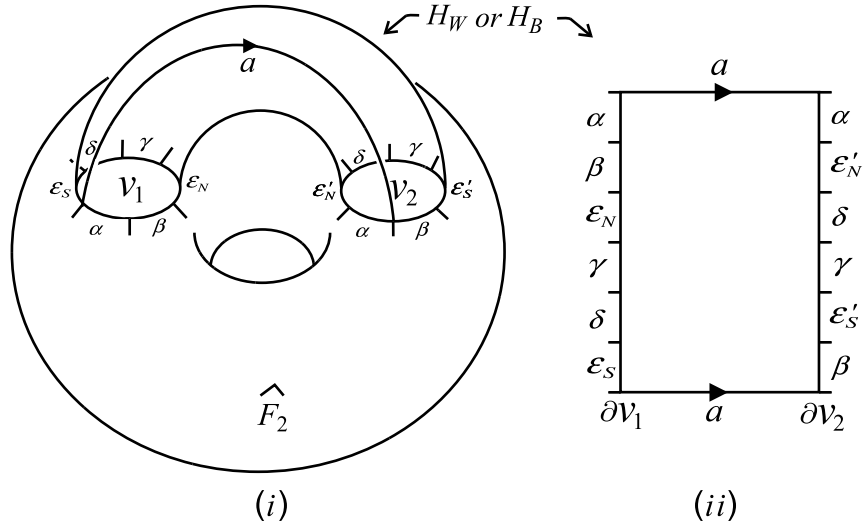


Figure 2.3: Two equivalent figures of  $H_W$  or  $H_B$ .

**Lemma 2.2.10.** *A  $B(\alpha, \beta)$  face is good.*

*Proof.* Suppose a  $B(\alpha, \beta)$  face is bad. Then it contains  $B(\alpha, \alpha)$ ,  $B(\alpha, \beta)$ ,  $B(\beta, \alpha)$ ,  $B(\beta, \beta)$  corners. These corners lie on  $H_B$  as in Figure 2.4. There are two cases. First, we assume Figure 2.4 (i). Figure 2.4 (ii) is similar. It follows from Figure 2.4 (i) that  $\omega(\epsilon') + \omega(\delta) + \omega(\gamma) + \omega(\epsilon') \leq \omega(\beta)$ . On the other hand,  $\omega(\alpha) + \omega(\epsilon') + \omega(\delta) + \omega(\gamma) + \omega(\epsilon') + \omega(\beta) = 3n_1$  since the number of all the labels around a vertex in  $G_2$  is  $3n_1$ . Therefore, combining this equation with the above inequality, we get the inequality  $\omega(\alpha) + 2\omega(\beta) \geq 3n_1$ . This implies that either  $\omega(\alpha) \geq n_1$  or  $\omega(\beta) \geq n_1$ , which contradicts [42, Lemma 1.5].  $\square$

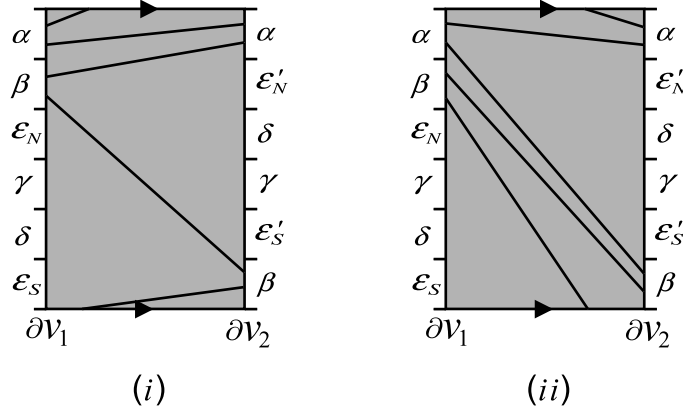


Figure 2.4: The intersection of  $H_B$  and the corners of a  $B(\alpha, \beta)$  face.

**Lemma 2.2.11.** *The black side  $\widehat{M}_B$  of  $M(r_2)$  is a Seifert fibered space over the disk with exactly two exceptional fibers. Moreover the Seifert fiber of this fibration is the curve on  $\widehat{F}_2$  formed by  $\alpha \cup \beta$ .*

*Proof.* Since  $\Lambda$  contains a  $B(\alpha, \beta)$  face, this follows immediately from Theorem 2.2.3 and Lemma 2.2.10.  $\square$

Before proving the next lemma, we observe that the edge classes of the three edges of a trigon in  $\Lambda$  cannot be all distinct by Lemma 2.2.4 and cannot be all same by Lemma 3.1 of [12].

**Lemma 2.2.12.** *If  $\Lambda$  contains a white bigon or a white trigon, the two edge classes of the edges of a white bigon or a white trigon are  $\lambda$  and  $\mu$  where  $\{\lambda, \mu\} = \{\alpha, \delta\}, \{\alpha, \gamma\}, \{\beta, \delta\}$  or  $\{\beta, \gamma\}$ .*

*Proof.* Let  $f$  be a white bigon in  $\Lambda$ .  $f$  is necessarily a good  $W(\lambda, \mu)$  face. Suppose  $\{\lambda, \mu\} = \{\alpha, \beta\}$  or  $\{\gamma, \delta\}$ . By Theorem 2.2.3 the white side  $\widehat{M}_W$  is a Seifert fibered space over the disk with exactly two exceptional fibers and the Seifert fiber of this fibration is the curve on  $\widehat{F}_2$  formed by  $\lambda \cup \mu$ . In other words,  $\widehat{M}_W = M_1 \cup_A M_2$  where  $M_1$  and  $M_2$  are solid tori and  $A$  is a properly embedded annulus in  $\widehat{M}_W$ , and the core of  $A$  is the fiber. On the other hand, the black side  $\widehat{M}_B = M_3 \cup_{A'} M_4$  where  $M_3$  and  $M_4$  are solid tori and the core of  $A'$  is the fiber. By the remark below Theorem 2.2.3, we may assume that the core of  $V_2$  lies on  $A \cup A'$ . Furthermore since two fibers of  $\widehat{M}_B$  and  $\widehat{M}_W$  coincide on  $\widehat{F}_2$ , we can isotope  $A$  and  $A'$  on  $\widehat{F}_2$  fixing the core of  $V_2$  so that  $A \cup A'$  is a torus  $\widehat{T}$ , say. Note that either side of  $\widehat{T}$  is a Seifert fibered space over the disk with two exceptional fibers, which implies that  $\widehat{T}$  is essential in  $M(r_2)$ . Pushing the core of  $V_2$  off  $\widehat{T}$ , we get an essential torus in  $M(r_2)$  which

misses the core of  $V_2$ , which is a contradiction to the choice of  $\widehat{F}_2$ . Therefore  $\{\lambda, \mu\} = \{\alpha, \delta\}, \{\alpha, \gamma\}, \{\beta, \delta\}$  or  $\{\beta, \gamma\}$ .

Let  $g$  be a white trigon in  $\Lambda$ . Hence  $g$  is also necessarily a good  $W(\lambda, \mu)$  face. The argument is now exactly same as in the case of a bigon above.  $\square$

**Lemma 2.2.13.** *Any two black bigons in  $G_1^+$  have the same pair of edge classes. Furthermore the pair is either  $\{\alpha, \beta\}$  or  $\{\gamma, \delta\}$ .*

*Proof.* The first statement follows from [15, Lemma 5.2] since  $M(r_2)$  does not contain a Klein bottle. The second follows from Lemma 2.2.7 since  $G_1^+$  contains a  $B(\alpha, \beta)$  face which is good by Lemma 2.2.10 and every bigon is a good face.  $\square$

The next theorem is the main result of the combinatorial arguments in this paper. To prove this, we use Lemma 2.2.16 and the main theorems in sections 2.3 and 2.4.

**Theorem 2.2.14.**  $\Lambda$  contains a  $W(\lambda, \mu)$  bigon, where  $\{\lambda, \mu\} = \{\alpha, \delta\}, \{\alpha, \gamma\}, \{\beta, \delta\}$  or  $\{\beta, \gamma\}$ .

*Proof.* Lemma 2.2.8 says that  $\Lambda$  contains a bigon  $f$ . If  $f$  is white, then we are done by Lemma 2.2.12.

Suppose  $\Lambda$  does not contain a white bigon. Then  $f$  is black. By Lemma 2.2.13, we may assume that  $f$  is a  $B(\alpha, \beta)$  bigon. Lemma 2.2.16 says that  $\Lambda$  contains a trigon. On the other hand, Theorems 2.3.1 and 2.4.1 imply that  $\Lambda$

does not contain a trigon. This contradiction shows that  $\Lambda$  contains a white bigon as desired.  $\square$

To prove Lemma 2.2.16, Theorems 2.3.1 and 2.4.1, we assume that  $\Lambda$  contains a  $B(\alpha, \beta)$  bigon and does not contain a white bigon.

Lemma 2.2.13 enables us to apply Lemmas 4.10 and 4.11 of [28] without change.

**Lemma 2.2.15.** *All interior vertices of  $\Lambda$  have valency at least 4 in  $\bar{\Lambda}$  and all boundary vertices of  $\Lambda$  but the exceptional vertex have valency at least 3 in  $\bar{\Lambda}$ .*

*Proof.* This is Lemma 4.10 of [28].  $\square$

**Lemma 2.2.16.**  *$\Lambda$  contains a trigon.*

*Proof.* This is Lemma 4.11 of [28].  $\square$

**Lemma 2.2.17.**  *$\Lambda$  contains an interior vertex.*

*Proof.* Suppose that  $\Lambda$  has no interior vertices. Lemma 2.2.15 guarantees that the number of vertices of  $\Lambda$  is greater than 3. Put  $\Lambda$  on an abstract disk  $D$  so that  $\Lambda$  lies in the interior of  $D$  and insert an edge connecting each vertex of  $\Lambda$  to  $\partial D$ . By taking the reduced graph of the resulting graph, we obtain a graph  $\Gamma$  satisfying the supposition of [2, Lemma 2.6.5]. In addition, since the number of vertices of  $\Gamma$  is greater than 3,  $\Gamma$  must satisfy (\*) in the proof of [2, Lemma 2.6.5]. In other words,  $\Gamma$  contains two vertices of valency at most

3. However this is impossible since all vertices of  $\Gamma$ , possibly except one, have valency at least 4 by Lemma 2.2.15.  $\square$

In section 2.3, we will show that  $\Lambda$  does not contain a black trigon and in section 2.4, we will show that  $\Lambda$  does not contain a white trigon.

### 2.3 A $B(\alpha, \beta)$ Bigon and a Black Trigon

Throughout this section, we assume that  $\Lambda$  contains a  $B(\alpha, \beta)$  bigon and does not contain a white bigon. Our goal in this section is to show the following.

**Theorem 2.3.1.** *If  $\Lambda$  contains a  $B(\alpha, \beta)$  bigon and does not contain a white bigon, then  $\Lambda$  does not contain a black trigon.*

The main idea is to define two dual graphs of  $\Lambda$  and use the fact that there is no triple of non-isomorphic disk faces in  $\Lambda$  and apply the index equation  $\sum_{\text{vertices}} I(v) + \sum_{\text{faces}} I(f) = 2$  of [5].

To prove Theorem 2.3.1, we suppose throughout this section that  $\Lambda$  contains a black trigon.

#### 2.3.1 Isomorphic Disk Faces and Dual Graph of $G^+$

We start this subsection with this lemma.

**Lemma 2.3.2.** *All black trigons of  $G_1^+$  have the same edge classes, i.e. two  $\gamma$ -edges and one  $\delta$ -edge, say.*

*Proof.* Let  $g$  be a black trigon of  $G_1^+$ . Lemma 2.2.4 excludes the case that the three edges of  $g$  have distinct edge classes. Thus  $g$  has two  $\lambda$ -edges and one  $\mu$ -edge. Since  $g$  is a good  $B(\lambda, \mu)$  face, we have the Seifert fibration of the black side  $\widehat{M}_B$  resulting from  $g$  whose fiber is represented by  $\{\lambda, \mu\}$ . Since  $M(r_2)$  does not contain a Klein bottle, by the uniqueness of the Seifert fibration,  $\{\lambda, \mu\} = \{\alpha, \beta\}$  or  $\{\gamma, \delta\}$  by Lemma 2.2.11.

Since  $\Lambda$  contains a  $B(\alpha, \beta)$  bigon, there are two corners, a  $B(\alpha, \beta)$  corner and a  $B(\beta, \alpha)$  corner. Then Lemma 2.2.4 eliminates the case that  $\{\lambda, \mu\} = \{\alpha, \beta\}$ . However Lemma 2.2.4 also excludes the case that  $\Lambda$  contains simultaneously two trigons with two  $\gamma$ -edges and one  $\delta$ -edge, and two  $\delta$ -edges and one  $\gamma$ -edge respectively. Hence we may assume that all trigons of  $G_1^+$  have the same edge classes, i.e. without loss of generality two  $\gamma$ -edges and one  $\delta$ -edge.  $\square$

**Lemma 2.3.3.**  $\Lambda$  cannot contain a  $B(\lambda, \mu)$  corner, where  $(\lambda, \mu) = (\alpha, \delta), (\beta, \gamma), (\gamma, \beta), (\delta, \alpha),$  or  $(\delta, \delta)$ .

*Proof.*  $\Lambda$  contains a black bigon  $f_1$  with one  $\alpha$ -edge and one  $\beta$ -edge, and contains a black trigon  $f_2$  with two  $\gamma$ -edges and one  $\delta$ -edge. Consider the intersection of all the corners of  $f_1$  and  $f_2$ , and  $H_B$ . See Figure 2.5. Then the above black corners are impossible.  $\square$

Since  $\Lambda$  contains a black face and a white face simultaneously by Lemma 2.2.15,  $M_B$  and  $M_W$  are handlebodies of genus 2 from [12, Lemma 8.3].

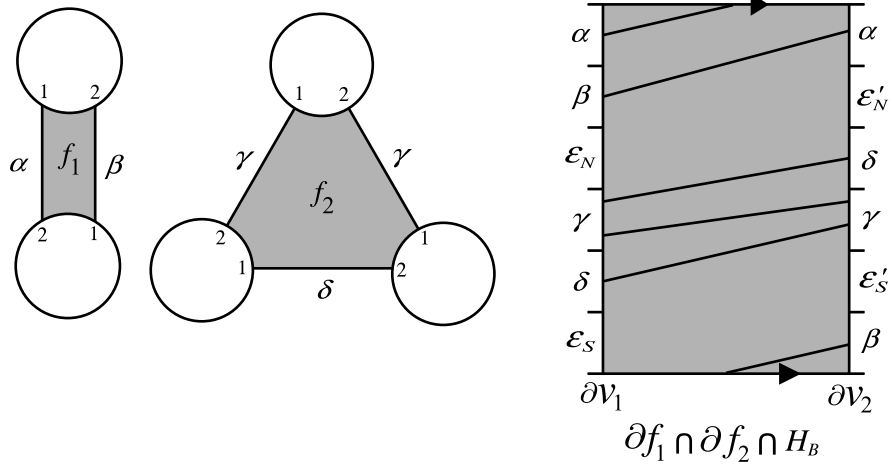


Figure 2.5: A  $B(\alpha, \beta)$  bigon, a  $B(\gamma, \delta)$  trigon and the intersection on  $H_B$ .

Traveling around the boundary of a disk face of  $G_1^+$  gives rise to a cyclic sequence of edge classes. We shall say that two disk faces of  $G_1^+$  of the same color are *isomorphic* if the cyclic sequences obtained by traveling in some directions are equal. See [15, Section 5].

Recall that  $H_B = V_2 \cap M_B$  and  $H_W = V_2 \cap M_W$ . Then  $\partial M_B = H_B \cup F_2$  and  $\partial M_W = H_W \cup F_2$ . Since all the vertices of  $\Lambda$  are parallel, each face of  $\Lambda$  is a non-separating disk in  $M_B$  or  $M_W$ . Note that any two faces of the same color in  $\Lambda$  are disjoint.

**Lemma 2.3.4.** *If two disk faces of  $G_1^+$  are parallel in  $M_B$  or  $M_W$ , then they are isomorphic.*

*Proof.* This is Lemma 4.13 of [28]. □

**Theorem 2.3.5.** *There is no triple of mutually non-isomorphic black disk faces in  $G_1^+$ , and there is no triple of mutually non-isomorphic white disk faces in  $G_1^+$ .*

To prove this theorem, we will show that there is a white binary disk face by using dual graphs of  $\Lambda$ .

For the purpose of the proof of Theorem 2.3.5, we assume for the time being that  $G_1 = G_1^+$ . Then every vertex of  $\Lambda$  except an exceptional vertex has valency 6 since all edges of  $G_1$  are positive.

Now we define a dual graph  $\Lambda^*$  to  $\Lambda$  as in [16, Section 3]. To do this, it is convenient to regard  $\Lambda$  as a graph in  $S^2$ , rather than a disk. In other words, we add an additional *outside face* to the set of faces of  $\Lambda$ . Then a *vertex* of  $\Lambda^*$  is a point in the interior of each face of  $\Lambda$  and a point of the outside face. An *edge* of  $\Lambda^*$  is the edge connecting the vertices of  $\Lambda^*$  corresponding to the faces of  $\Lambda$  on either side of each edge of  $\Lambda$ , and meeting each edge transversely in a single point.

We give two orientations  $\omega$  and  $\omega'$  to the edges of  $\Lambda^*$  as follows;

$\omega$  : *an edge of  $\Lambda^*$  dual to an edge of  $\Lambda$  in an edge class  $\in \{\alpha, \delta\}$  (resp.  $\{\beta, \gamma\}$ ) is oriented from the W-side to the B-side (resp. from the B-side to the W-side).*

$\omega'$  : an edge of  $\Lambda^*$  dual to an edge of  $\Lambda$  in an edge class  $\in \{\beta, \delta\}$  (resp.  $\{\alpha, \gamma\}$ )  
 is oriented from the  $W$ -side to the  $B$ -side (resp. from the  $B$ -side to the  
 $W$ -side).

See Figure 2.6.

*Note.* For an edge  $e$  of  $\Lambda$  in the boundary of the outside face, we regard the side of  $e$  contained in the outside face as being locally colored with the color opposite to that of the face of  $\Lambda$  that contains  $e$ .

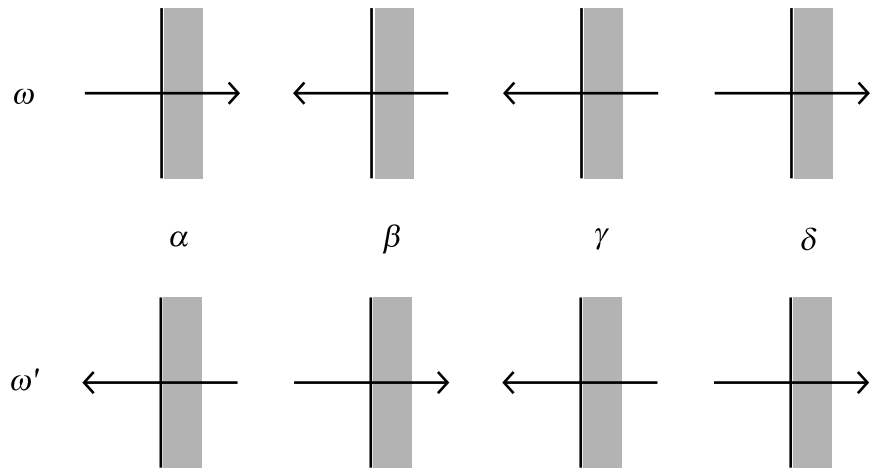


Figure 2.6: Two orientations  $\omega$  and  $\omega'$  to the edges of  $\Lambda^*$ .

As defined in [11], the *index* of a vertex  $v$  and a face  $f$  of a graph in  $S^2$  with oriented edges is defined by  $I(v) = 1 - s(v)/2$  and  $I(f) = \chi(f) - s(f)/2$  where  $s(v)$  and  $s(f)$  are switches at  $v$  and of  $f$  respectively. A *sink* or a *source*

is a vertex of index 1, and a *cycle* is a face of index 1. We say an *exceptional cycle* if it is dual to an exceptional vertex.

**Lemma 2.3.6.**  $\Lambda^*$  does not contain a cycle except an exceptional cycle with respect to  $\omega, \omega'$ .

*Proof.* Suppose  $v$  is a non-exceptional vertex dual to a cycle with respect to  $\omega$ . Since  $v$  has valency 6, the edge classes of three edges which are incident to  $v$  at the label 1 belong to either  $\{\alpha, \delta\}$  or  $\{\beta, \gamma\}$ . Therefore two of them have the same edge class at the same label. This contradicts Lemma 2.2.5. The same argument applies to  $\omega'$ .  $\square$

Let  $s$  and  $s'$  be the number of sinks and sources of  $\Lambda^*$  at vertices dual to the faces of  $\Lambda$  (i.e. we exclude the outside face.) with respect to  $\omega, \omega'$  respectively.

**Lemma 2.3.7.**  $s > 0$  and  $s' > 0$ .

*Proof.* By Lemma 2.3.6, the only possible cycle is an exceptional cycle. However if  $\Lambda^*$  has an exceptional cycle, then it cannot contain the sink or source dual to the outside face at the same time. Hence it follows from the equation  $\sum_{vertices} I(v) + \sum_{faces} I(f) = 2$  that  $s, s' > 0$ .  $\square$

A sink or source of  $\omega, \omega'$  in  $\Lambda^*$  that does not correspond to the outside face of  $\Lambda$  is a binary face of  $\Lambda$ .

**Lemma 2.3.8.** *There is a white binary face in  $\Lambda$  dual to a sink or source with respect to  $\omega$ .*

*Proof.* By Lemma 2.3.7, there is a binary face in  $\Lambda$  dual to a sink or source with respect to  $\omega$ . We show that this binary face is white.

Suppose that a binary face in  $\Lambda$  dual to a sink or source with respect to  $\omega$  is black. Then such a black binary face is either a  $B(\alpha, \delta)$  face or a  $B(\beta, \gamma)$  face. The former contains a  $B(\alpha, \delta)$  corner and the latter contains a  $B(\beta, \gamma)$  corner. This contradicts Lemma 2.3.3.  $\square$

So far, we have shown that under the assumption that  $G_1 = G_1^+$  Lemma 2.3.8 holds. Now we are ready to prove Theorem 2.3.5.

*Proof of Theorem 2.3.5.* We follow the proof of Lemma 4.16 of [28]. Let  $f_1, f_2, f_3$  be three mutually non-isomorphic black faces of  $G_1^+$ . Then these faces cut  $M_B$  into two 3-balls by Lemma 2.3.4.

Let  $f$  be a black face of  $G_1$  other than  $f_1, f_2, f_3$ . Since  $f$  lies in the complement of  $f_1 \cup f_2 \cup f_3$  in  $M_B$ ,  $f$  must be a disk, otherwise it would be compressible in  $M_B$ , so  $F_1$  would be compressible in  $M$ , a contradiction to the fact that  $F_1$  is incompressible. Each component of  $\partial f \cap F_2$  is an edge of  $G_2$ .  $\partial f$  must be an essential curve in  $\partial M_B = F_2 \cup H_B$ , otherwise some component of  $\partial f \cap F_2$  would be a trivial loop in  $G_2$ . Hence  $f$  is an essential disk in  $M_B$ , so it must be parallel to one of the faces  $f_1, f_2$  and  $f_3$ . Therefore any black face

of  $G_1$  is a disk face isomorphic to one of  $f_1, f_2, f_3$  by Lemma 2.3.4. It follows that all the edges of  $G_1$  are positive, i.e.  $G_1 = G_1^+$ .

Next, we will show that any white face of  $G_1$  is a disk face. Note that if every white face of  $G_1$  is a disk face, then  $G_1$  is connected. Suppose a white face  $g$  of  $G_1$  is not a disk face. Lemma 2.3.8 guarantees the existence of a white binary disk face  $g_1$ . Furthermore, there must be a white disk face  $g_2$  other than  $g_1$  in  $\Lambda$  which is non-isomorphic to  $g_1$ , otherwise there are three edges in the same edge class incident to an interior vertex, contradicting Lemma 2.2.5. Thus the complement of  $g_1 \cup g_2$  in  $M_W$  is a 3-ball. So,  $g$  is compressible in  $M_W$ , which implies that  $F_1$  is compressible, a contradiction.

We have shown that  $G_1 = G_1^+$  and  $G_1$  is connected. Therefore,  $F_1$  is nonseparating, which contradicts [29, Theorem 1.1]. This completes the proof that there is no triple of mutually non-isomorphic black disk faces in  $G_1^+$ . Similarly, we can apply the same argument to show that there is no triple of non-isomorphic white disk faces, by using a  $B(\alpha, \beta)$  bigon.  $\square$

### 2.3.2 Ordinary Cycles and Boundary Cycles

Now we go back to the subgraph  $\Lambda$  as in subsection 2.2.1 and continue with the proof of Theorem 2.3.1. Since  $\Lambda$  contains a  $B(\alpha, \beta)$  bigon and a  $B(\gamma, \delta)$  trigon with two  $\gamma$ -edges and one  $\delta$ -edge by Lemma 2.3.2, Theorem 2.3.5 implies the following.

**Lemma 2.3.9.** *Any black disk face of  $G_1^+$  is isomorphic to either a  $B(\alpha, \beta)$  bigon or a  $B(\gamma, \delta)$  trigon with two  $\gamma$ -edges and one  $\delta$ -edge.*

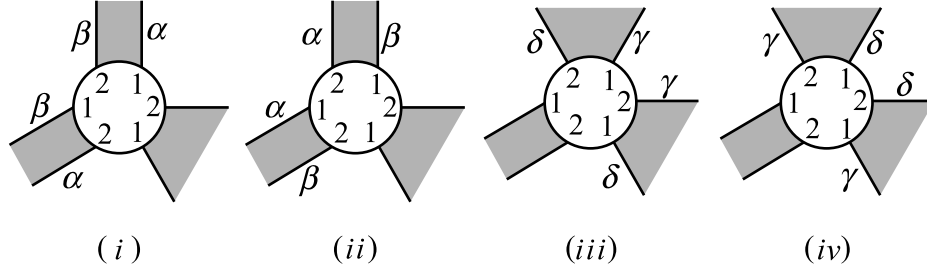


Figure 2.7: Four distinct types of interior vertices.

We define the dual graph  $\Lambda^*$  with two orientations  $\omega, \omega'$  as in the case  $G_1 = G_1^+$ . The cycle dual to an interior vertex in  $\Lambda$  is said to be an *ordinary cycle*. The cycle dual to a boundary vertex (except an exceptional vertex) is called a *boundary cycle*. The cycle dual to an exceptional vertex is said to be an *exceptional cycle*. Thus when we say a boundary cycle dual to a boundary vertex, we do not allow it to be the cycle dual to an exceptional vertex.

**Lemma 2.3.10.**  $\Lambda^*$  does not contain a sink or source dual to a black face of  $\Lambda$  with respect to  $\omega, \omega'$ .

*Proof.* Lemma 2.3.9 says that any black disk face is either a  $B(\alpha, \beta)$  bigon or a  $B(\gamma, \delta)$  trigon with two  $\gamma$ -edges and one  $\delta$ -edge. However, either black disk face is not dual to a sink or source with respect to  $\omega, \omega'$ .  $\square$

It is guaranteed by Lemma 2.2.17 that  $\Lambda$  contains an interior vertex.

Note that there are only four distinct types of interior vertices. See Figure 2.7.

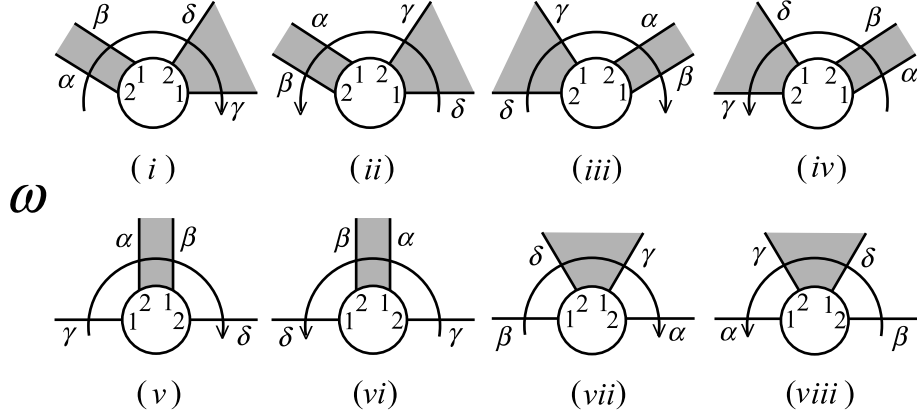


Figure 2.8: Boundary cycles with respect to  $\omega$ .

**Lemma 2.3.11.**  $\Lambda^*$  does not contain an ordinary cycle with respect to  $\omega, \omega'$ .

*Proof.* Since any interior vertex has valency 6, this follows from the proof of Lemma 2.3.6.  $\square$

**Lemma 2.3.12.** A boundary cycle dual to a boundary vertex with respect to  $\omega, \omega'$  is one of those illustrated in Figure 2.8 and Figure 2.9 respectively.

*Proof.* If a boundary vertex  $v$  dual to a boundary cycle has valency 5 or 6, then at least two edges incident to  $v$  have the same edge class at the same label, contradicting Lemma 2.2.5. Hence any boundary vertex dual to a boundary cycle has valency 4. Furthermore, any boundary vertex has two  $\alpha$ - or  $\beta$ -edges and also two  $\gamma$ - or  $\delta$ -edges by the property (1) of  $\Lambda$ . Then the proof follows from Lemma 2.3.9.  $\square$

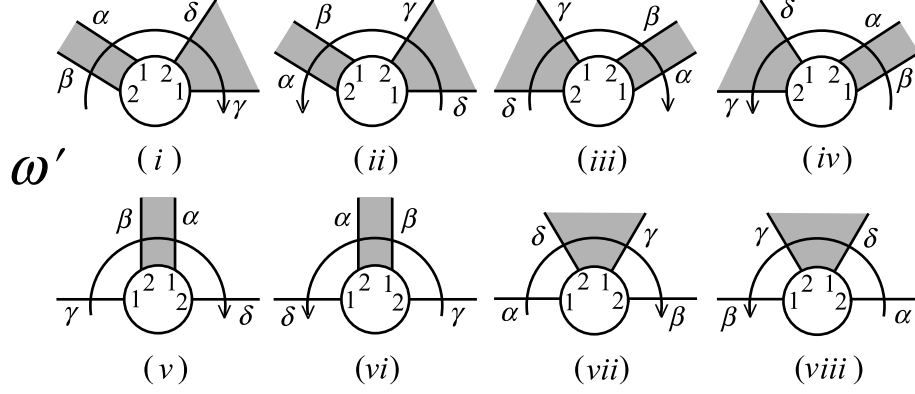


Figure 2.9: Boundary cycles with respect to  $\omega'$ .

**Lemma 2.3.13.**  $\Lambda^*$  does not contain a boundary cycle with respect to  $\omega'$ .

*Proof.* Assume for contradiction that  $\Lambda$  contains a boundary cycle dual to a boundary vertex  $u_x$ . In  $G_2$ , the label  $x$  appears either three times around  $v_1$  at the ends of  $\alpha$ -,  $\gamma$ - and  $\epsilon$ -edges and three times around  $v_2$  at the ends of  $\beta$ -,  $\delta$ - and  $\epsilon'$ -edges, or three times around  $v_1$  at the ends of  $\beta$ -,  $\delta$ - and  $\epsilon$ -edges and three times around  $v_2$  at the ends of  $\alpha$ -,  $\gamma$ - and  $\epsilon'$ -edges. The odd-numbered types in Figure 2.9 have the first case and the even-numbered types have the second case.

**Claim.** In  $G_2$ , the label  $x$  appears at  $\epsilon_N$  (resp.  $\epsilon_S$ ) of the  $\epsilon$ -edge class at  $v_1$  if and only if it appears at  $\epsilon'_S$  (resp.  $\epsilon'_N$ ) of the  $\epsilon'$ -edge class at  $v_2$ .

*Proof.* Assume the first case i.e. the label  $x$  appears three times around the vertex  $v_1$  at the ends of  $\alpha$ -,  $\gamma$ - and  $\epsilon$ -edges and three times around the vertex

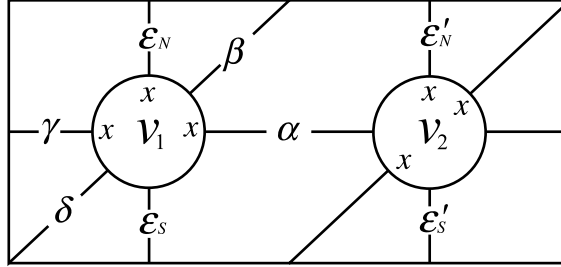


Figure 2.10: Three occurrences of label  $x$  on  $v_1$  and  $v_2$ .

$v_2$  at the ends of  $\beta$ -,  $\delta$ - and  $\epsilon'$ -edges. The second case is similar.

Suppose, for example, that  $x$  appears at  $\epsilon_N$  and at  $\epsilon'_N$  of  $\epsilon$ - and  $\epsilon'$ -edges respectively at the same time. See Figure 2.10. At the vertex  $v_1$  the edge classes  $\delta$  and  $\epsilon_S$  do not have the label  $x$ . Then the sum of the weights of  $\delta$  and  $\epsilon$  is less than  $n_1$ . On the other hand, at the vertex  $v_2$  the edge classes  $\delta$  and  $\epsilon'_N$  have the label  $x$  twice, which implies that the sum of the weights of  $\delta$  and  $\epsilon'$  is greater than  $n_1$ . However, these two inequalities conflict since the weights of  $\epsilon$  and  $\epsilon'$  are same.  $\square$

Assume that the boundary vertex  $u_x$  is dual to one of the types (i)–(iv). Then we have a  $B(\epsilon, \epsilon')$  corner. In Figure 2.5 of Lemma 2.3.3,  $(\epsilon, \epsilon')$  should be  $(\epsilon_N, \epsilon'_N)$  or  $(\epsilon_S, \epsilon'_S)$ . This contradicts the claim.

For the type (v), we have two black corners, a  $B(\gamma, \epsilon')$  corner, a  $B(\epsilon, \delta)$  corner. However, from Figure 2.5 of Lemma 2.3.3,  $(\epsilon, \epsilon')$  should be  $(\epsilon_N, \epsilon'_N)$ , which is a contradiction to the claim. The other types are also impossible by

the same argument. This completes the proof.  $\square$

*Note.* The claim in the proof of Lemma 2.3.13 doesn't work with the orientation  $\omega$ .

**Lemma 2.3.14.**  $\Lambda^*$  does not contain a boundary cycle with respect to  $\omega$ .

*Proof.* Lemmas 2.3.10, 2.3.11, 2.3.13 and the equation  $\sum_{vertices} I(v) + \sum_{faces} I(f) = 2$  imply that there is a sink or source dual to a white disk face with respect to  $\omega'$ . In other words, there is a  $W(\beta, \delta)$  or  $W(\alpha, \gamma)$  face. There are eight types of boundary cycles with respect to  $\omega$  as in Figure 2.8. The first four types have a  $B(\epsilon, \epsilon')$  corner. However, by Figure 2.5,  $(\epsilon, \epsilon')$  must be either  $(\epsilon_N, \epsilon'_N)$  or  $(\epsilon_S, \epsilon'_S)$ . Assume we have the type (i). If we let  $u_x$  be a boundary vertex of the type (i), then the label  $x$  appears three times around the vertex  $v_1$  at the ends of  $\beta$ -,  $\gamma$ - and  $\epsilon$ -edges and three times around the vertex  $v_2$  at the ends of  $\alpha$ -,  $\delta$ - and  $\epsilon'$ -edge. Applying an argument similar to the claim in Lemma 2.3.13,  $(\epsilon, \epsilon')$  must be  $(\epsilon_S, \epsilon'_S)$ . Thus, we have a  $W(\beta, \delta)$  corner, a  $W(\epsilon_S, \alpha)$  corner, and a  $W(\gamma, \epsilon'_S)$  corner. Since we have a  $W(\beta, \delta)$  or  $W(\alpha, \gamma)$  face and  $\lambda$  is assumed to have no white bigon, there are  $W(\delta, \delta)$  or  $W(\beta, \beta)$  corners in a  $W(\beta, \delta)$  face by the remark below the proof of Lemma 4.4 in [16], or there are  $W(\alpha, \gamma)$  corners in a  $W(\alpha, \gamma)$  face. Then neither a  $W(\beta, \beta)$  corner, a  $W(\delta, \delta)$  corner nor a  $W(\alpha, \gamma)$  corner satisfies Lemma 2.2.4 with  $W(\beta, \delta)$ ,  $W(\epsilon_S, \alpha)$ , and  $W(\gamma, \epsilon'_S)$  corners. Therefore type (i) cannot happen. A similar argument applies to the other types (ii), (iii) and (iv).

For the type  $(v)$ , we have a  $W(\beta, \delta)$  corner, a  $W(\gamma, \alpha)$  corner and a  $W(\epsilon, \epsilon')$  corner. Then Lemma 2.2.4 forces  $(\epsilon, \epsilon')$  to be either  $(\epsilon_N, \epsilon'_S)$  or  $(\epsilon_S, \epsilon'_N)$ . If  $(\epsilon, \epsilon') = (\epsilon_N, \epsilon'_S)$ , the boundary vertex has a  $B(\gamma, \epsilon'_S)$  corner, which is impossible by Figure 2.5. If  $(\epsilon, \epsilon') = (\epsilon_S, \epsilon'_N)$ , then the boundary vertex has a  $B(\epsilon_S, \delta)$  corner, which is also impossible by Figure 2.5. For the other types, we can apply a similar argument.  $\square$

### 2.3.3 Proof of Theorem 2.3.1

*Proof.* Lemmas 2.3.10, 2.3.11 and 2.3.13 guarantee that  $\Lambda$  contains a  $W(\lambda_1, \lambda_2)$  face where  $\{\lambda_1, \lambda_2\} = \{\beta, \delta\}$  or  $\{\alpha, \gamma\}$  by the index equation  $\sum_{vertices} I(v) + \sum_{faces} I(f) = 2$ . Also Lemmas 2.3.10, 2.3.11 and 2.3.14 guarantee that  $\Lambda$  contains a  $W(\mu_1, \mu_2)$  face where  $\{\mu_1, \mu_2\} = \{\alpha, \delta\}$  or  $\{\beta, \gamma\}$ . Hence a  $W(\lambda_1, \lambda_2)$  face and a  $W(\mu_1, \mu_2)$  face are the only two non-isomorphic white disk faces in  $\Lambda$  by Theorem 2.3.5.

If  $\{\lambda_1, \lambda_2\} = \{\beta, \delta\}$  and  $\{\mu_1, \mu_2\} = \{\alpha, \delta\}$ , then no  $\gamma$ -edges are incident to interior vertices, which is impossible since there are only four types of interior vertices. See Figure 2.7. Similarly for the case that  $\{\lambda_1, \lambda_2\} = \{\beta, \delta\}$  and  $\{\mu_1, \mu_2\} = \{\beta, \gamma\}$ , in which case no  $\alpha$ -edges are incident to interior vertices, and the case that  $\{\lambda_1, \lambda_2\} = \{\alpha, \gamma\}$  and  $\{\mu_1, \mu_2\} = \{\alpha, \delta\}$ , in which case no  $\beta$ -edges are incident to interior vertices.

Then the only remaining case is that  $\{\lambda_1, \lambda_2\} = \{\alpha, \gamma\}$  and  $\{\mu_1, \mu_2\} = \{\beta, \gamma\}$ , i.e.  $\Lambda$  has a  $W(\alpha, \gamma)$  face and a  $W(\beta, \gamma)$  face, in which case no  $\delta$ -edges are interior edges and are incident to interior vertices, which is possible when

an interior vertex is of type (i) or (ii) of Figure 2.7. These faces cannot be both bad by Lemma 2.2.6 and cannot be both good by Lemma 2.2.7.

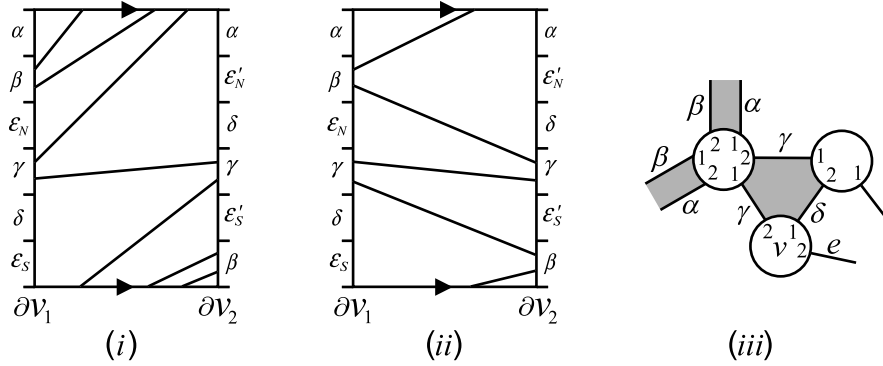


Figure 2.11: The intersection of the white corners of a bad  $W(\beta, \gamma)$  face and  $H_W$ , and the local configuration at an interior vertex of type (i).

Assume that a  $W(\alpha, \gamma)$  face is good and a  $W(\beta, \gamma)$  face is bad. Then every interior vertex is of type (i) by Lemma 2.2.6. Consider the intersection of the white corners of a bad  $W(\beta, \gamma)$  face and  $H_W$  where there are two possibilities as in Figure 2.11 (i), (ii), and the local configuration at an interior vertex of type (i) as in Figure 2.11 (iii). However, Figure 2.11 (ii) is impossible since there is a  $W(\alpha, \gamma)$  corner. In Figure 2.11 (iii)  $e$  must be  $\gamma$  from Figure 2.11 (i). Then the vertex  $v$  has two  $\gamma$ -edges at the same label, which is a contradiction to Lemma 2.2.5.

Assume that a  $W(\alpha, \gamma)$  face is bad and a  $W(\beta, \gamma)$  face is good. Then every interior vertex is of type (ii) by Lemma 2.2.6. Consider the intersection of the white corners of a  $W(\alpha, \gamma)$  face and  $H_W$  and the local configuration at

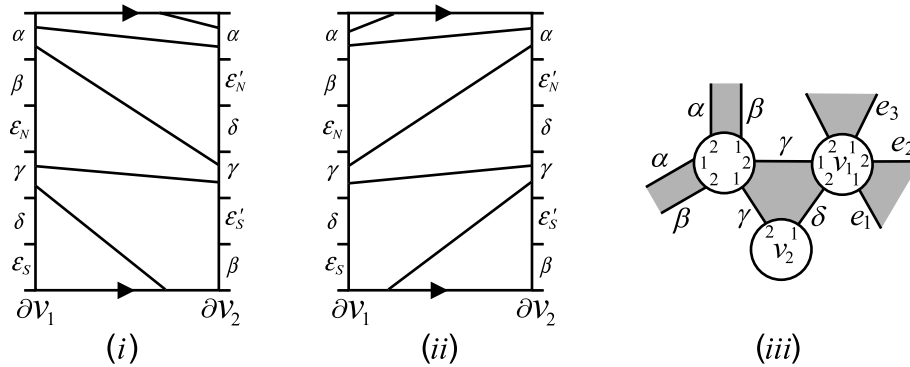


Figure 2.12: The intersection of the white corners of a  $W(\alpha, \gamma)$  face and  $H_W$ , and the local configuration at an interior vertex of type  $(ii)$ .

an interior vertex of type  $(ii)$ . See Figure 2.12. There are two possibilities for the intersection of the white corners of a  $W(\alpha, \gamma)$  face and  $H_W$  as in Figure 2.12  $(i), (ii)$ . Figure 2.12  $(ii)$  is impossible since there is a  $W(\beta, \gamma)$  corner. In Figure 2.12  $(iii)$  suppose that  $v_1$  is not an exceptional vertex. Recall that no  $\delta$ -edge is an interior edge in  $\Lambda$ . Then  $e_1$  must be an  $\alpha$ -edge and must be a boundary edge since the  $\delta$ -edge adjacent to  $e_1$  is a boundary edge. This implies that  $e_2$  is an interior edge and then a  $\beta$ -edge. Also,  $e_3$  must be a  $\gamma$ -edge from Figure 2.12  $(i)$ . This is a contradiction to Lemma 2.2.5. If  $v_1$  is an exceptional vertex, consider the vertex  $v_2$  in Figure 2.12  $(iii)$  and apply the same argument. Hence we have finished the proof of Theorem 2.3.1.  $\square$

## 2.4 A $B(\alpha, \beta)$ Bigon and a White Trigon

In this section, we assume that  $\Lambda$  contains a  $B(\alpha, \beta)$  bigon and does not contain a white bigon. Then the main goal of this section is to prove the following theorem.

**Theorem 2.4.1.** *If  $\Lambda$  contains a  $B(\alpha, \beta)$  bigon and does not contain a white bigon, then  $\Lambda$  does not contain a white trigon.*

Suppose that  $\Lambda$  contains a white trigon. Then Lemma 2.2.12 says that a white trigon is either a  $W(\alpha, \delta)$ ,  $W(\beta, \gamma)$ ,  $W(\beta, \delta)$  or  $W(\alpha, \gamma)$  trigon.

Note that Theorem 2.3.5 still holds by using a white trigon instead of a white binary disk face in the proof of Theorem 2.3.5. Furthermore, by Lemma 2.2.17, there is an interior vertex in  $\Lambda$ .

### 2.4.1 A $W(\alpha, \delta)$ Trigon with Two $\delta$ -edges and One $\alpha$ -edge

Assume that there is a  $W(\alpha, \delta)$  trigon with two  $\delta$ -edges and one  $\alpha$ -edge in  $\Lambda$ . Then we consider the orientation  $\omega'$  of  $\Lambda^*$ .

**Lemma 2.4.2.**  *$\Lambda^*$  does not contain a boundary cycle with respect to  $\omega'$ .*

*Proof.* Consider the intersection of the white corners of a  $W(\alpha, \delta)$  trigon and  $H_W$  where there are two cases as in Figure 2.13 (i), (ii), and the intersection of the black corners of a  $B(\alpha, \beta)$  bigon and  $H_B$  as in Figure 2.13 (iii). Let  $v$  be a boundary vertex dual to a boundary cycle with respect to  $\omega'$ . As in the proof of Lemma 2.3.12, there are only 4 positive edges incident to  $v$ . There are

two types of local configuration at  $v$  as shown in Figure 2.14 (i), (ii), where  $e_1, e_2, e_3$  and  $e_4$  are positive edges and  $e_5$  and  $e_6$  are negative edges.

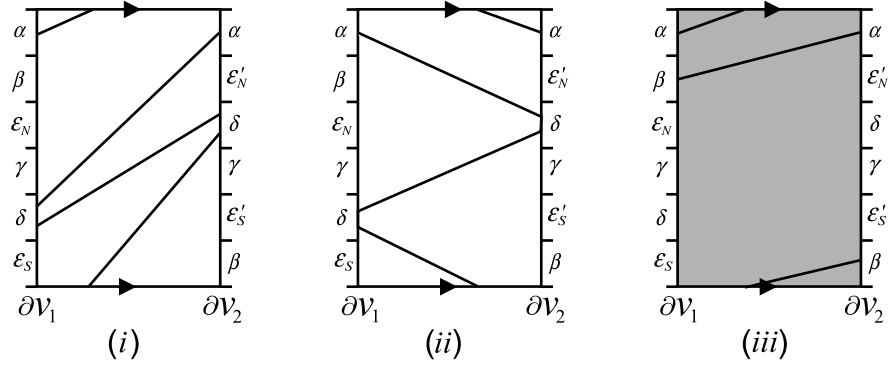


Figure 2.13: The intersection of the white corners of a  $W(\alpha, \delta)$  trigon and the intersection of the black corners of a  $B(\alpha, \beta)$  bigon and  $H_B$ .

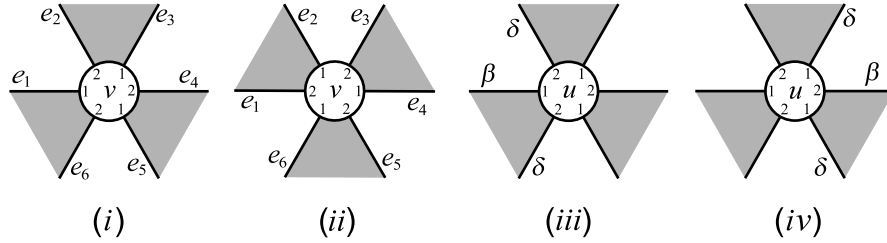


Figure 2.14: Local configurations of a boundary vertex (i), (ii), and an interior vertex with a  $\delta$ -edge incident (iii), (iv).

Assume we have Figure 2.13 (ii). Then the only possible white corner with one  $\beta$ -edge is a  $W(\beta, \delta)$  corner or a  $W(\delta, \beta)$  corner, which makes a boundary vertex not to be a cycle with respect to  $\omega'$  since a  $\beta$ -edge and a  $\delta$ -edge have the same orientation with respect to  $\omega'$ . Now assume Figure 2.13

(i).

1) The first type as in Figure 2.14 (i); Note that  $(e_5, e_6) = (\epsilon_N, \epsilon'_S)$  from the intersection of the white corners of a  $W(\alpha, \delta)$  trigon and  $H_W$  as shown in Figure 2.13 (i).

Assume there is a clockwise boundary cycle. There are only two cases for  $e_1$  i.e.  $e_1$  is either  $\alpha$  or  $\gamma$ . First if  $e_1 = \alpha$ , then  $e_2$  must be  $\delta$  from Figure 2.13 (i) since there is a  $W(\epsilon_N, \epsilon'_S)$  corner. Then  $e_3 = \gamma$  and  $e_4 = \beta$ . Thus, we have a  $B(\gamma, \delta)$  corner and a  $B(\epsilon_N, \beta)$  corner. However this cannot happen from the intersection of the black corners of a  $B(\alpha, \beta)$  bigon and  $H_B$  as in Figure 2.13 (iii).

Second, if  $e_1 = \gamma$ ,  $e_2$  must be  $\beta$  since there is a  $W(\epsilon_N, \epsilon'_S)$  corner. Then  $e_3 = \alpha$  and  $e_4 = \delta$ . Hence we have two black corners, i.e. a  $B(\gamma, \epsilon'_S)$  corner and a  $B(\epsilon_N, \delta)$  corner. We can observe from Figure 2.13 (iii) with a  $B(\gamma, \epsilon'_S)$  corner and a  $B(\epsilon_N, \delta)$  corner inserted that the only positive edge from which a black corner runs to a  $\gamma$ -edge is a  $\gamma$ -edge. Thus if a  $\gamma$ -edge is an interior edge, then there is a face all edges of which are  $\gamma$ -edges, which contradicts Lemma 3.1 of [12]. Consequently, no  $\gamma$ -edge is incident to interior vertices. For an interior vertex  $u$ , a  $\delta$ -edge must be incident to  $u$ , otherwise there are three  $\alpha$  or  $\beta$ -edges incident to  $u$ , which is a contradiction to Lemma 2.2.5. However at whatever label a  $\delta$ -edge is incident to  $u$ , there is another  $\delta$ -edge incident to  $u$  at the same label from Figure 2.13 (i) with a  $W(\epsilon_N, \epsilon'_S)$  corner inserted and Figure 14 (iii) with a  $B(\gamma, \epsilon'_S)$  corner and a  $B(\epsilon_N, \delta)$  corner inserted, which is a contradiction to Lemma 2.2.5. See Figure 2.14 (iii), (iv).

Assume there is a anticlockwise boundary cycle. If  $e_1 = \beta$ , then  $e_2 = \gamma$ ,  $e_3 = \delta$  and  $e_4 = \alpha$  since there is a  $W(\epsilon_N, \epsilon'_S)$  corner. Thus, we have a  $B(\delta, \gamma)$  corner and a  $B(\beta, \epsilon'_S)$  corner. However these two black corners cannot happen at the same time from the intersection of the black corners of a  $B(\alpha, \beta)$  bigon and  $H_B$  as in Figure 2.13 (iii). If  $e_1 = \delta$ , then  $e_2 = \alpha$ ,  $e_3 = \beta$  and  $e_4 = \gamma$ . Hence we have two black corners, i.e. a  $B(\epsilon_N, \gamma)$  corner and a  $B(\delta, \epsilon'_S)$  corner at  $v$ . We can observe that the only positive edge class to which a black corner runs from a  $\gamma$ -edge is a  $\gamma$ -edge. The argument is then completely the same as that of the case of a clockwise boundary cycle.

2) The second type as in Figure 2.14 (ii); We use an argument similar to the proof of Lemma 2.3.13. If we let  $u_x$  be a boundary vertex dual to a boundary cycle, then the label  $x$  appears either three times around  $v_1$  at the ends of  $\alpha$ -,  $\gamma$ - and  $\epsilon$ -edges and three times around  $v_2$  at the ends of  $\beta$ -,  $\delta$ - and  $\epsilon'$ -edges, or three times around  $v_1$  at the ends of  $\beta$ -,  $\delta$ - and  $\epsilon$ -edges and three times around  $v_2$  at the ends of  $\alpha$ -,  $\gamma$ - and  $\epsilon'$ -edges. By the claim in Lemma 2.3.13,  $(e_5, e_6)$  is either  $(\epsilon_N, \epsilon'_S)$  or  $(\epsilon_S, \epsilon'_N)$ . However, one of  $e_1$  and  $e_4$  must be either  $\alpha$  or  $\gamma$ . Thus by Figure 2.13 (i),  $(e_5, e_6) = (\epsilon_N, \epsilon'_S)$ . Figure 2.13 (iii) with a  $B(\epsilon_N, \epsilon'_S)$  corner inserted shows that if one edge of a black corner is a  $\delta$ -edge, then the other of the corner must be a  $\beta$ -edge. Therefore there is no boundary cycle with respect to  $\omega'$ . This completes the proof.  $\square$

*Remark:* Figure 2.9 in section 2.3 is not applicable in the proof of Lemma 2.4.2. For, we used Lemma 2.3.9 to get Figure 2.9. However, in this section, we cannot apply Lemma 2.3.9.

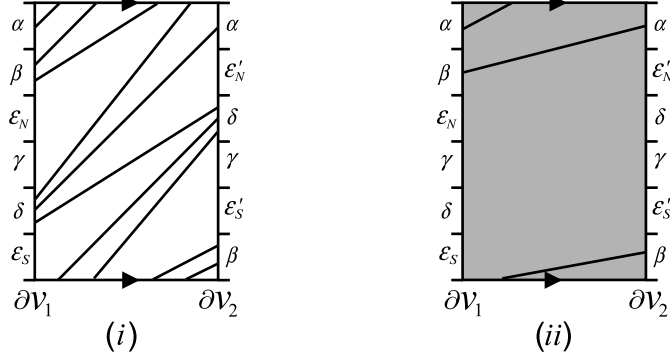


Figure 2.15: The intersection of  $H_W$  and the white corners of a  $W(\alpha, \delta)$  trigon and a bad  $W(\beta, \delta)$  face, and the intersection of the black corners of a  $B(\alpha, \beta)$  bigon and  $H_B$ .

**Lemma 2.4.3.** *There is no source or sink dual to a white face in  $\Lambda^*$  with respect to  $\omega'$ .*

*Proof.* Suppose there is a source or sink dual to a white face with respect to  $\omega'$ , i.e. there is a  $W(\lambda, \mu)$  face where  $\{\lambda, \mu\} = \{\alpha, \gamma\}$  or  $\{\beta, \delta\}$ . Since  $\Lambda$  contains a  $W(\alpha, \delta)$  trigon, which is good, Lemma 2.2.7 implies that a  $W(\lambda, \mu)$  face is bad. If  $\{\lambda, \mu\} = \{\alpha, \gamma\}$  i.e.  $\Lambda$  contains a bad  $W(\alpha, \gamma)$  face, then we have a  $W(\alpha, \alpha)$  corner, a  $W(\gamma, \gamma)$  corner and a  $W(\delta, \delta)$  corner. This is impossible by Lemma 2.2.6. Therefore we assume that  $\Lambda$  has a bad  $W(\beta, \delta)$  face. Note that Theorem 2.3.5 implies that every white face in  $\Lambda$  is either a  $W(\alpha, \delta)$  trigon or a bad  $W(\beta, \delta)$  face. Consider the intersection of the white corners of a  $W(\alpha, \delta)$  trigon, the white corners of a bad  $W(\beta, \delta)$  face and  $H_W$  where there is only one case, and the intersection of the black corners of a  $B(\alpha, \beta)$  bigon and  $H_B$ .

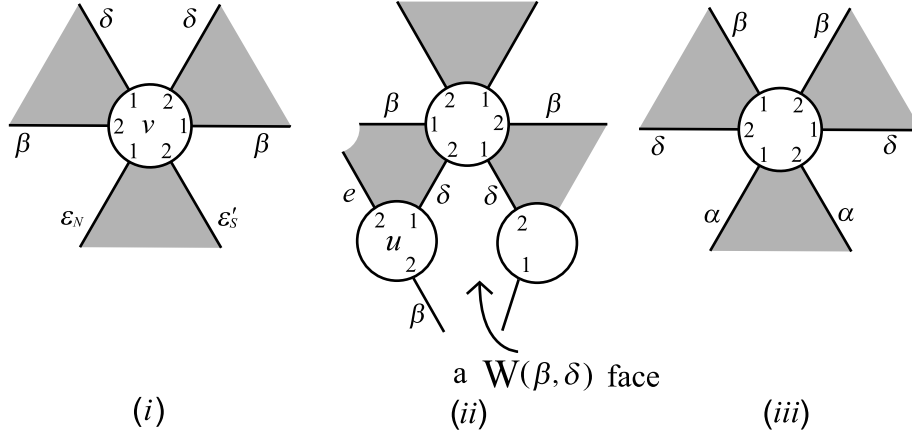


Figure 2.16: A non-exceptional vertex having a  $W(\delta, \delta)$  corner (i), a vertex having a  $W(\delta, \beta)$  corner of a  $W(\beta, \delta)$  face (ii), and an interior vertex (iii).

See Figure 2.15. Since  $\Lambda$  has a  $W(\alpha, \delta)$  trigon and a bad  $W(\beta, \delta)$  face, there are at least two  $W(\delta, \delta)$  corners. Since no vertex can have two  $W(\delta, \delta)$  corners by Lemma 2.2.5, there are at least two vertices which have a  $W(\delta, \delta)$  corner. Let  $v$  be such a non-exceptional vertex.

**Claim.** *There is only one local configuration at  $v$  as shown in Figure 2.16 (i).*

*Proof.* If at least five positive edges are incident to  $v$ , then there are at least two white corners at  $v$  which are corners of white disk faces in  $\Lambda$ . One is a  $W(\delta, \delta)$  corner. The other corner must be a  $W(\beta, \beta)$  corner because every white face in  $\Lambda$  is either a  $W(\alpha, \delta)$  trigon or a bad  $W(\beta, \delta)$  face and no vertex has three edges incident to it in the same edge class. The one remaining white corner at  $v$  must be a  $W(\alpha/\gamma/\epsilon, \alpha/\gamma/\epsilon')$  corner, which is impossible by Figure

2.15 (i). If four edges incident to  $v$  are positive, the local configuration at  $v$  must be as in Figure 2.16 (i) since a  $W(\epsilon, \epsilon')$  corner cannot occur by Figure 2.15 (i).  $\square$

Suppose a  $W(\delta, \delta)$  corner of a bad  $W(\beta, \delta)$  face does not appear at an exceptional vertex. The bad  $W(\beta, \delta)$  face contains a vertex  $u$  as shown in Figure 2.16 (ii). Since there is only one local configuration at the vertex containing a  $W(\delta, \delta)$  corner,  $e$  is positive. However,  $e$  cannot be  $\alpha, \gamma$  and  $\delta$  from Figure 2.15 (ii) because there is a  $B(\epsilon_N, \epsilon'_S)$  corner by the claim. Also,  $e$  cannot be  $\beta$  by Lemma 2.2.5.

Finally, every  $W(\delta, \delta)$  corner of a  $W(\beta, \delta)$  face must appear at an exceptional vertex. Therefore there is only one  $W(\beta, \delta)$  face  $X$ , say. Thus there is only one possible sink or source dual to a white face. Note that an exceptional vertex is not dual to a cycle in  $\Lambda^*$  because it contains a  $W(\delta, \delta)$  corner. On the other hand, every white face in  $\Lambda$  is either a  $W(\alpha, \delta)$  trigon or a bad  $W(\beta, \delta)$  face. Thus there is a unique type of interior vertices as in Figure 2.16 (iii) since a  $B(\epsilon_N, \epsilon'_S)$  corner coming from the claim and Figure 2.15 (ii) exclude a  $B(\delta, \delta)$  corner. Since there are only two non-isomorphic black disk faces in  $\Lambda$ , one black disk face has an  $\alpha$ -,  $\beta$ - and  $\delta$ -edges coming from the local picture at an interior vertex as shown in Figure 2.16 (iii). The other black disk face is a  $B(\alpha, \beta)$  bigon. Hence there is no sink or source dual to a black disk face. Since there is no cycle by Lemmas 2.3.11 and 2.4.2, the only possible positive index takes place at  $X$  or the outside face. However, the index of an

interior vertex is  $-1$ . This is a contradiction to the equation  $\sum_{vertices} I(v) + \sum_{faces} I(f) = 2$ .  $\square$

**Lemma 2.4.4.** *There is no source or sink dual to a black face in  $\Lambda^*$  with respect to  $\omega'$ .*

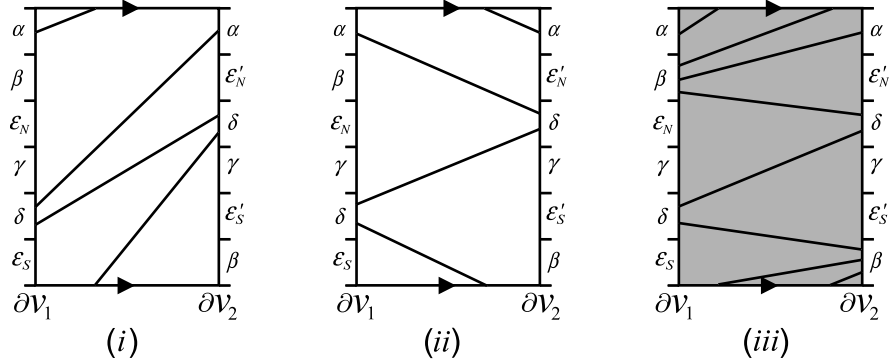


Figure 2.17: The intersection of the white corners of a  $W(\alpha, \delta)$  trigon and  $H_W$ , and the intersection of  $H_B$  and the black corners of a  $B(\alpha, \beta)$  bigon and a bad  $B(\beta, \delta)$  face.

*Proof.* Suppose there is a source or sink dual to a black face with respect to  $\omega'$ , i.e. there is a  $B(\lambda, \mu)$  face where  $\{\lambda, \mu\} = \{\alpha, \gamma\}$  or  $\{\beta, \delta\}$ . Then a  $B(\lambda, \mu)$  face must be bad by Lemma 2.2.7 because of the existence of a  $B(\alpha, \beta)$  bigon.

Suppose we have a bad  $B(\beta, \delta)$  face. Consider the intersection of the black corners of a  $B(\alpha, \beta)$  bigon, the black corners of a bad  $B(\beta, \delta)$  face and  $H_B$  as shown in Figure 2.17 (iii), and the intersection of the white corners of a  $W(\alpha, \delta)$  trigon and  $H_W$  where there are two cases as shown in Figure 2.17

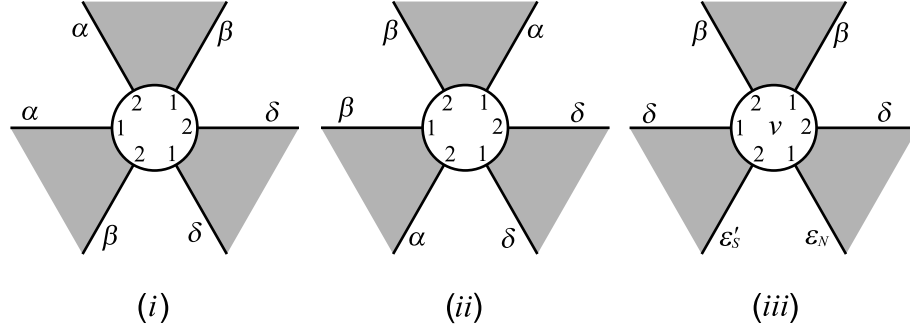


Figure 2.18: Local configurations of an interior vertex (i), (ii), and a non-exceptional vertex having a  $B(\beta, \beta)$  corner (iii).

(i), (ii). By Theorem 2.3.5, every black face is either a  $B(\alpha, \beta)$  bigon or a bad  $B(\beta, \delta)$  face. Also, since three edges in the same edge class cannot be incident to a vertex, there are only two types of local configuration at interior vertices. See Figure 2.18 (i) (ii). Note that Figure 2.17 (i) excludes the first type of interior vertices because a  $W(\alpha, \alpha)$  corner and a  $W(\delta, \beta)$  corner cannot exist simultaneously in Figure 2.17 (i), and Figure 2.17 (ii) rules out the second type of interior vertices since no  $W(\beta, \beta)$  corner survives in Figure 2.17 (ii).

Let  $v$  be a vertex containing a  $B(\beta, \beta)$  corner of a bad  $B(\beta, \delta)$  face. Suppose  $v$  is a non-exceptional vertex. Now apply an argument similar to the proof of the claim in Lemma 2.4.3 by using Figure 2.17 (iii). Then the local configuration at  $v$  looks like Figure 2.18 (iii). However, a  $W(\epsilon_N, \epsilon'_S)$  corner is impossible because in the case of Figure 2.17 (i) the second type of interior vertices contains a  $W(\beta, \beta)$  corner, and in the case of Figure 2.17 (ii) a  $W(\epsilon_N, \epsilon'_S)$  corner cannot exist.

Consequently,  $v$  must be an exceptional vertex and then there is only one bad  $B(\beta, \delta)$  face  $Y$ , say, containing only one  $B(\beta, \beta)$  corner. Note that since  $v$  contains a  $B(\beta, \beta)$  corner, the exceptional vertex  $v$  is not dual to a cycle in  $\Lambda^*$ . We already showed in Lemma 2.4.3 that there are no  $W(\beta, \delta)$  faces and no  $W(\alpha, \gamma)$  faces in  $\Lambda$ . Furthermore, no  $B(\alpha, \gamma)$  faces exist since we have a bad  $B(\beta, \delta)$  face. Therefore, there are only two possible sinks or sources in  $\Lambda^*$ . One is dual to  $Y$  and the other the outside face.

Since there is no cycle in  $\Lambda^*$  by Lemmas 2.3.11 and 2.4.2, in order to get a contradiction to the equation  $\sum_{vertices} I(v) + \sum_{faces} I(f) = 2$ , it suffices to show that either there is a vertex of index  $-1$  or the outside face is not dual to a sink or source. Let  $u$  be a vertex containing a  $B(\beta, \delta)$  corner of  $Y$ . Then  $u$  is not an exceptional vertex. Also  $u$  is a boundary vertex since the local picture at interior vertices looks like Figure 2.18 (i) (ii). We can observe that two negative edges are not incident to  $u$  since neither a  $W(\epsilon, \epsilon')$  corner nor a  $B(\epsilon, \epsilon')$  corner exists by Figure 2.17 with white corners of an interior vertex added. If at most one negative edge is incident to  $u$ , it is easy to see using Figure 2.17 that either  $u$  has index  $-1$  or the outside face is not dual to a sink or a source.

Suppose we have a bad  $B(\alpha, \gamma)$  face in  $\Lambda$ . Apply an argument similar to the case of a  $B(\beta, \delta)$  face. First use a  $B(\alpha, \alpha)$  corner instead of a  $B(\beta, \beta)$  corner to show that there is only one  $B(\alpha, \gamma)$  face in  $\Lambda$ . However unlike the case of a  $B(\beta, \delta)$  face, there is only one type of local configuration at interior vertices and furthermore the index of an interior vertex is  $-1$ . Use the equation

$\sum_{vertices} I(v) + \sum_{faces} I(f) = 2$  to get a contradiction.  $\square$

By Lemmas 2.3.11 and 2.4.2 – 2.4.4 and the index equation  $\sum_{vertices} I(v) + \sum_{faces} I(f) = 2$ , we have proved Theorem 2.4.1 for the case that  $\Lambda$  contains a  $W(\alpha, \delta)$  trigon with two  $\delta$ -edges and one  $\alpha$ -edge.

### 2.4.2 A $W(\alpha, \delta)$ Trigon with Two $\alpha$ -edges and One $\delta$ -edge

In this subsection, we suppose  $\Lambda$  contains a  $W(\alpha, \delta)$  trigon with two  $\alpha$ -edges and one  $\delta$ -edge.

**Lemma 2.4.5.**  *$\Lambda^*$  does not contain a boundary cycle with respect to  $\omega'$ .*

*Proof.* The proof of this lemma is exactly analogous as that of Lemma 2.4.2.  $\square$

**Lemma 2.4.6.** *There is no source or sink dual to a white face in  $\Lambda^*$  with respect to  $\omega'$ .*

*Proof.* Suppose there is a source or sink dual to a white face with respect to  $\omega'$ , i.e. there is a  $W(\lambda, \mu)$  face where  $\{\lambda, \mu\} = \{\alpha, \gamma\}$  or  $\{\beta, \delta\}$ . Then a  $W(\lambda, \mu)$  face must be a bad  $W(\alpha, \gamma)$  face by Lemmas 2.2.6 and 2.2.7. Consider the intersection of the white corners of a  $W(\alpha, \delta)$  trigon, the white corners of a bad  $W(\alpha, \gamma)$  face and  $H_W$  where there is only one case, and the intersection of the black corners of a  $B(\alpha, \beta)$  bigon and  $H_B$ . See Figure 2.19. Since  $\Lambda$  contains a  $W(\alpha, \delta)$  trigon and a bad  $W(\alpha, \gamma)$  face, there are at least two vertices which have a  $W(\alpha, \alpha)$  corner. Let  $v$  be such a non-exceptional vertex.

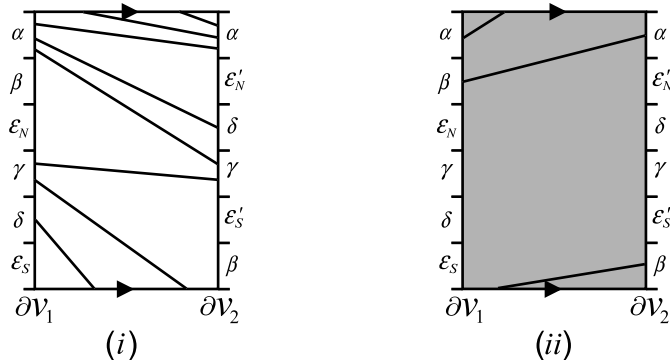


Figure 2.19: The intersection of  $H_W$  and the white corners of a  $W(\alpha, \delta)$  trigon and a bad  $W(\alpha, \gamma)$  face, and the intersection of the black corners of a  $B(\alpha, \beta)$  bigon and  $H_B$ .

**Claim.** *There is only one local configuration at  $v$  as shown in Figure 2.20 (i).*

*Proof.* Follow the proof of the claim in Lemma 2.4.3 with  $\beta, \delta$  replaced by  $\gamma, \alpha$  respectively.  $\square$

Let  $u$  be an interior vertex in  $\Lambda$ . Since every white face in  $\Lambda$  is either a  $W(\alpha, \delta)$  trigon or a bad  $W(\alpha, \gamma)$  face by Theorem 2.3.5, there are only two possible types of the local configuration at  $u$  by Lemma 2.2.5. See Figure 2.20 (ii), (iii). However either type is also impossible since a  $B(\delta, \gamma)$  corner in Figure 2.20 (ii) and a  $B(\delta, \delta)$  corner in Figure 2.20 (iii) cannot happen by the existence of a  $B(\epsilon_N, \epsilon'_S)$  corner coming from the local configuration at  $v$  in the claim. This completes the proof.  $\square$

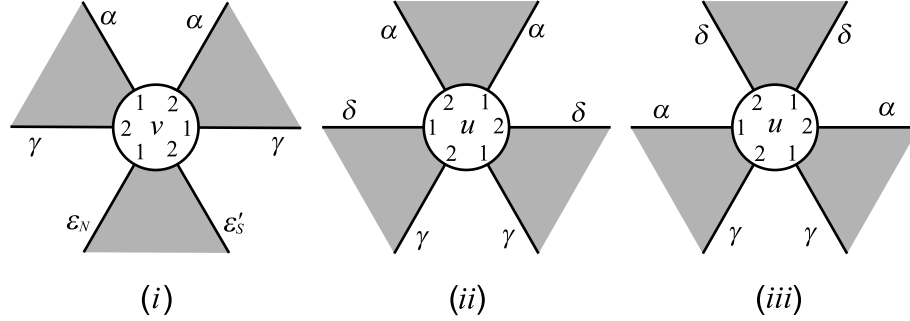


Figure 2.20: A non-exceptional vertex having a  $W(\alpha, \alpha)$  corner (i), and local configurations of an interior vertex (ii), (iii).

**Lemma 2.4.7.** *There is no source or sink dual to a black face in  $\Lambda^*$  with respect to  $\omega'$ .*

*Proof.* Suppose there is a source or sink dual to a black face with respect to  $\omega'$ , i.e. there is a  $B(\lambda, \mu)$  face where  $\{\lambda, \mu\} = \{\alpha, \gamma\}$  or  $\{\beta, \delta\}$ . Then a  $B(\lambda, \mu)$  face must be bad by Lemma 2.2.7 since  $\Lambda$  contains a  $B(\alpha, \beta)$  bigon.

Suppose we have a bad  $B(\beta, \delta)$  face. Consider the intersection of the black corners of a  $B(\alpha, \beta)$  bigon, the black corners of a bad  $B(\beta, \delta)$  face and  $H_B$  as in Figure 2.21 (iii), and the intersection of the white corners of a  $W(\alpha, \delta)$  trigon and  $H_W$  where there are two cases as in Figure 2.21 (i), (ii). By Theorem 2.3.5, every black face is either a  $B(\alpha, \beta)$  bigon or a bad  $B(\beta, \delta)$  face. Also, since three edges in the same edge class cannot be incident to a vertex, there are only two types of the local configuration at interior vertices. See Figure 2.22 (i), (ii). Note that the white corners of an interior vertex rule

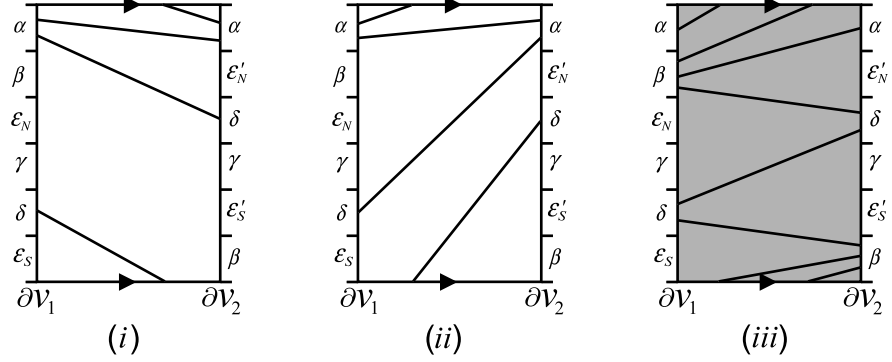


Figure 2.21: The intersection of the white corners of a  $W(\alpha, \delta)$  trigon and  $H_W$ , and the intersection of  $H_B$  and the black corners of a  $B(\alpha, \beta)$  bigon and a bad  $B(\beta, \delta)$  face.

out Figure 2.21 (ii).

**Claim.** *If a bad  $B(\beta, \delta)$  face has a  $B(\beta, \beta)$  corner which appears at a non-exceptional vertex  $w$ , then the dual cycle to  $w$  has index  $-1$ . Hence a bad  $B(\beta, \delta)$  face and  $w$  contribute 0 to the sum  $\sum_{vertices} I(v) + \sum_{faces} I(f)$ .*

*Proof.* An argument similar to the proof of the claim in Lemma 2.4.3 shows that the local configuration at  $w$  looks like Figure 2.22 (iii). Then  $w$  has index  $-1$ . This completes the proof.  $\square$

Suppose no  $B(\beta, \beta)$  corners appear at an exceptional vertex. Lemmas 2.3.11, 2.4.5, 2.4.6 and the claim imply that the only possible positive index comes from the cycle dual to an exceptional vertex or the sink or source dual to the outside face. However both cannot happen simultaneously so we get a contradiction to the equation  $\sum_{vertices} I(v) + \sum_{faces} I(f) = 2$ . Hence there is

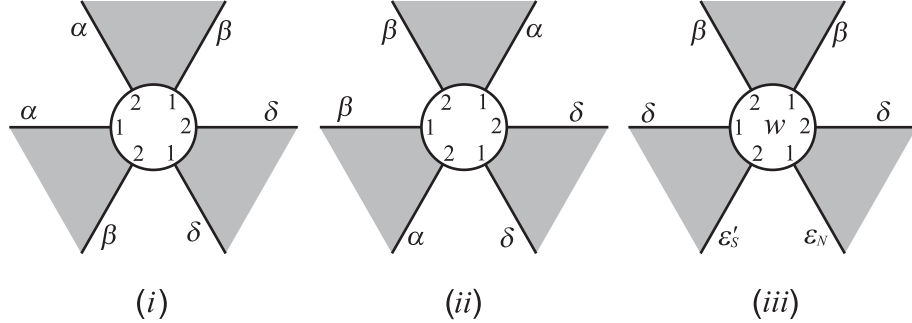


Figure 2.22: Local configurations at an interior vertex (i), (ii), and a non-exceptional vertex having a  $B(\beta, \beta)$  corner of a bad  $B(\beta, \delta)$  face (iii).

a  $B(\beta, \beta)$  corner of a  $B(\beta, \delta)$  face which must appear at an exceptional vertex. Then the rest of the proof is similar to the fourth and the fifth paragraphs of the proof of Lemma 2.4.4.

For the case that there is a bad  $B(\alpha, \gamma)$  face in  $\Lambda$ , apply an argument similar to the case of a  $B(\beta, \delta)$  face.  $\square$

By Lemmas 2.3.11 and 2.4.5 – 2.4.7 and the index equation  $\sum_{vertices} I(v) + \sum_{faces} I(f) = 2$ , we have proved Theorem 2.4.1 for the case that  $\Lambda$  contains a  $W(\alpha, \delta)$  with two  $\alpha$ -edges and one  $\delta$ -edge.

### 2.4.3 A $W(\beta, \gamma)$ Trigon, a $W(\beta, \delta)$ Trigon and a $W(\alpha, \gamma)$ Trigon

For the case of a  $W(\beta, \gamma)$  trigon, we can apply the same argument as in the case of a  $W(\alpha, \delta)$  trigon by interchanging  $\alpha$  and  $\beta$ , and by interchanging  $\gamma$  and  $\delta$ .

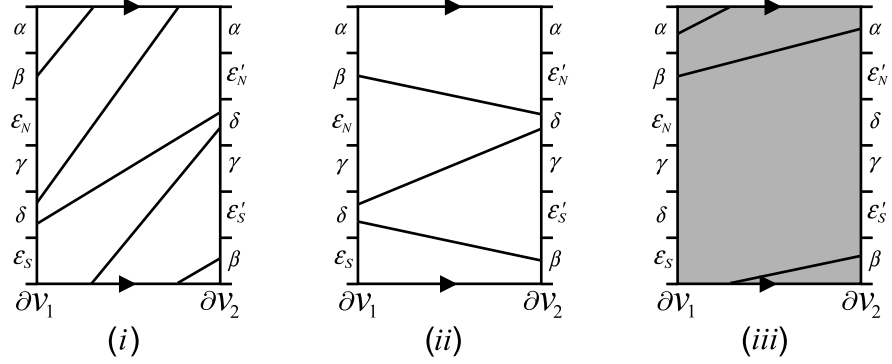


Figure 2.23: The intersection of the white corners of a  $W(\beta, \delta)$  trigon and  $H_W$ , and the intersection of the black corners of a  $B(\alpha, \beta)$  bigon and  $H_B$ .

Now suppose  $\Lambda$  contains a  $W(\beta, \delta)$  trigon with two  $\delta$ -edges and one  $\beta$ -edge. Here, instead of using the orientation  $\omega'$ , we will use the orientation  $\omega$ .

**Lemma 2.4.8.**  $\Lambda^*$  does not contain a boundary cycle with respect to  $\omega$ .

*Proof.* Consider the intersection of the white corners of a  $W(\beta, \delta)$  trigon and  $H_W$ , where there are two cases as in Figure 2.23 (i), (ii), and the intersection of the black corners of a  $B(\alpha, \beta)$  bigon and  $H_B$  as in Figure 2.23 (iii). Let  $v$  be a boundary vertex dual to a boundary cycle with respect to  $\omega$ . There are two types of the local configuration at  $v$  as shown in Figure 2.24 where  $e_1, e_2, e_3$  and  $e_4$  are positive edges, and  $e_5$  and  $e_6$  are negative edges.

First we assume Figure 2.23 (i); then if one edge of a white corner is an  $\alpha$ -edge, then the other edge of the corner must be a  $\delta$ -edge. Since an  $\alpha$ -edge

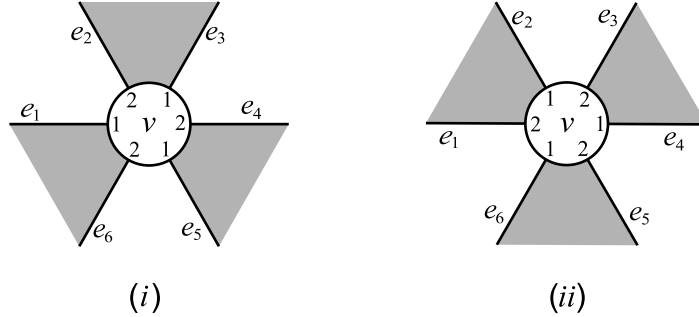


Figure 2.24: Local configurations at a boundary vertex.

and a  $\delta$ -edge have the same orientation with respect to  $\omega$ , there is no boundary cycle, as desired.

Second we assume Figure 2.23 (ii); then

1) The first type as in Figure 2.24 (i); Note that  $(e_5, e_6) = (\epsilon_S, \epsilon'_N)$  from the intersection of the white corners of a  $W(\beta, \delta)$  trigon and  $H_W$  as in Figure 2.23 (ii). That is, there is a  $W(\epsilon_S, \epsilon'_N)$  corner. Then Figure 2.23 (ii) with this corner inserted shows that if one edge of a white corner in  $\Lambda$  is an  $\alpha$ -edge, then the other edge must be a  $\delta$ -edge. Therefore, there is no boundary cycle.

2) The second type as in Figure 2.24 (ii); Assume there is a clockwise boundary cycle. If  $e_2 = \gamma$  and  $e_4 = \beta$ , then  $e_1 = \alpha$  and  $e_3 = \delta$ . In other words, we have a  $B(\gamma, \alpha)$  corner and a  $B(\beta, \delta)$  corner, which is impossible by Figure 2.23 (iii). If  $e_2 = \beta$  and  $e_4 = \gamma$ , then  $e_5$  must be  $\delta$  by Figure 2.23 (ii), which is also impossible because  $e_5$  is a negative edge.

Assume there is a anticlockwise boundary cycle. If  $e_1 = \gamma$ ,  $e_6$  must be

$\delta$  by Figure 2.23 (ii), which is impossible. If  $e_1 = \beta$  and  $e_3 = \gamma$ , then  $e_2 = \delta$  and  $e_4 = \alpha$ . In other words, we have a  $B(\alpha, \gamma)$  corner and a  $B(\delta, \beta)$  corner, which is impossible by Figure 2.23 (iii).  $\square$

*Remark:* As in the remark above Lemma 2.4.3, Figure 2.8 is not applicable in the proof of Lemma 2.4.8.

**Lemma 2.4.9.** *There is no source or sink dual to a white face in  $\Lambda^*$  with respect to  $\omega$ .*

*Proof.* Apply exactly the same argument as that of Lemma 2.4.3 by interchanging  $\alpha$  and  $\beta$ .  $\square$

**Lemma 2.4.10.** *There is no source or sink dual to a black face in  $\Lambda^*$  with respect to  $\omega$ .*

*Proof.* The proof is exactly the same as that of Lemma 2.4.4 with  $\alpha$  and  $\beta$  interchanged.  $\square$

In conclusion, by Lemmas 2.3.11, 2.4.8 – 2.4.10 and the index equation  $\sum_{\text{vertices}} I(v) + \sum_{\text{faces}} I(f) = 2$ , we have proved Theorem 2.4.1 for the case that  $\Lambda$  contains a  $W(\beta, \delta)$  trigon with two  $\delta$ -edges and one  $\beta$ -edge.

Now suppose  $\Lambda$  contains a  $W(\beta, \delta)$  with two  $\beta$ -edges and one  $\delta$ -edge.

**Lemma 2.4.11.**  *$\Lambda^*$  does not contain a boundary cycle with respect to  $\omega$ .*

*Proof.* The proof is completely similar as that of Lemma 2.4.8.  $\square$

**Lemma 2.4.12.** *There is no source or sink dual to a white face in  $\Lambda^*$  with respect to  $\omega$ .*

*Proof.* The proof is exactly the same as that of Lemma 2.4.6 with  $\alpha$  and  $\beta$  interchanged.  $\square$

**Lemma 2.4.13.** *There is no source or sink dual to a black face in  $\Lambda^*$  with respect to  $\omega$ .*

*Proof.* The proof is exactly the same as that of Lemma 2.4.7 with  $\alpha$  and  $\beta$  interchanged.  $\square$

In conclusion, by Lemmas 2.4.11, 2.4.12, and 2.4.13 and the equation  $\sum_{\text{vertices}} I(v) + \sum_{\text{faces}} I(f) = 2$ , we have proved Theorem 2.4.1 for the case that  $\Lambda$  contains a  $W(\beta, \delta)$  trigon with two  $\beta$ -edges and one  $\delta$ -edge.

For the case of a  $W(\alpha, \gamma)$  trigon, we can apply the same argument by interchanging  $\alpha$  and  $\beta$ , and by exchanging  $\gamma$  and  $\delta$ .

Finally, this completes the proof of Theorem 2.4.1.

## Chapter 3

### The Toroidal Dehn Filling

In this chapter, we give two descriptions of the toroidal Dehn filling  $M(r_2)$ .

#### 3.1 Topological Description of the Toroidal Dehn Filling $M(r_2)$

In this section, we show that the toroidal Dehn filling  $M(r_2)$  is the union of  $M_1$  and  $M_2$ , where  $M_i$ ,  $i = 1, 2$  is a Seifert fibered space over the disk with two exceptional fibers, along an incompressible torus.

Theorem 2.2.14 says that  $G_1$  contains a  $B(\alpha, \beta)$  face and a  $W(\lambda, \mu)$  bigon, where  $\{\lambda, \mu\} = \{\alpha, \delta\}, \{\alpha, \gamma\}, \{\beta, \delta\}$  or  $\{\beta, \gamma\}$ . We may assume without loss of generality that  $G_1$  contains a  $B(\alpha, \beta)$  face and a  $W(\alpha, \delta)$  bigon.

The next proposition will be used to prove Theorem 3.1.4.

**Proposition 3.1.1.**  *$G_1$  contains either a black bigon with two positive edges or a trigon.*

*Remark:* There are two types of trigons in  $G_1$ ; one is a trigon with all positive edges and the other is a trigon with one positive edge and two negative edges.

To prove Proposition 3.1.1, we need two lemmas.

**Lemma 3.1.2.** *There is no bigon in  $G_1$  whose edges are negative with a  $(\epsilon_N, \epsilon'_S)$  corner and a  $(\epsilon_S, \epsilon'_N)$  corner as shown in Figure 3.1 (i).*

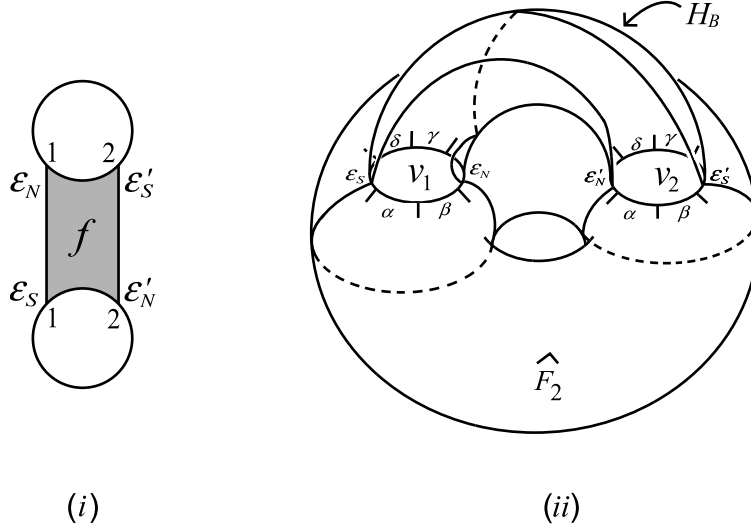


Figure 3.1: A black bigon with negative edges and with a  $(\epsilon_N, \epsilon'_S)$  corner and a  $(\epsilon_S, \epsilon'_N)$  corner.

*Proof.* Let  $f$  be such a bigon as in the hypothesis. We assume without loss of generality that  $f$  is black. Recall that  $\widehat{F}_2$  is an incompressible torus containing the graph  $G_2$  and  $H_B$  is the intersection of  $V_2$  and a black side of  $M$ .  $\partial f$  appears on  $\widehat{F}_2 \cup H_B$  as in Figure 3.1 (ii).

The two endpoints of the negative edges  $\epsilon$  and  $\epsilon'$  of  $f$  separate  $\partial v_1$  and  $\partial v_2$  into two arcs respectively. Let  $a$  (resp.  $b$ ) be the arc on  $\partial v_1$  (resp.  $\partial v_2$ )

which contains the endpoints of  $\alpha$ -,  $\beta$ -edges at  $v_1$  (resp.  $\gamma$ -,  $\delta$ -edges at  $v_2$ ). Then  $\epsilon \cup a$  and  $\epsilon' \cup b$  are circles which cobound an annulus on  $\widehat{F}_2$ , denoted by  $A$ . Also the two corners of  $f$  separate  $\overline{H_B - (v_1 \cup v_2)}$  into two disks; let  $D$  be one which contains  $a$  and  $b$ . Then  $A \cup D$  is an once punctured Klein bottle. Therefore  $A \cup D \cup f$  is a Klein bottle, which is a contradiction.  $\square$

**Lemma 3.1.3.** *No white  $(\epsilon_N, \epsilon'_N)$  or  $(\epsilon_S, \epsilon'_S)$  corners exist in  $G_1$ .*

*Proof.* Since there is a  $W(\alpha, \delta)$  bigon, we have a  $W(\alpha, \delta)$  corner and a  $W(\delta, \alpha)$  corner. Then it follows from Lemma 2.2.4 that a white  $(\epsilon_N, \epsilon'_N)$  or  $(\epsilon_S, \epsilon'_S)$  corner cannot exist.  $\square$

*Proof of Proposition 3.1.1.* Suppose for contradiction that  $G_1$  does not contain a black bigon with positive edges and does not contain a trigon. Observe that Lemmas 3.1.2 and 3.1.3 imply that  $G_1$  does not contain a white bigon with two negative edges. Let  $\overline{G}$  be a connected component of the reduced graph  $\overline{G}_1$  of  $G_1$ . Note that  $\overline{G}$  is a graph on the sphere  $\widehat{F}_1$ .

**Claim.** *Every vertex in  $\overline{G}$  has valency at least 4.*

*Proof.* Since  $G_1$  does not contain a black bigon with positive edges and does not contain a white bigon with negative edges, it is easy to see that no vertex in  $\overline{G}$  has valency 1 or 2. Suppose a vertex  $v$  in  $\overline{G}$  has valency 3. Then there are four types of the local configuration at  $v$  in  $G_1$ . See Figure 3.2.

For the first and second types, since there is no black bigon with positive edges, the edges of the black bigons in Figure 3.2 (i), (ii) are negative. Thus

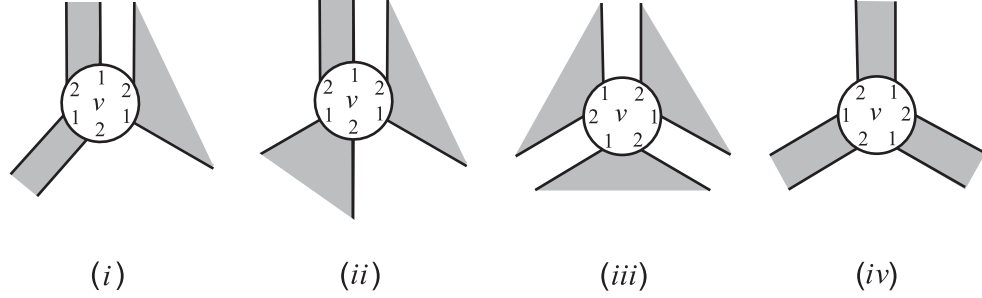


Figure 3.2: A vertex of valency 3 in  $\overline{G}$ .

the adjacent white bigon has two negative edges, which is a contradiction.

For the third type, all edges of the three white bigons in Figure 3.2 (iii) are positive since there is no white bigon with negative edges in  $G_1$ . By [15, Lemma 5.2], all the three white bigons are  $W(\alpha, \delta)$  bigons. Therefore there are two edges in the same edge class at the same label at  $v$ , which is a contradiction to Lemma 2.2.5.

If we have the fourth type as in Figure 3.2 (iv), all black bigons have negative edges. By Lemma 3.1.2, all the corners of these black bigons are either  $B(\epsilon_N, \epsilon'_N)$  corners or  $B(\epsilon_S, \epsilon'_S)$  corners. This condition forces one of the three white corners at  $v$  to be either a white  $(\epsilon_N, \epsilon'_N)$  corner or a white  $(\epsilon_S, \epsilon'_S)$  corner, which is impossible by Lemma 3.1.3.

Therefore, every vertex in  $\overline{G}$  has valency at least 4. □

Let  $V, E, F$  be the number of vertices, edges and faces respectively in  $\overline{G}$ . Since no trigons exist in  $G_1$ , no trigons exist in  $\overline{G}$ . So every face except one

in  $\overline{G}$  has at least 4 edges. Hence,  $4F - 4 \leq 2E$ . Combined with  $V - E + F = 2$ , we get  $2E \leq 4V - 4$ . On the other hand, by the claim,  $4V \leq 2E$ . This is a contradiction.  $\square$

For the purpose of the next theorem, let  $D^2(p, q)$  be a Seifert fibered space over the disk with two exceptional fibers of orders  $p$  and  $q$  respectively. Recall that  $M(r_2)$  is a toroidal Dehn filling.

**Theorem 3.1.4.**  *$M(r_2)$  is either  $D^2(2, q) \cup_T D^2(2, s)$ ,  $D^2(2, 3) \cup_T D^2(r, s)$  or  $D^2(2, q) \cup_T D^2(3, s)$  where  $T$  is an incompressible torus in  $M(r_2)$ . Furthermore, the fibers of the two Seifert fibered subspaces of  $M(r_2)$  intersect exactly once on  $T$ .*

*Proof.*  $G_1$  contains a  $W(\alpha, \delta)$  bigon and a  $B(\alpha, \beta)$  face. Then Theorem 2.2.3 and Lemma 2.2.11 imply that  $M(r_2)$  is  $D^2(2, q) \cup_T D^2(r, s)$  where  $T$  is  $\widehat{F}_2$  and the two fibers are induced from an  $\alpha \cup \delta$  curve and an  $\alpha \cup \beta$  curve respectively which intersect exactly once on  $T$ .

On the other hand, Proposition 3.1.1 guarantees the existence of either a black bigon with two positive edges or a trigon in  $G_1$ . If  $G_1$  contains a black bigon with two positive edges,  $M(r_2)$  is  $D^2(2, q) \cup_T D^2(2, s)$ , which is the first case.

If  $G_1$  contains a trigon with three positive edges, which is a good face, then by Theorem 2.2.3 one of orders of the four exceptional fibers is 3. Then  $M(r_2)$  is either  $D^2(2, 3) \cup_T D^2(r, s)$  or  $D^2(2, q) \cup_T D^2(3, s)$  depending on which side the trigon lies in.

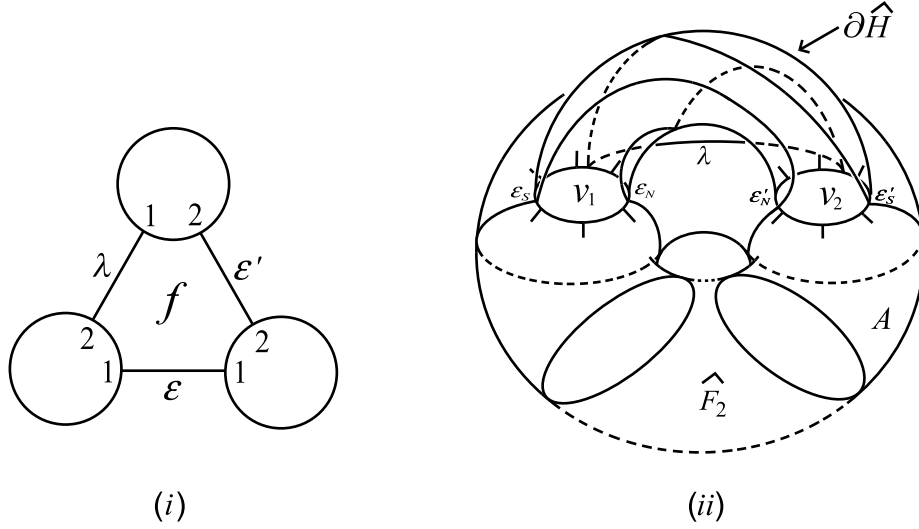


Figure 3.3: A trigon with two negative edges and one positive edge.

The only remaining case is when  $G_1$  has a trigon with two negative edges and one positive edge. Let  $f$  be a trigon with one  $\lambda$ -edge and two negative edges where  $\lambda \in \{\alpha, \beta, \gamma, \delta\}$  as in Figure 3.3 (i). Then Lemma 2.2.4 (if  $f$  is black) and Lemma 3.1.3 (if  $f$  is white) imply that the  $(\epsilon, \epsilon')$  corner of  $f$  must be either a  $(\epsilon_N, \epsilon'_S)$  corner or a  $(\epsilon_S, \epsilon'_N)$  corner.

Recall that  $\widehat{F}_2$  is an incompressible torus containing the graph  $G_2$ . Let  $\widehat{H}$  be the intersection of  $V_2$  and the side of  $M(r_2)$  where  $f$  lies.  $\partial f$  appears on  $\widehat{F}_2 \cup \partial \widehat{H}$  as in Figure 3.3 (ii). Let  $A$  be an annulus on  $\widehat{F}_2$  containing all the edges of  $f$ . Let  $N$  be the regular neighborhood of  $\widehat{H} \cup A \cup f$  in the side where  $f$  lies. Then it is easy to see that the fundamental group of  $N$  is isomorphic to the group  $\langle x, y \mid x^2 y^3 = 1 \rangle$ . Therefore  $N$  is homeomorphic to  $D^2(2, 3)$ . This implies the second case of  $M(r_2)$ .  $\square$

### 3.2 A Link Surgery Description of the Toroidal Dehn Filling $M(r_2)$

In this section, we interpret the toroidal Dehn filling  $M(r_2)$  as the manifold obtained by Dehn surgery on some link  $L$  in  $S^3$  by using a black good face and a white good face.

$G_1$  contains a  $B(\alpha, \beta)$  face and a  $W(\alpha, \delta)$  bigon. We denote them by  $f_1$  and  $f_2$  respectively. Note that a  $B(\alpha, \beta)$  face is good by Lemma 2.2.10.

Then we are exactly in the same situation as in [16, Section 5]. Thus we go through the same terminology and arguments as in [16, Section 5].

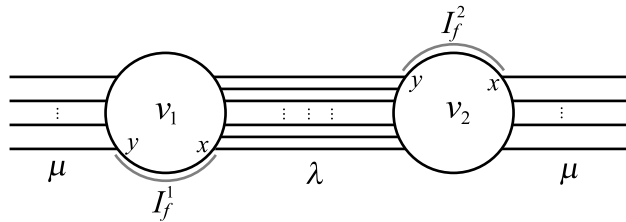


Figure 3.4: The external interval of  $f$ .

Let  $f$  be a good  $(\lambda, \mu)$  face in  $\Lambda$ . Then by Lemma 4.2 in [16], there are vertices  $x, y$  of  $f$  in  $\Lambda$ , representing corners of  $\partial f$ , such that the edges of  $\partial f$  on  $G_2$  are, up to homeomorphism, as in Figure 3.4. The interval  $[x, y]$  on vertex  $v_i$ ,  $i = 1, 2$ , that contains no edges of  $\partial f$  in its interior, is called *the external interval of  $f$  on vertex  $v_i$* , denoted by  $I_f^i$ . In particular, if  $f$  is a bigon, there are two such intervals. Then we denote the external interval of  $f_i$  at vertex  $v_j$  by  $I_i^j$ ,  $j = 1, 2$ . There are two choices on  $I_2^j$ :

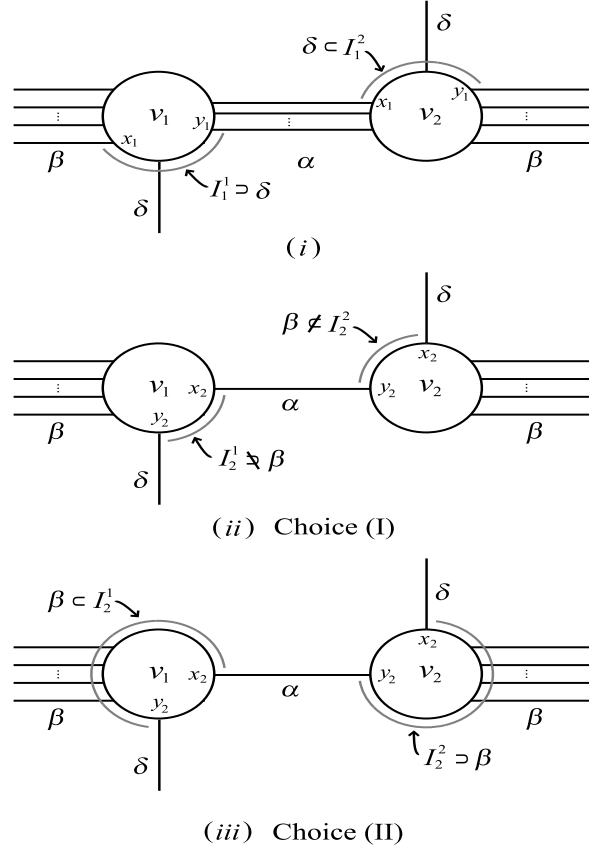


Figure 3.5: The external intervals of  $f_1$  and  $f_2$ .

- Choice (I).  $I_2^j$  does not contain the endpoints of the edge class  $\beta$ .
- Choice (II).  $I_2^j$  contains the endpoints of the edge class  $\beta$ .

Note that  $I_1^j$  contains the endpoints of the edge class  $\delta$ . See Figure 3.5.

Recall that  $M(r_2) = \widehat{M}_B \cup_{\widehat{F}_2} \widehat{M}_W$  and  $\widehat{H}_B$  (resp.  $\widehat{H}_W$ ) =  $V_2 \cap \widehat{M}_B$  (resp.  $\widehat{M}_W$ ). For convenience, we change indices  $B, W$  into  $1, 2$  respectively

and we let  $V$  be the attached solid torus to  $M$ . Recall that  $r_1$  and  $r_2$  are slopes on  $\partial_0 M = \partial V$  such that  $M(r_1)$  is reducible and  $M(r_2)$  is toroidal and the boundary components of  $F_1$  have slopes  $r_1$ .

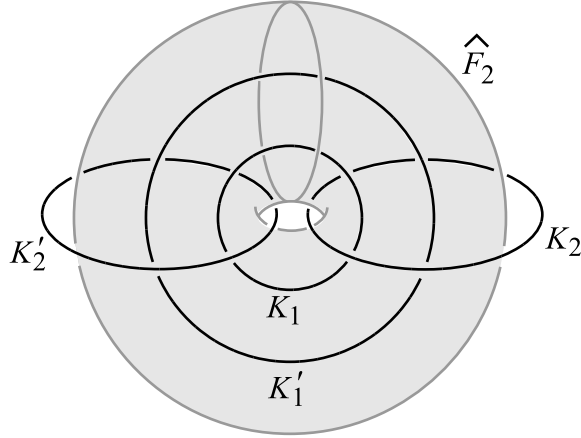


Figure 3.6: The link  $L_0 = K_1 \cup K'_1 \cup K_2 \cup K'_2$ .

Now follow the argument from page 452 through page 457 in [16, Section 5] with some notations changed, i.e. with  $\epsilon, \delta_1, \delta_2, H_1, H_2, \mu, \tau, Q, T$  and  $M_i$  replaced by  $\alpha, \beta, \delta, \widehat{H}_1, \widehat{H}_2, r_1, r_2, F_1, F_2$ , and  $\widehat{M}_i$ .

Then from page 456 and page 457 in [16, Section 5], we have the following:  $(M(r_2), K_{r_2})$  is obtained from  $(S^3, K_0)$  by some Dehn surgery on  $L_0$  where  $K_{r_2}$  is the core of  $V$  in  $M(r_2)$ . That is, the exterior of  $K_{r_2}$  is obtained from the exterior of  $K_0$  in  $S^3$  by a Dehn surgery on  $L_0$ . Moreover, given the 0-framing of  $K_0$  in  $S^3$ , the meridian of  $K_0$  corresponds to the slope  $r_2$  on  $\partial V$ .

Here, as in Section 5 in [16],  $K_0$  means the core of  $V = \widehat{H}_1 \cup \widehat{H}_2 \subset S^3$

and  $L_0$  means the link  $K_1 \cup K'_1 \cup K_2 \cup K'_2$  in  $S^3$  depicted in Figure 3.6. Also let  $L$  be the link  $L = K_1 \cup K'_1 \cup K_2 \cup K'_2 \cup K_0$ . Then  $L$  looks like Figure 3.7 according to the two choices (I), (II) on  $I_2^j$ . Note that  $L$  in Choice (II) is the reflection of  $L$  in Choice (I) (in which  $K_i \mapsto K_i$ ,  $0 \leq i \leq 2$ , and  $K'_i \mapsto K'_i$ ,  $i = 1, 2$ ). Therefore under this reflection the  $r_1$ -framing on  $K_0$  goes to the  $(-r_1)$ -framing (and the longitude to the longitude).

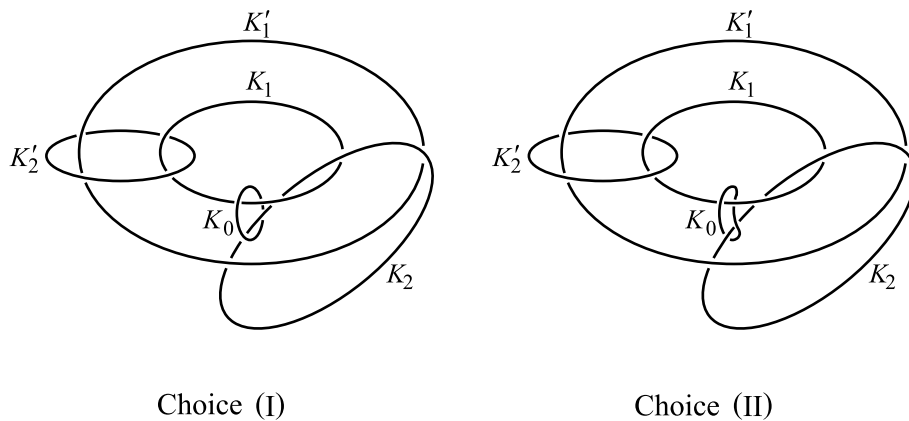


Figure 3.7: The link  $L = K_1 \cup K'_1 \cup K_2 \cup K'_2 \cup K_0$ .

Let  $L(\theta, \varphi, \psi, \omega, \pi)$  be the Dehn filling on the exterior of  $L$  where  $\theta, \varphi, \psi, \omega, \pi$  denote the filling slopes on  $K_1, K'_1, K_2, K'_2, K_0$  respectively. When one of the filling slopes is an asterisk (\*), then no filling is done on the corresponding component.

**Proposition 3.2.1.**  $M = L(\theta, \varphi, \psi, \omega, *)$  where  $L$  is the link from Choice (I) as in Figure 3.7. Furthermore, the reducible Dehn filling  $M(r_1)$  is  $L(\theta, \varphi, \psi, \omega, 1/3)$  and the toroidal Dehn filling  $M(r_2)$  is  $L(\theta, \varphi, \psi, \omega, 1/0)$ .

*Proof.* From the above discussion, we need only to show that  $\pi = 1/3$  for  $M(r_1)$ . In other words, with respect to the framing of  $K_0$ , the slope  $r_1$  is  $1/3$ . Let  $a$  be a vertex in  $G_1$  which contains a  $B(\beta, \alpha)$  corner of a  $B(\alpha, \beta)$  face  $f_1$ . That is,  $v_1$  in  $G_2$  has the label  $a$  at the endpoint of a  $\beta$ -edge and  $v_2$  in  $G_2$  has the label  $a$  at the endpoint of an  $\alpha$ -edge. Let  $b$  be a vertex in  $G_1$  which contains a  $W(\alpha, \delta)$  corner of a  $W(\alpha, \delta)$  bigon  $f_2$ . Then it suffices to show that  $\partial b$  has slope  $1/3$ .

$\partial b$  consists of three black corners and three white corners, one of which is a  $W(\alpha, \delta)$  corner. There are three occurrences of the label  $b$  at  $v_1$  and  $v_2$ . Let  $b_1, b_2$  and  $b_3$  be the labels representing three occurrences of  $b$  at  $v_1$  and  $v_2$  such that  $b_i$  at  $v_1$  and  $b_i$  at  $v_2$  are connected by a black corner of the vertex  $b$ , and  $b_i$  at  $v_2$  and  $b_{i+1}$  at  $v_1$  are connected by a white corner of the vertex  $b$ ,  $i = 1, 2, 3$  (let  $b_4 = b_1$ ). We assume that a  $W(\alpha, \delta)$  corner connects  $b_3$  at  $v_2$  and  $b_1$  at  $v_1$ . The labels  $b_1, b_2$  and  $b_3$  on  $\partial v_1$  and  $\partial v_2$  occur either in the order  $b_1 b_2 b_3$  or in the order  $b_1 b_3 b_2$ .

First, we assume the order  $b_1 b_2 b_3$ . Then we take Choice (I) for  $I_2^j$ . Since the  $r_1$ -framings on  $\widehat{H}_1$  and  $\widehat{H}_2$  are shown Figure 5.16 and Figure 5.17 Case (I) in [16] respectively, a  $B(\beta, \alpha)$  corner and a  $W(\alpha, \delta)$  corner, which are uniquely determined on  $\partial \widehat{H}_1$  and  $\partial \widehat{H}_2$  respectively are given in Figure 3.8 (i). Therefore,  $\partial v$  has slope  $1/3$ .

Second, we assume the order  $b_1 b_3 b_2$ . Then we take Choice (II) for  $I_2^j$ . The  $r_1$ -framing on  $\widehat{H}_2$  is shown in Figure 5.17 Case (II) in [16]. Thus,  $\partial v$  has slope  $-1/3$ . See Figure 3.8 (ii). Under the reflection sending  $L$  in Choice (II)

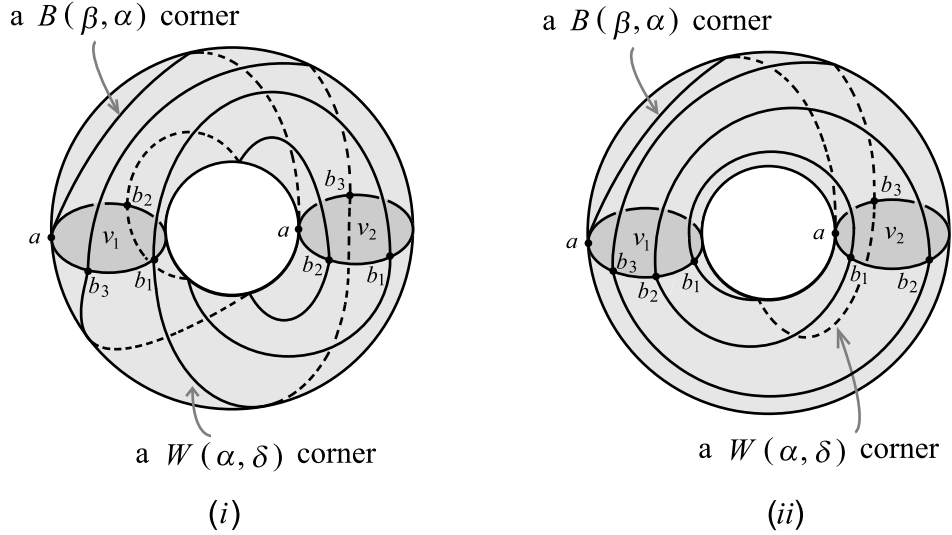


Figure 3.8: The  $r_1$ -framing.

to  $L$  in Choice (I),  $-1/3$  in Choice (II) goes to  $1/3$  in Choice (I). Therefore we may assume without loss of generality that  $\pi = 1/3$  in Choice (I). This completes the proof of  $\pi = 1/3$ .  $\square$

**Lemma 3.2.2.**  $\psi$  is equal to 2 in Choice (I) and  $-2$  in Choice (II).

*Proof.*  $\psi$  is the filling slope on  $K_2$ , which is a core of  $V_2$  disjoint from  $\widehat{H}_2 \cup R_2$ . Also  $(W_2; \widehat{H}_2, R_2)$  is obtained from  $(V_2; \widehat{H}_2, R_2)$  by  $\psi$ -Dehn filling on  $K_2$  as described in the page 456 in [16]. Recall that  $W_2 = \text{nbhd}(A_2 \cup \widehat{H}_2 \cup f_2)$ . Since  $f_2$  is a  $W(\alpha, \delta)$  bigon,  $W_2$  is the neighborhood of a Möbius band. Then with the standard framing on  $K_2$  which is shown in Figure 5.17 Case (I) of [16], we easily see that  $\psi = 2$  in Choice (I). For Choice (II), notice that the longitude has the opposite orientation to Choice (I). Therefore,  $\psi = -2$  in

Choice (II).



## Chapter 4

# Dehn Fillings on a Link and Tangle Fillings on a Tangle

### 4.1 Tangle Description of $M$ with Tangle Slopes

From now on,  $L$  is the link in Choice (I) as in Figure 3.7. Proposition 3.2.1 says that  $M$ , the reducible Dehn filling  $M(r_1)$  and the toroidal Dehn filling  $M(r_2)$  are obtained by Dehn surgery on  $L$ .  $L$  is strongly invertible and the quotient of the exterior under this involution gives rise to a tangle. Therefore  $M$ ,  $M(r_1)$  and  $M(r_2)$  are double branched covers of  $S^3$  along some tangles or some links which are obtained by rational tangle fillings on the tangle obtained from the quotient of the exterior of  $L$ .

We will use the same convention on rational tangles and the same terminology as in [16, Section 6]. Let  $T(\alpha_1, \dots, \alpha_n)$  be a filling of a tangle  $T$  where  $\alpha_i \in \mathbf{Q} \cup \{1/0\}$ ,  $1 \leq i \leq n$ . Then the double branched cover of  $S^3$  along the link  $T(\alpha_1, \dots, \alpha_n)$  is a closed 3-manifold denoted by  $\tilde{T}(\alpha_1, \dots, \alpha_n)$ .

By Proposition 3.2.1,  $M = L(\theta, \varphi, \psi, \omega, *)$ . Figure 4.1 (i) shows that  $L$  is strongly invertible and depicts the quotient along with its fixed set. Then the quotient of  $(S^3, L)$  under this strong inversion is  $P(\frac{0}{1}, \frac{1}{1}, \frac{0}{1}, \frac{1}{1}, \frac{0}{1})$  as in Figure 4.1 (ii), where  $P$  is the pentangle (see [16, Section 6] for the definition of

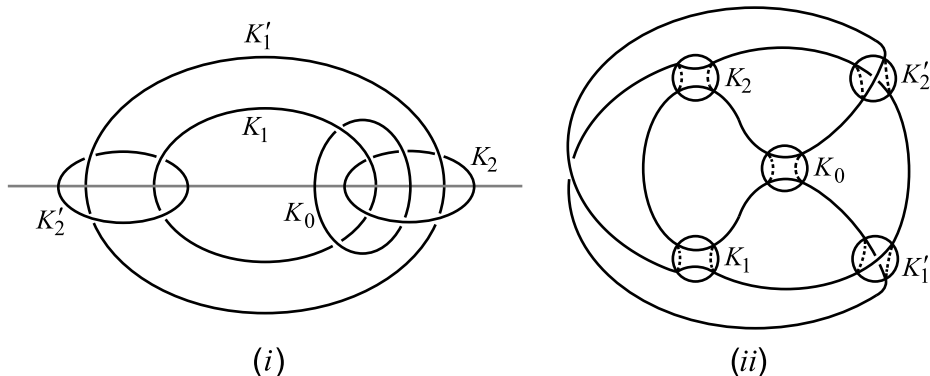


Figure 4.1: The strong invertibility of  $L$  and the quotient of  $(S^3, L)$ .

the pentangle) and invariant regular neighborhoods of  $L$  become tangle balls in the quotient. In other words, the quotient of the exterior  $E(L)$  of  $L$  in  $S^3$  under the involution is the pentangle  $P$ . The longitude framings of  $\partial E(L)$  pass to the  $\frac{1}{0}$  framings of the tangle balls as indicated by the dashed lines. The meridian framings of  $\partial E(L)$  pass to the  $\frac{0}{1}$  framings of the tangle balls for  $K_0, K_1, K_2$  and  $\frac{1}{1}$  framings for  $K'_1, K'_2$  as indicated by the solid lines. In particular the (meridian, longitude)-framings of  $K_0, K_2$  pass to the  $(\frac{0}{1}, \frac{1}{0})$ -framing of the corresponding tangle spheres of  $P$ , which implies with Proposition 3.2.1 and Lemma 3.2.2 that the reducible Dehn filling  $M(r_1) = L(\theta, \varphi, 2, \omega, 1/3)$  is  $\tilde{P}(\theta', \varphi', 1/2, \omega', 3)$  and the toroidal Dehn filling  $M(r_2) = L(\theta, \varphi, 2, \omega, 1/0)$  is  $\tilde{P}(\theta', \varphi', 1/2, \omega', 0/1)$ .

However we can regard the pentangle  $P(\theta', \varphi', 1/2, \omega', *)$  as the tangle  $Q(-1/\theta', -1/\varphi', -1/\omega', *)$  by rotating the pentangle by  $-\pi/2$  where  $Q$  is the tangle as shown in Figure 4.2 (ii). Note that the tangle  $Q$  admits a

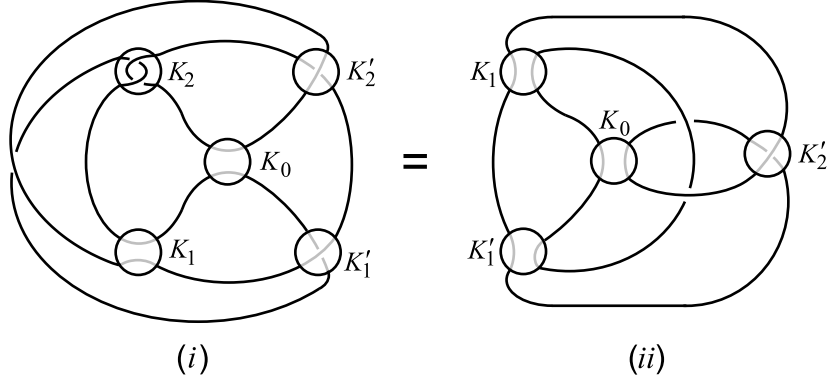


Figure 4.2: The pentangle  $P(\theta', \varphi', 1/2, \omega', *) =$  the tangle  $Q(-1/\theta', -1/\varphi', -1/\omega', *)$ .

symmetry by rotation in the horizontal axis. Without ambiguity, if we let  $\theta, \varphi, \omega$  be  $-1/\theta', -1/\varphi', -1/\omega'$  respectively, then  $M = \tilde{Q}(\theta, \varphi, \omega, *)$ ,  $M(r_1) = \tilde{Q}(\theta, \varphi, \omega, -1/3)$  and  $M(r_2) = \tilde{Q}(\theta, \varphi, \omega, 1/0)$ .

Then we will show that  $\theta = 2, \varphi = p - 2$  and  $\omega = 1/p$  where  $p$  is an integer less than  $-2$ . In other words, we will prove the following in the rest of the sections.

**Theorem 4.1.1.**  $M = \tilde{Q}(2, p - 2, 1/p, *)$ ,  $M(r_1) = \tilde{Q}(2, p - 2, 1/p, -1/3)$  and  $M(r_2) = \tilde{Q}(2, p - 2, 1/p, 1/0)$ . where  $p$  is an integer and  $p \leq -2$ .

*Remark:* In Theorem 4.1.1, the tangle  $Q(2, p - 2, 1/p, *)$  is the reflection of the tangle given in Figure 1.1 (i) on page 2. Hence Theorem 4.1.1 implies Theorem 1.4.1.

## 4.2 Some Restrictions on Tangle Slopes $\theta, \varphi$ and $\omega$

We do a series of computations describing the double branched covers of certain tangle filling of  $Q$  and combining this with certain Dehn filling theorems, we put restrictions on the tangle slopes  $\theta, \varphi$  and  $\omega$ .

**Lemma 4.2.1.** *Let  $M$  be an irreducible 3-manifold with  $\partial M$  a torus. Let  $\theta, \varphi$  be slopes on  $\partial M$  such that  $M(\theta)$  is reducible ( $\neq S^2 \times S^1$ ) and  $M(\varphi)$  is either reducible, a lens space, or  $S^3$ . Then  $\Delta(\theta, \varphi) \leq 1$ .*

*Proof.* This is exactly Lemma 8.1 of [16]. □

*Remark:* In the proof of Lemma 8.1 of [16] it is overlooked that  $M(\theta)$  could be  $S^2 \times S^1$ . In order for the proof to be correct,  $M(\theta)$  should not be  $S^2 \times S^1$ .

**Lemma 4.2.2.**  $\theta, \varphi \notin \{-1, 0, 1, 1/0\}$  and  $\omega \notin \{-1, 0, 1, 1/0, 1/2\}$ .

*Proof.* Let  $W(*)$  be  $Q(*, \varphi, \omega, 1/0)$ . Then  $W(\theta) = Q(\theta, \varphi, \omega, 1/0)$  and  $\widetilde{W}(\theta) = \widetilde{Q}(\theta, \varphi, \omega, 1/0)$  ( $= M(r_2)$ ). Theorem 3.1.4 says that  $M(r_2) = \widetilde{W}(\theta)$  is a toroidal manifold and is not a Seifert fibered space. Moreover, by [14],  $\widetilde{W}(\theta)$  is also irreducible since  $\Delta(r_1, r_2) = \Delta(1/0, -1/3) = 3$ . Consider the rational tangle fillings  $W(-1), W(0), W(1)$  and  $W(1/0)$ . See Figure 4.3. Then the double branched cover of each tangle filling is either a Seifert fibered space or a reducible manifold, which is impossible. Therefore,  $\theta \notin \{-1, 0, 1, 1/0\}$ . On the other hand, the tangle  $Q$  admits a symmetry by rotation in the horizontal axis, which interchanges  $\theta, \varphi$ . Therefore  $\varphi \notin \{-1, 0, 1, 1/0\}$ .

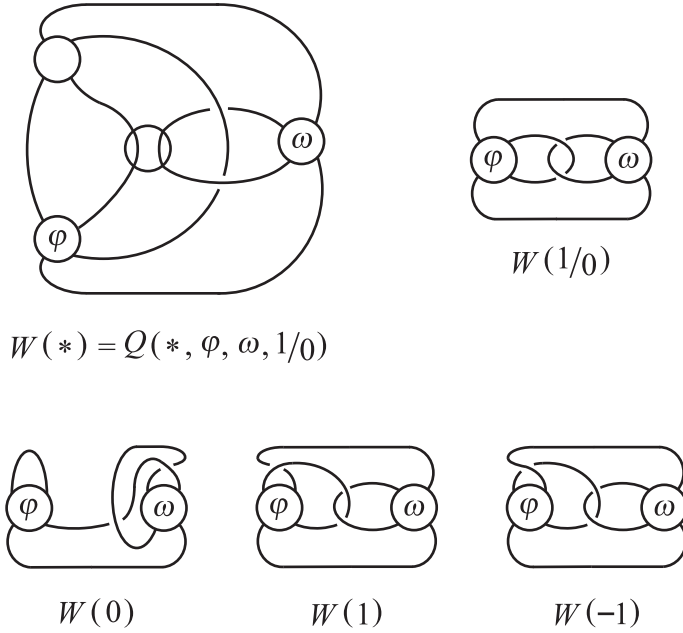


Figure 4.3:  $W(*) = Q(*, \varphi, \omega, 1/0)$  and the rational tangle fillings.

For  $\omega$ , let  $W'(*)$  be  $Q(\theta, \varphi, *, 1/0)$ . Then  $M(r_2) = \widetilde{W}'(\omega)$  is a toroidal and irreducible manifold and is not a Seifert fibered space. Consider the rational tangle fillings illustrated in Figure 4.4. The double branched cover of each tangle filling is either a Seifert fibered space or a reducible manifold, which is impossible. Hence  $\omega \notin \{-1, 0, 1, 1/0\}$ .

If  $\omega = 1/2$ , then  $M(r_2) = \widetilde{W}'(1/2)$  contains a Klein bottle from figure 4.4, which is a contradiction. Thus  $\omega \neq 1/2$ . □

Recall that  $D^2(a, b)$  is a Seifert fibered space over  $D^2$  with two exceptional fibers of orders  $a, b$ . Similarly, let  $S^2(a, b, c)$  be a Seifert fibered space over  $S^2$  with three exceptional fibers of orders  $a, b, c$ .

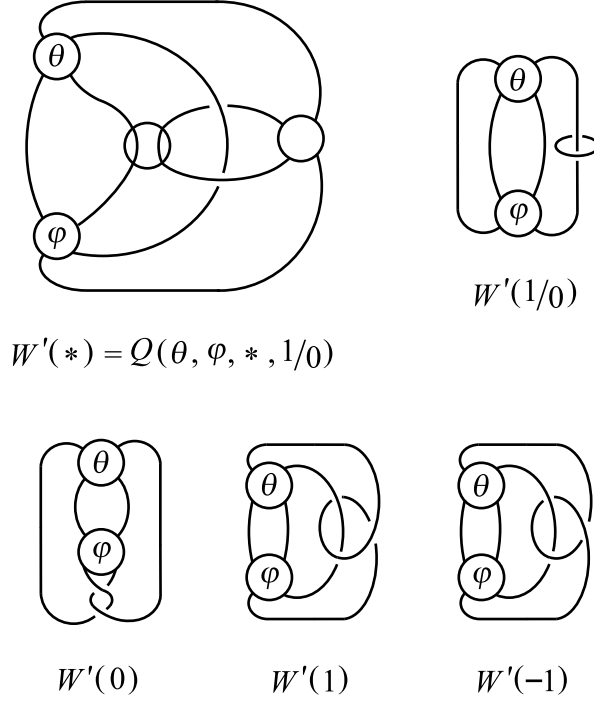


Figure 4.4:  $W'(*) = Q(\theta, \varphi, *, 1/0)$  and the rational tangle fillings.

**Lemma 4.2.3.**  $\theta, \varphi$  are integers and  $\omega$  is  $1/k$  where  $k$  is an integer.

*Proof.* First, we show that  $\theta$  is an integer. Let  $W(*) = Q(*, \varphi, \omega, -1/3)$ . Then  $\widetilde{W}(\theta) = \widetilde{Q}(\theta, \varphi, \omega, -1/3)$  is  $M(r_1)$ , which is reducible. We perform the rational tangle fillings shown in Figure 4.5. Observe that  $\widetilde{W}(1/0)$  is either  $S^3$ ,  $S^2 \times S^1$  or a lens space. Hence  $\Delta(\theta, 1/0) \leq 1$  by Lemma 4.2.1, provided that  $\widetilde{W}(*)$  is irreducible. Note that  $\widetilde{W}(\theta) = M(r_1)$  is not  $S^2 \times S^1$  by [29]. Since  $\theta \neq 1/0$  by Lemma 4.2.2,  $\theta$  is an integer. Thus, to show that  $\theta$  is an integer, it remains to show that  $\widetilde{W}(*)$  is irreducible.

Suppose for contradiction that  $\widetilde{W}(*)$  is reducible, i.e.  $\widetilde{W}(*) = X \#$

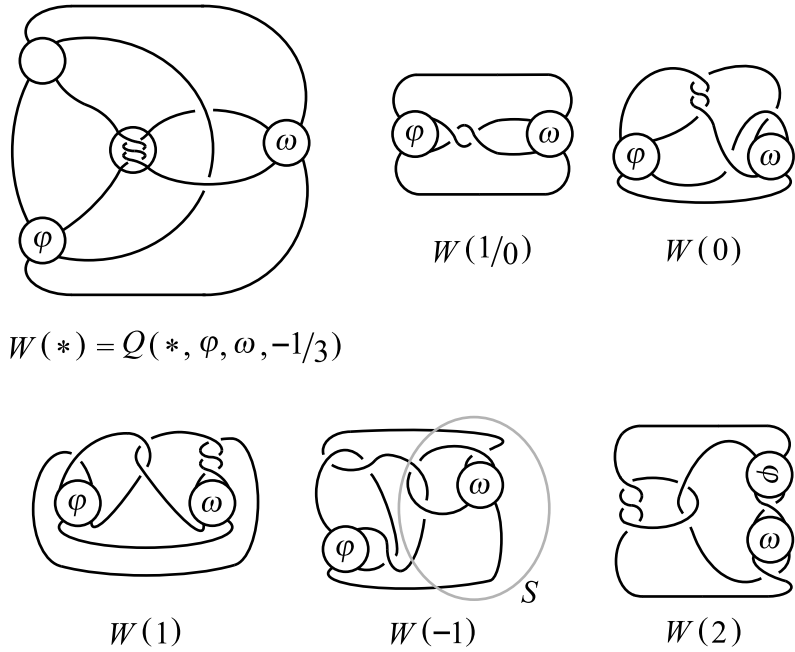


Figure 4.5:  $W(*) = Q(*, \varphi, \omega, -1/3)$  and the rational tangle fillings.

$Y(*)$  where  $Y$  contains the torus boundary component where Dehn fillings are performed. Note that if there are two slopes  $p$  and  $q$  such that  $\widetilde{W}(p)$  and  $\widetilde{W}(q)$  are prime manifolds, then  $\widetilde{W}(p) = \widetilde{W}(q)$ . However  $\widetilde{W}(1/0)$  is either  $S^3$ ,  $S^2 \times S^1$  or a lens space, which are all prime. Thus  $\widetilde{W}(p)$  is either  $S^3$ ,  $S^2 \times S^1$  or a lens space if  $\widetilde{W}(p)$  is prime. From Figure 4.5,  $\widetilde{W}(0)$  and  $\widetilde{W}(-1)$  are prime manifolds because  $\varphi, \omega \notin \{-1, 0, 1, 1/0\}$ , whence they must be either  $S^3$ ,  $S^2 \times S^1$  or a lens space.

Suppose  $\varphi \neq 1 + 1/a$  for an integer  $a$ . If  $\omega \neq 1/(1 + 1/b)$  for an integer  $b$ , then  $\widetilde{W}(-1)$  is a toroidal prime manifold, which is neither  $S^3$ ,  $S^2 \times S^1$  nor a lens space. If  $\omega = 1/(1 + 1/b)$  for some integer  $b$ , then  $\widetilde{W}(-1)$  is  $S^2(e, f, g)$

where  $e, f, g \geq 2$  since  $\omega \neq 0, 1/2$ , which is neither  $S^3, S^2 \times S^1$  nor a lens space, a contradiction. Therefore  $\varphi$  must be  $1+1/a$  for some integer  $a$ . Then  $\widetilde{W}(1) = S^2(|2a+1|, 2, t)$  for some integer  $t$ . Note that  $|2a+1| \neq 0, 1$  because  $\varphi \notin \{-1, 0, 1, 1/0\}$ . If  $\omega \neq 1/3$  i.e.  $t \neq 0$ , then  $\widetilde{W}(1)$  is a prime manifold, which must be either  $S^3, S^2 \times S^1$  or a lens space. Hence  $\omega$  must be  $1/(3+1/s)$  for some integer  $s$ . This implies that  $\widetilde{W}(-1) = S^2(|2a+1|, 2, |2s+1|)$ . However, since  $\varphi \neq -1, 0, 1$  and  $\omega \neq -1, 0, 1, 1/2$ ,  $|2a+1| \geq 2$  and  $|2s+1| \geq 2$ , whence  $\widetilde{W}(-1)$  is neither  $S^3, S^2 \times S^1$  nor a lens space, a contradiction. If  $\omega = 1/3$ , then  $\widetilde{W}(-1) = S^2(|2a+1|, 2, 2)$ , which is neither  $S^3, S^2 \times S^1$  nor a lens space, a contradiction. This completes the proof that  $\widetilde{W}(\ast)$  is irreducible.

By the symmetry by rotation in the horizontal axis on the tangle  $Q$ ,  $\varphi$  is also an integer.

To show that  $\omega$  is  $1/k$  for some integer  $k$ , a similar argument to the above applies. Let  $W'(\ast) = Q(\theta, \varphi, \ast, -1/3)$ . Then  $\widetilde{W}'(\omega) = \widetilde{Q}(\theta, \varphi, \omega, -1/3)$  is  $M(r_1)$ , which is reducible and is not  $S^2 \times S^1$  by [29]. We perform the rational tangle fillings shown in Figure 4.6. Since  $\widetilde{W}'(0)$  is either  $S^3, S^2 \times S^1$  or a lens space,  $\omega$  is  $1/k$  for some integer  $k$  by Lemma 4.2.1, provided that  $\widetilde{W}'(\ast)$  is irreducible.  $\widetilde{W}'(1/2)$  is  $S^2(a, b, c)$ ,  $a, b, c \geq 2$ , since  $\theta, \varphi \notin \{-1, 0, 1, 1/0\}$  and  $\theta$  and  $\varphi$  are integers. Thus  $\widetilde{W}'(1/2)$  is prime and  $\widetilde{W}'(1/2) \neq \widetilde{W}'(0)$ . So  $\widetilde{W}'(\ast)$  is irreducible. The proof is complete.  $\square$

**Lemma 4.2.4.**  $\theta, \varphi \neq -2$ .

*Proof.* Suppose  $\varphi = -2$ . Let  $W(\ast) = Q(\ast, -2, \omega, -1/3)$ . Then  $\widetilde{W}(\theta)(=$

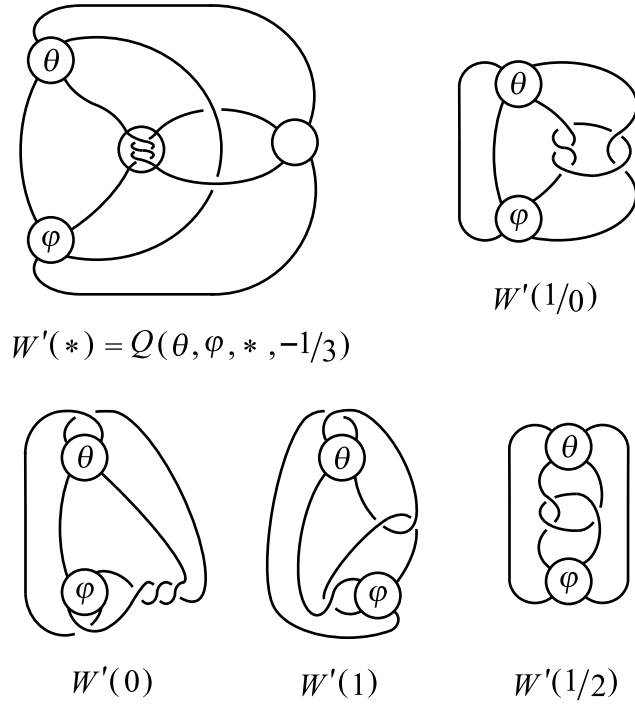


Figure 4.6:  $W'(*) = Q(\theta, \varphi, *, -1/3)$  and the rational tangle fillings.

$M(r_1)$ ) is reducible and is not  $S^2 \times S^1$  by [29]. Consider the rational tangle fillings shown in Figure 4.5 with the  $-2$ -rational tangle substituted for  $\varphi$ . Note that  $\widetilde{W}(1)$  is  $S^3$ , a lens space or a reducible manifold. Since  $\widetilde{W}(1/0)$  and  $\widetilde{W}(-1)$  are prime and they are not homeomorphic,  $\widetilde{W}(*)$  is irreducible. Therefore we can apply Lemma 4.2.1 to get  $\Delta(\theta, 1) \leq 1$ . Thus  $\theta = 0, 1, 2$ . However 0 and 1 are impossible by Lemma 4.2.2. Then  $\theta = 2$ . We will show that 2 is also impossible.

Consider the toroidal Dehn filling  $M(r_2) = \widetilde{Q}(\theta, \varphi, \omega, 1/0)$ . Since  $\theta = 2$  and  $\varphi = -2$ ,  $M(r_2)$  contains a Klein bottle, which is a contradiction to the

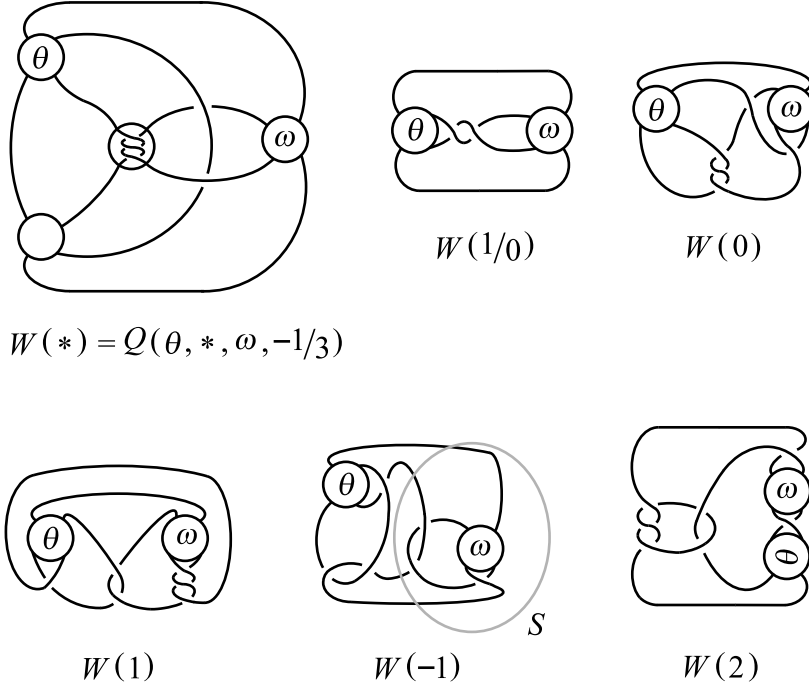


Figure 4.7:  $W(*) = Q(\theta, *, \omega, -1/3)$  and the rational tangle fillings.

assumption that  $M(r_2)$  does not contain a Klein bottle.

By the symmetry on  $Q$ ,  $\theta \neq -2$ . □

**Lemma 4.2.5.**  $\omega \neq 1/3$ .

*Proof.* Suppose that  $\omega = 1/3$ . Let  $W(*) = Q(\theta, *, 1/3, -1/3)$ . Then  $\widetilde{W}(\varphi)$  is  $M(r_1)$ , which is reducible and is not  $S^2 \times S^1$  by [29]. Consider the rational tangle fillings shown in Figure 4.7 with the  $1/3$ -rational tangle substituted for  $\omega$ . Note that  $\widetilde{W}(0)$  is a lens space and  $\widetilde{W}(1)$  is either a reducible manifold or a lens space. Therefore Lemma 4.2.1 says that  $\Delta(\varphi, 0) \leq 1$  and  $\Delta(\varphi, 1) \leq 1$

provided that  $\widetilde{W}(\ast)$  is irreducible. Hence  $\varphi$  is 0 or 1 which is impossible by Lemma 4.2.2. However  $\widetilde{W}(0)$  and  $\widetilde{W}(-1)$  are prime manifolds and are not homeomorphic. This implies that  $\widetilde{W}(\ast)$  is irreducible.  $\square$

### 4.3 The Proof of $\theta = 2$

In this section we show that  $\theta = 2$ .

**Proposition 4.3.1.**  *$\theta$  is 2 up to the symmetry by rotation in the horizontal axis on  $Q$ .*

Before proving Proposition 4.3.1, we need to consider several special cases.

#### 4.3.1 The Case that $\varphi = -3$

**Lemma 4.3.2.** *If  $\varphi = -3$ , then  $\theta = 2$ .*

*Proof.* Assume that  $\varphi = -3$ . Let  $W(\ast) = Q(\ast, -3, \omega, -1/3)$ . Then  $\widetilde{W}(\theta)$  is reducible. Consider the rational tangle fillings shown in Figure 4.5 with the  $-3$ -rational tangle substituted for  $\varphi$ .

Assume  $\widetilde{W}(\ast)$  is hyperbolic. Notice that  $\widetilde{W}(1) = S^2(2, 2, |1/\omega - 3|)$  and  $\widetilde{W}(-1)$  is toroidal since  $\omega \notin \{-1, 0, 1, 1/0, 1/2\}$ . Then  $\widetilde{W}(\ast)$  admits a reducible Dehn filling  $\widetilde{W}(\theta)$ , a toroidal Dehn filling  $\widetilde{W}(-1)$ , and a Dehn filling of the form  $S^2(2, 2, 1/\omega - 3)$ . By Corollary 1.3 in [28],  $\Delta(\theta, 1) \leq 2$  and by Theorem 1.1 in [34],  $\Delta(\theta, -1) \leq 3$ . Thus  $\theta = -1, 0, 1$  or  $2$ . However, Lemma

4.2.2 leads to  $\theta = 2$ . The proof is complete under the assumption that  $\widetilde{W}(\ast)$  is hyperbolic.

We show that  $\widetilde{W}(\ast)$  is hyperbolic. Equivalently, it suffices to show that  $\widetilde{W}(\ast)$  is irreducible,  $\partial$ -irreducible, non-Seifert fibered and atoroidal. Since  $\widetilde{W}(1/0)$  and  $\widetilde{W}(-1)$  are prime and are not homeomorphic,  $\widetilde{W}(\ast)$  is irreducible.

Suppose  $\widetilde{W}(\ast)$  is a Seifert fibered space. Since  $\widetilde{W}(1/0)$  is a lens space,  $\widetilde{W}(\ast)$  is a Seifert fibered space over  $D^2$  with at most 2 exceptional fibers. Hence  $\widetilde{W}(r)$  is a Seifert fibered space over  $S^2$  with at most three exceptional fibers except for one slope  $r$ , for which  $\widetilde{W}(r)$  is reducible. Figure 4.5 shows that  $\widetilde{W}(-1)$  is irreducible. Hence  $\widetilde{W}(-1) = S^2(e, f, g)$  where  $e, f, g \geq 1$ , which does not contain a separating incompressible torus. On the other hand,  $\widetilde{W}(-1)$  contains a separating incompressible torus which is the double branched cover of  $S$  in Figure 4.5, since  $\omega \notin \{-1, 0, 1, 1/0, 1/2\}$ . This is a contradiction. Therefore  $\widetilde{W}(\ast)$  is not a Seifert fibered space.

Suppose  $\widetilde{W}(\ast)$  is  $\partial$ -reducible. After  $\partial$ -compression, the torus boundary becomes a sphere which must bound a 3-ball since  $\widetilde{W}(\ast)$  is irreducible. This implies that  $\widetilde{W}(\ast)$  is a solid torus, which is a Seifert fibered space, a contradiction.

Suppose  $\widetilde{W}(\ast)$  is toroidal. Let  $T$  be an essential torus in  $\widetilde{W}(\ast)$ . Since  $\widetilde{W}(1/0)$  is a lens space,  $T$  must be separating, which allows us to let  $\widetilde{W}(\ast) = A \cup_T B(\ast)$  where  $B$  contains the torus boundary of  $\widetilde{W}(\ast)$ .

**Claim.**  *$T$  is compressible in  $\widetilde{W}(-1)$ .*

*Proof.* Suppose  $T$  is incompressible in  $\widetilde{W}(-1)$ . Figure 4.5 shows that there is a unique incompressible torus up to isotopy in  $\widetilde{W}(-1)$ , which must be the double branched cover of the sphere  $S$  as in Figure 4.5. Therefore  $\widetilde{W}(-1) = D^2(2, 4) \cup_T D^2(2, |1/\omega - 1|)$ . Thus  $A$  is either  $D^2(2, 4)$  or  $D^2(2, |1/\omega - 1|)$ . Observe from Figure 4.5 that  $\widetilde{W}(0) = S^2(3, 3, |1/\omega - 2|)$ ,  $\widetilde{W}(1) = S^2(2, 2, |1/\omega - 3|)$  and  $\widetilde{W}(2) = S^2(3, 2, |1/\omega + 1|)$ . Hence  $A$  is  $D^2(2, 3)$  and  $\omega = 1/4$ .  $A = D^2(2, 3)$  is the complement of the trefoil knot i.e. the  $(2, 3)$  torus knot  $T_{2,3}$ .  $\widetilde{W}(1) = S^2(2, 2, 1)$  becomes a lens space. It is easy to see that  $\widetilde{W}(1) = L(8, -3)$ . Since  $B(1)$  is a solid torus,  $\widetilde{W}(1) = L(8, -3)$  is obtained by Dehn filling on  $A = T_{2,3}$ . This is impossible by Corollary 7.4 in [8].  $\square$

$T$  is compressible in  $\widetilde{W}(1/0)$ ,  $\widetilde{W}(0)$ ,  $\widetilde{W}(1)$ ,  $\widetilde{W}(-1)$  and  $\widetilde{W}(2)$ . Since  $\Delta(2, -1) = \Delta(2, 0) = \Delta(1, -1) \geq 2$ , by Lemma 2.4 in [4]  $B(*)$  is a cable space  $C(p, q)$  with the cabling slope  $1/0$ . (See Section 3 in [10] for the definition of a cable space.). Moreover, since  $\Delta(\theta, 1/0) = 1$ ,  $B(\theta)$  is a solid torus, which makes  $T$  compressible in  $\widetilde{W}(\theta)$ . Therefore  $\widetilde{W}(1/0) = A(r_{1/0}) \# L(q, p)$  and  $\widetilde{W}(\theta) = A(r_\theta)$  for some slopes  $r_{1/0}, r_\theta$  on  $T$  with  $\Delta(r_{1/0}, r_\theta) = |q|\Delta(\theta, 1/0) = |q|$ . Since  $\widetilde{W}(1/0)$  is a lens space,  $A(r_{1/0})$  must be  $S^3$ . Then  $|q|$  must be 1 by Lemma 4.2.1 since  $A$  is irreducible,  $A(r_{1/0})$  is  $S^3$  and  $A(r_\theta)$  is reducible. The fact that  $q = 1$  or  $-1$  implies that  $T$  is  $\partial$ -parallel in  $\widetilde{W}(*)$ , which is a contradiction to the assumption that  $T$  is essential in  $\widetilde{W}(*)$ . Thus  $\widetilde{W}(*)$  is atoroidal.  $\square$

### 4.3.2 The Case that $\varphi = 3$

**Lemma 4.3.3.** *If  $\varphi = 3$ , then  $\theta = 2$ .*

*Proof.* Assume that  $\varphi = 3$ . Let  $W(*) = Q(*, 3, \omega, -1/3)$ . Then  $\widetilde{W}(\theta)$  is reducible. Consider the rational tangle fillings shown in Figure 4.5 with the 3-rational tangle substituted for  $\varphi$ .

Assume  $\widetilde{W}(*)$  is hyperbolic.  $\widetilde{W}(-1)$  is toroidal since  $\omega \notin \{-1, 0, 1, 1/0, 1/2\}$ .  $\widetilde{W}(\theta)$  is reducible. Thus  $\Delta(\theta, -1) \leq 3$ . The possible values of  $\theta$  are  $-4, -3, -2, 2$  since  $\theta \notin \{-1, 0, 1, 1/0\}$ . If  $\theta$  is 2, we are done. If  $\theta$  is  $-3$ , then this belongs to the case of  $\varphi = -3$  by the symmetry on  $Q$ , whence we are done. Also,  $\theta \neq -2$  by Lemma 4.2.4. The remaining case is  $\theta = -4$ .

Suppose  $\theta = -4$ . Let  $W'(*) = Q(-4, 3, *, -1/3)$ . Then  $\widetilde{W}'(\omega)$  is reducible. Similarly, we can easily see from Figure 39 that  $\widetilde{W}'(1/0)$  is the lens space  $L(7, -2)$  and  $\widetilde{W}'(1)$  is  $S^2(4, 2, 3)$ . They are non-homeomorphic prime manifolds. Thus  $\widetilde{W}'(*)$  is irreducible. Moreover, Lemma 4.2.1 leads to  $\Delta(1/0, \omega) \leq 1$ . Since  $\omega$  is of the form  $1/k$  for some integer  $k$ ,  $\omega$  is 1 or  $-1$ , which is impossible by Lemma 4.2.2. Hence  $\theta \neq -4$ .

To complete the proof of the lemma, it remains to show that  $\widetilde{W}(*)$  is hyperbolic.

$\widetilde{W}(*)$  is irreducible because  $\widetilde{W}(1/0)$  and  $\widetilde{W}(-1)$  are prime and are not homeomorphic. The way of proving that  $\widetilde{W}(*)$  is  $\partial$ -irreducible and not a Seifert fibered space is exactly the same as for the case  $\varphi = -3$ .

Suppose  $\widetilde{W}(\ast)$  is toroidal. Let  $T$  be an essential torus in  $\widetilde{W}(\ast)$ . Since  $\widetilde{W}(1/0)$  is a lens space,  $T$  must be separating. Let  $\widetilde{W}(\ast) = A \cup_T B(\ast)$  where  $B$  contains the torus boundary of  $\widetilde{W}(\ast)$ .

**Claim.**  $T$  is compressible in  $\widetilde{W}(-1)$ .

*Proof.* Suppose for the contradiction  $T$  is incompressible in  $\widetilde{W}(-1)$ . Let  $T'$  be the double branched cover of  $S$  as shown in Figure 4.5.  $\widetilde{W}(-1) = D^2(2, 2) \cup_{T'} D^2(2, |1/\omega - 1|)$ . Then  $T'$  is the unique incompressible torus up to isotopy in  $\widetilde{W}(-1)$  unless  $\omega \in \{-1, 0, 1, 1/0, 1/2, 1/3\}$ . If  $\omega = 1/3$ , then  $\widetilde{W}(1)$  is reducible from Figure 4.5. Thus by Lemma 4.2.1,  $\Delta(\theta, 1) \leq 1$  i.e.  $\theta = 2$  since  $\theta \neq 0, 1$ , in which case we are done. Therefore we may assume that  $T'$  is the unique incompressible torus up to isotopy in  $\widetilde{W}(-1)$ . Thus,  $T = T'$ . In other words,  $\widetilde{W}(-1) = D^2(2, 2) \cup_T D^2(2, |1/\omega - 1|)$ . Hence  $A$  is either  $D^2(2, 2)$  or  $D^2(2, |1/\omega - 1|)$ . Observe from Figure 4.5 that  $\widetilde{W}(0) = S^2(3, 3, |1/\omega - 2|)$ ,  $\widetilde{W}(1) = S^2(4, 2, |1/\omega - 3|)$  and  $\widetilde{W}(2) = S^2(3, 2, |1/\omega - 5|)$ . Hence  $A$  is  $D^2(2, 3)$  and  $\omega = 1/4$ .  $A = D^2(2, 3)$  is the complement of the trefoil knot i.e. the  $(2, 3)$  torus knot  $T_{2,3}$ . Now apply the same argument as in the case  $\varphi = -3$  using  $\widetilde{W}(1) = L(10, -3)$ . □

$T$  is compressible in  $\widetilde{W}(1/0)$ ,  $\widetilde{W}(0)$ ,  $\widetilde{W}(1)$ ,  $\widetilde{W}(-1)$  and  $\widetilde{W}(2)$ . Then the rest of the proof is exactly the same as for the case  $\varphi = -3$ . □

### 4.3.3 The Case that $\omega = -1/3$

**Lemma 4.3.4.** *If  $\omega = -1/3$ , then  $\theta = 2$ .*

*Proof.* Assume that  $\omega = -1/3$ . Let  $W(*) = Q(\theta, *, -1/3, -1/3)$ . Then  $\widetilde{W}(\varphi)$  is reducible. Consider the rational tangle fillings shown in Figure 4.7 with the  $-1/3$ -rational tangle substituted for  $\omega$ . Then  $\widetilde{W}(-1)$  is toroidal unless  $\theta = 1/0, 0, 1, 2$  (by Lemma 4.2.2,  $\theta = 2$ , in which case we are done.). Hence we may assume that  $\widetilde{W}(-1)$  is toroidal.

Assume  $\widetilde{W}(*)$  is hyperbolic.  $\widetilde{W}(\varphi)$  is reducible and  $\widetilde{W}(-1)$  is toroidal. Thus  $\Delta(\varphi, -1) \leq 3$ . By Lemma 4.2.2  $\varphi = -4, -3, -2$  or  $2$ . If  $\varphi = -3$ , then  $\theta = 2$  by Lemma 4.3.2. If  $\varphi = 2$ , we are done by using the symmetry by rotation in the horizontal axis on  $Q$ . Also,  $\varphi \neq -2$  by Lemma 4.2.4.

Suppose  $\varphi = -4$ . Let  $W'(*) = Q(*, -4, -1/3, -1/3)$ . Then  $\widetilde{W}'(\theta)$  is reducible and is not  $S^2 \times S^1$  by [29]. Similarly, we can easily see from Figure 4.5 with  $W$  replaced by  $W'$  that  $\widetilde{W}'(2)$  is the lens space  $L(5, 1)$  and  $\widetilde{W}'(0)$  is  $S^2(3, 4, 5)$ . These are non-homeomorphic prime manifolds. Thus  $\widetilde{W}'(*)$  is irreducible. Since  $\widetilde{W}'(2)$  is a lens space and  $\widetilde{W}'(\theta)$  is reducible, by Lemma 4.2.1,  $\Delta(\theta, 2) \leq 1$ . Thus  $\theta$  is  $1, 2$  or  $3$ . However  $1$  is ruled out by Lemma 4.2.2. If  $\theta = 2$ , then we are done. The case  $\theta = 3$  belongs to the case  $\varphi = 3$  by the symmetry on  $Q$ . Thus  $\theta = 2$  by Lemma 4.3.3.

To complete the proof of the lemma, it remains to show that  $\widetilde{W}(*)$  is hyperbolic.

$\widetilde{W}(*)$  is irreducible because  $\widetilde{W}(1/0)$  and  $\widetilde{W}(-1)$  are prime and not homeomorphic. In the proof of Lemma 4.3.2, in order to prove that  $\widetilde{W}(*)$  is not a Seifert fibered space, we used the fact that  $\widetilde{W}(-1)$  is irreducible and contains

a separating incompressible torus. In this case,  $\widetilde{W}(-1)$  is also irreducible and contains a separating incompressible torus unless  $\theta = -1, 0, 1, 2$ , in which cases we are done by Lemma 4.2.2. Now we can apply the same argument as in the case  $\varphi = -3$  to show that  $\widetilde{W}(*)$  is  $\partial$ -irreducible and not a Seifert fibered space.

Suppose  $\widetilde{W}(*)$  is toroidal. Let  $T$  be an essential torus in  $\widetilde{W}(*)$ . Since  $\widetilde{W}(1/0)$  is a lens space,  $T$  must be separating. Let  $\widetilde{W}(*) = A \cup_T B(*)$  where  $B$  contains the torus boundary of  $\widetilde{W}(*)$ .

**Claim.**  $T$  is compressible in  $\widetilde{W}(-1)$ .

*Proof.* Suppose  $T$  is incompressible in  $\widetilde{W}(-1)$ . Let  $T'$  be the double branched cover of  $S$  as shown in Figure 4.7.  $\widetilde{W}(-1) = D^2(2, 4) \cup_{T'} D^2(2, |\theta - 1|)$ . Then  $T'$  is the unique incompressible torus up to isotopy in  $\widetilde{W}(-1)$  unless  $\theta = -1, 0, 1, 1/0, 2$ , in which cases we are done by Lemma 4.2.2. Therefore  $T' = T$ . That is,  $\widetilde{W}(-1) = D^2(2, 4) \cup_T D^2(2, |\theta - 1|)$ . Thus  $A$  is either  $D^2(2, 4)$  or  $D^2(2, |\theta - 1|)$ . Observe from Figure 4.7 that  $\widetilde{W}(0) = S^2(3, 5, |\theta|)$ ,  $\widetilde{W}(1) = S^2(2, 6, |\theta + 1|)$  and  $\widetilde{W}(2) = S^2(3, 2, |\theta + 5|)$ . Hence  $A$  is  $D^2(2, 3)$  and  $\theta = -2$ .  $A = D^2(2, 3)$  is the complement of the trefoil knot i.e. the  $(2, 3)$  torus knot  $T_{2,3}$ . Now apply the same argument as in the case  $\varphi = -3$  using  $\widetilde{W}(1) = L(16, -5)$ .  $\square$

$T$  is compressible in  $\widetilde{W}(1/0)$ ,  $\widetilde{W}(0)$ ,  $\widetilde{W}(1)$ ,  $\widetilde{W}(-1)$  and  $\widetilde{W}(2)$ . Then the rest of the proof is exactly the same as for the case  $\varphi = -3$ .  $\square$

#### 4.3.4 The Proof of Proposition 4.3.1

*Proof.* Theorem 3.1.4 says that the toroidal manifold  $M(r_2)$  is either  $D^2(2, q) \cup_T D^2(2, s)$ ,  $D^2(2, 3) \cup_T D^2(r, s)$  or  $D^2(2, q) \cup_T D^2(3, s)$ . On the other hand,  $M(r_2)$  is the double branched cover  $\tilde{Q}(\theta, \varphi, \omega, 1/0)$  over the link  $Q(\theta, \varphi, \omega, 1/0)$  as shown in Figure 4.8. Let  $S$  be the sphere shown in Figure 4.8. The double branched cover of  $S$  is an incompressible torus in  $M(r_2)$ . Since there is the unique incompressible torus in  $M(r_2)$  up to isotopy,  $T$  is the double branched cover of  $S$ . Therefore, by Lemma 4.2.3  $M(r_2) = D^2(|\theta|, |\varphi|) \cup_T D^2(2, |1/\omega|)$ .

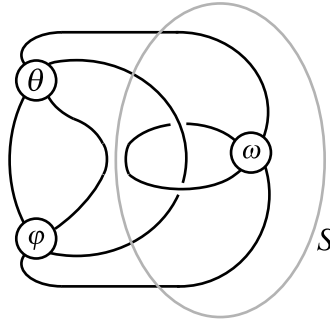


Figure 4.8:  $Q(\theta, \varphi, \omega, 1/0)$ .

(1) Assume  $M(r_2) = D^2(2, q) \cup_T D^2(2, s)$ . Then  $\theta$  must be 2 or  $-2$ .

Lemma 4.2.4 implies that  $\theta$  is 2.

(2) Assume  $M(r_2) = D^2(2, q) \cup_T D^2(3, s)$ . Then there are two cases: either  $\{|\theta|, |\varphi|\} = \{3, s\}$  or  $\{2, |1/\omega|\} = \{3, s\}$ .

If  $\{|\theta|, |\varphi|\} = \{3, s\}$ , then up to the symmetry, we may assume that  $|\varphi| = 3$ . Therefore by Lemmas 4.3.2 and 4.3.3,  $\theta$  is 2.

If  $\{2, |1/\omega|\} = \{3, s\}$ , then  $|1/\omega| = 3$ . Lemmas 4.3.4 and 4.2.5 imply that  $\theta$  is 2.

(3) Assume  $M(r_2) = D^2(2, 3) \cup_T D^2(r, s)$ . There are two cases:  $\{|\theta|, |\varphi|\} = \{2, 3\}$  or  $\{2, |1/\omega|\} = \{2, 3\}$ . In either case, Lemmas 4.2.5 and 4.3.2 – 4.3.4 show that  $\theta$  is 2.  $\square$

#### 4.4 The Proof of Theorem 4.1.1

*Proof.* Proposition 4.3.1 says that  $\theta = 2$ . Then  $M(r_1) = \tilde{Q}(2, \varphi, \omega, -1/3)$  is  $S^2(2, 3, |\varphi + 2 - 1/\omega|)$ . See  $W(2)$  in Figure 4.5. However since  $M(r_1) = \tilde{Q}(2, \varphi, \omega, -1/3)$  is reducible,  $\varphi + 2 - 1/\omega$  must be 0. Thus if we let  $\omega = 1/p$  where  $p$  is an integer, then  $\varphi = p - 2$ . Hence  $M = \tilde{Q}(2, p - 2, 1/p, *)$ ,  $M(r_1) = \tilde{Q}(2, p - 2, 1/p, -1/3)$  and  $M(r_2) = \tilde{Q}(2, p - 2, 1/p, 1/0)$ . However Lemma 4.2.2 implies that  $p \neq -1, 0, 1, 2, 3$ . If  $p$  is either  $-2$  or  $4$ , then  $M(r_2) = \tilde{Q}(2, p - 2, 1/p, 1/0)$  contains a Klein bottle, which is a contradiction. Therefore  $p \leq -3$  or  $p \geq 5$ . Observe that the tangle  $Q(2, p - 2, 1/p, *)$  is isotopic to the tangle  $Q(2, -p, 1/(-p + 2), *)$ . Therefore, we may assume that  $p \leq -3$ .

To complete the proof of the theorem, we need only to show that  $\tilde{Q}(2, p - 2, 1/p, *)$  is hyperbolic. However, the proof of this is exactly the same as the proof of Theorem 4.2 in [4].  $\square$

## Bibliography

- [1] S. Boyer and X. Zhang, *On Culler-Shalen seminorms and Dehn filling*, Topology and its Applications, **68** (1996), 285-303.
- [2] M. Culler, C. McA. Gordon, J. Luecke, and P. B. Shalen, *Dehn surgery on knots*, Ann. of Math. **125** (1987), 237-300.
- [3] M. Dehn, *Über die Topologie des dreidimensionalen Raumes*, Math. Ann. **69** (1910), 137-168.
- [4] M. Eudave-Muñoz and Y. Q. Wu, *Nonhyperbolic Dehn fillings on hyperbolic 3-manifolds*, Pacific J.Math. **190** (1999), 261-275.
- [5] L. Glass, *A combinatorial analog of the Poincaré index theorem*, J. Combin. Theory Ser. B **15** (1973), 264-268.
- [6] C. McA. Gordon, *Boundary slopes on punctured tori in 3-manifolds*, Trans. Amer. Math. Soc. **350** (1998), 1713-1790.
- [7] C. McA. Gordon, *Combinatorial methods in Dehn surgery* Proceedings of Knots 96, S. Suzuki, ed., World Scientific Publishing (1997), 263-290.
- [8] C. McA. Gordon, *Dehn surgery and satellite knots*, Trans. Amer. Math. Soc. **275** (1983), 687-708.

- [9] C. McA. Gordon, *Small surfaces and Dehn filling*, Geometry and Topology Monographs Vol. 2, Proceedings of the Kirbyfest, 1999, 177-199.
- [10] C. McA. Gordon and R. A. Litherland, *Incompressible planar surfaces in 3-manifolds*, Topology Appl. **18** (1984), 121-144.
- [11] C. McA. Gordon and J. Luecke, *Knots are determined by their complements*, J. Amer. Math. Soc. **2** (1989), 371-415.
- [12] C. McA. Gordon and J. Luecke, *Dehn surgeries on knots creating essential tori, I*, Communications in Analysis and Geometry **3** (1995), 597-644.
- [13] C. McA. Gordon and J. Luecke, *Knots are determined by their complements*, J. Amer. Math. Soc. **2** (1989), 371-415.
- [14] C. McA. Gordon and J. Luecke, *Reducible manifolds and Dehn surgery*, Topology **35** (1996), 385-409.
- [15] C. McA. Gordon and J. Luecke, *Toroidal and boundary-reducing Dehn fillings*, Topology Appl. **93** (1999), 77-90.
- [16] C. McA. Gordon and J. Luecke, *Non-integral toroidal Dehn surgeries*, Communications in Analysis and Geometry **12** (2004), 417-485.
- [17] C. McA. Gordon and Y.-Q. Wu, *Toroidal and annular Dehn fillings*, Proc. London Math. Soc. **78** (1999), 662-700.
- [18] C. McA. Gordon and Y.-Q. Wu, *Annular Dehn fillings*, Comm. Math. Helv. **75** (2000), 430-456.

- [19] C. McA. Gordon and Y.-Q. Wu, *Toroidal Dehn fillings on hyperbolic 3-manifolds*, Memoirs Amer. Math. Soc. vol. 194, no. 909, American Mathematical Society, Providence, RI, 2008.
- [20] W. Jaco, *Lectures on three-manifold topology*, Regional Conf. Series in Math. **43** (1997).
- [21] W.H. Jaco and P.B. Shalen, *Seifert fibered spaces in 3-manifolds*, Memoirs Amer. Math. Soc. vol. 21, no. 220, American Mathematical Society, Providence, RI, 1979.
- [22] K. Johannson, *Homotopy Equivalences of 3-Manifolds with Boundaries*, Lecture Notes in Mathematics 761, Springer-Verlag, Berlin, Heidelberg, 1979.
- [23] S. Kang, *Reducible and toroidal Dehn fillings with distance 3*, Topology **47** (2008), 277-315.
- [24] H. Kneser, *Geschlossene Flächen in dreidimensionale Mannigfaltigkeiten*, Jahresber. Deutsch. Math.-Verein. **38** (1929), 248-260.
- [25] M. Lackenby and R. Meyerhoff, *The maximal number of exceptional Dehn surgeries*, arXiv:0808.1176
- [26] S. Lee, *Boundary reducing and toroidal Dehn fillings at the maximal distance*, preprint.

- [27] S. Lee, *Reducing and annular Dehn fillings*, Trans. Amer. Math. Soc. **359** (2007), 227-247.
- [28] S. Lee, *Reducing and Toroidal Dehn fillings on 3-manifold bounded by two tori*, Mathematical Research Letters **12** (2005), 10001-10014.
- [29] S. Lee, *Toroidal Dehn surgeries on Knots in  $S^1 \times S^2$* , J. Knot Theory Ramifications **14** (2005), 657-664.
- [30] S. Lee, S. Oh and M. Teragaito, *Dehn fillings and small surfaces*, Preprint 2003. <http://de.arxiv.org/abs/math.GT/0303156>.
- [31] W.B.R. Lickorish, *A representation of orientable combinatorial 3-manifolds*, Ann. of Math. **76** (1962), 531-540.
- [32] R.A. Litherland, *Surgery on knots in solid tori. II*, J. London Math. Soc. **22** (1980), 559-569.
- [33] R. Myers, *Simple knots in compact, orientable 3-manifolds*, Trans. Amer. Math. Soc. **273** (1982), 75-91.
- [34] S. Oh, *Reducible and toroidal manifolds obtained by Dehn fillings*, Topology Appl. **75** (1997), 93-104.
- [35] G. Perelman, *The entropy formula for the Ricci flow and its geometric applications*, arXiv:math.DG/0211159.

- [36] G. Perelman, *Ricci flow with surgery on three-manifolds*, arXiv:math.DG/0303109.
- [37] G. Perelman, *Finite extinction time for the solutions to the Ricci flow on certain three-manifolds*, arXiv:math.DG/0307245.
- [38] W. Thurston, *Three dimensional manifolds, Kleinian groups and hyperbolic geometry*, Bull. Amer. Math. Soc. **6** (1982), 357-381.
- [39] W. Thurston, *Three-Dimensional Geometry and Topology*, Vol. 1, Princeton University Press (1997).
- [40] A.H. Wallace, *Modifications and cobounding manifolds*, Can. J. Math. **12** (1960), 503-528.
- [41] Y. Q. Wu, *The reducibility of surgered 3-manifolds*, Topology Appl. **43** (1992), 213-218.
- [42] Y. Q. Wu, *Dehn fillings producing reducible manifolds and toroidal manifolds*, Topology **37** (1998), 95-108.

## Vita

Sungmo Kang was born in Damyang, Jullanamdo in Korea on 7 May 1975, the son of Wonyong Kang and Yeungja Park. He received the Bachelor of Science degree in Mathematics from Korea University in 2000 and received the Master of Science degree in Mathematics from Korea University in 2002. In Fall 2002, he applied to the University of Texas at Austin for enrollment in their mathematics program. He was accepted and started graduate studies in August, 2002.

Permanent address: 773 Youngjuri Damyangup Damyangun,  
Jullanamdo 517-800, The Republic of Korea

This dissertation was typeset with  $\text{\LaTeX}^\dagger$  by the author.

---

<sup>†</sup> $\text{\LaTeX}$  is a document preparation system developed by Leslie Lamport as a special version of Donald Knuth's  $\text{\TeX}$  Program.